

**Identification of a novel receptor of bacterial  
PAMP RsE in *Arabidopsis* using genomic tools**

**Dissertation**

der Mathematisch-Naturwissenschaftlichen Fakultät

der Eberhard Karls Universität Tübingen

zur Erlangung des Grades eines

Doktors der Naturwissenschaften

(Dr. rer. nat.)

vorgelegt von

Li Fan

aus Henan

Tübingen

2015

Gedruckt mit Genehmigung der Mathematisch-Naturwissenschaftlichen  
Fakultät der Eberhard Karls Universität Tübingen.

Tag der mündlichen Qualifikation: 18.02.2016

Dekan: Prof. Dr. Wolfgang Rosenstiel

1. Berichterstatter: Prof. Dr. Thorsten Nürnberger

2. Berichterstatter: Prof. Dr. Georg Felix

## Summary

Plant innate immunity is triggered when a pathogen invades the cell and pathogen associated molecular patterns (PAMPs) are recognized by plant pattern recognition receptors (PRRs). Contrasting to the large amount of PAMPs identified so far, only a limited number of PRRs are known. RsE2 is a novel PAMP that was partially purified from the bacterial pathogen, *Ralstonia solanacearum* (Melzer, 2013). This pathogen colonizes xylem of plants and causes wilt in a wide range of host species. RsE2 could be effectively identified and elicits several early immunity responses such as ethylene response, oxidative burst in the plants and extracellular alkalization in cell suspensions of *Arabidopsis thaliana*. Further studies disclosed substantial natural variation in the RsE2-mediated ethylene response among different ecotypes of *Arabidopsis thaliana*. I hypothesized that the genetic variation in the RsE2-recognizing PRR gene in ecotypes is responsible for the phenotypical variation in the RsE2-caused response.

To identify the RsE2-recognizing PRRs, I screened for RsE2-induced/triggered ethylene response in multiple *Arabidopsis thaliana* ecotypes and conducted a genome wide associated study (GWAS). Meanwhile, I developed a F2 mapping population. Using a NGS-assisted (Next Generation Sequencing) QTL (Quantitative Trait Locus) mapping approach, I mapped RsE2 sensitivity to an 1.1 Mb region on Chr 3. This region overlaps with one of four candidate framed in GWAS as significant. Forward genetic analysis further identified that receptor like protein RLP32 is the receptor of RsE2 in Arabidopsis. My work showed great advantages to identify the RsE2-recognizing PRR using genomic tools.

Furthermore, I showed that RLP32-mediated RsE2 perception was compromised in the bak1/bkk1 double mutant or sobir1 mutant. The RLP32/Bak1/SOBIR1 tripartite-receptor provides a good system to study how a RLP-type PRR mediates signal transduction during PAMP-triggered immunity (PTI).

Finally, the transient expression of RLP32 from *Brassicaceae* plant family in *N. benthamiana* seedling could confer the capability of elicitor perception in

*Solanaceae* plant family, which suggests the potential application of engineered RsE2-recognizing system to enhance plant disease resistance.



## Zusammenfassung

Die angeborene Immunität der Pflanzen wird aktiviert, wenn Pathogene in die Pflanze eindringen und Pathogen-assoziierte molekulare Muster (PAMPs, pathogen associated molecular patterns) von pflanzlichen Mustererkennungsrezeptoren erkannt werden. Im Gegensatz zur großen Zahl bereits identifizierter PAMPs sind bisher nur wenige Mustererkennungsrezeptoren bekannt. RsE2 ist ein neues PAMP, das aus dem bakteriellen Pathogen *Ralstonia solanacearum* aufgereinigt wurde (Melzer 2013). Dieses Pathogen kolonisiert das Xylem der Pflanzen und verursacht Welke in einem weiten Wirtspflanzenkreis. Es konnte gezeigt werden, dass RsE2 von Pflanzen effektiv erkannt wird und eine Reihe von Immunantworten wie die Produktion von Ethylen und reaktiven Sauerstoffspezies sowie die Alkalisierung extrazellulären Mediums in Zellkulturen von *Arabidopsis thaliana* auslöst. Weitere Studien zeigten, dass die durch RsE2 ausgelöste Ethylenproduktion innerhalb verschiedener Ökotypen von *A. thaliana* sehr unterschiedlich ist. Daraus kann man schlussfolgern, dass genetische Variation im Gen des RsE2-erkennenden Mustererkennungsrezeptors für die beobachtete phänotypische Variation bei der durch RsE2 ausgelösten Antwort verantwortlich ist.

Um den Mustererkennungsrezeptor für RsE2 zu identifizieren, testete ich die RsE2-induzierte Ethylenantwort in einer großen Zahl von *A. thaliana* Ökotypen und führte eine GWAS-Analyse (GWAS, genome wide associated study) durch. Parallel dazu entwickelte ich eine F2 Population zur weiteren Kartierung. Mittels NGS-unterstützter QTL-Kartierung (NGS, next generation sequencing; QTL, quantitativ trait locus) konnte ich die RsE2-Sensitivität einer 1,1 Mb großen Region auf dem Chromosom 3 zuordnen. Dieses Ergebnis deckt sich ebenfalls mit einem von vier Kandidaten der GWAS-Studie. Durch weitere genetische Analysen konnte ich das Protein RLP32 als Rezeptor für RsE2 identifizieren.

Desweiteren konnte in der vorliegenden Arbeit gezeigt werden, dass RLP32-vermittelte RsE2-Perzeption in bak1/bkk1 Doppelmutanten und in sobir1-Mutanten beeinträchtigt ist. Der trimere Rezeptorkomplex aus

RLP32/BAK1/SOBIR1 stellt somit ein gutes Beispiel dafür dar, wie RLP-Rezeptoren zur PAMP-induzierten Immunität von Pflanzen beitragen.

## Contents

Summary .....	I
Zusammenfassung.....	III
Table directory .....	VIII
Table of figures .....	IX
Abbreviations .....	XI
<b>1. Acknowledgements .....</b>	<b>1</b>
<b>2. Introduction .....</b>	<b>2</b>
<b>2.1. Plant innate immunity--PTI and ETI .....</b>	<b>2</b>
<b>2.2. PAMPs and receptors.....</b>	<b>3</b>
2.2.1. A large variety of microbial patterns are recognized by plants .....	3
2.2.2. Pattern recognition receptors (PRRs).....	6
<b>2.3. Approaches to identify and clone immune receptors.....</b>	<b>11</b>
<b>2.4. The application of pathogen recognition systems in crop improvement.....</b>	<b>13</b>
<b>2.5. The scope of current thesis.....</b>	<b>14</b>
<b>3. Materials and methods .....</b>	<b>16</b>
<b>3.1 Protein biochemistry.....</b>	<b>16</b>
3.1.1 Buffer conditions for FPLC.....	16
3.1.2 Partial purification of PAMP Rse2 from <i>Ralstonia solanacearum</i> .	16
<b>3.2 Plant materials and growth conditions.....</b>	<b>17</b>
<b>3.3 Bio-assay.....</b>	<b>18</b>
3.3.1 Ethylene assay .....	18
3.3.2 Callose assay .....	19
<b>3.4 GBS based QTL .....</b>	<b>19</b>
3.4.1 Arabidopsis genomic DNA isolation for F2 populations.....	19
3.4.2 PstI-MseI GBS .....	20
3.4.3 Sequence Processing.....	23

---

3.4.4 rQTL mapping.....	24
<b>3.5 Software and Web tools .....</b>	<b>25</b>
<b>3.6 Molecular biology .....</b>	<b>25</b>
3.6.1 qRT-PCR validation .....	25
3.6.2 Primers for genotyping T-DNA lines .....	26
3.6.3 Cloning and Protoplast transformation .....	26
3.6.4 Transient expression in <i>N. benthamiana</i> .....	28
3.6.5 Arabidopsis transformation and selection.....	28
<b>4. Results .....</b>	<b>30</b>
<b>4.1 Natural variation within Arabidopsis ecotypes for RsE2 sensitivity 30</b>	
4.1.1 Use of a double mutant system to identify the RsE2 receptor.....	30
4.1.2 RsE1 and RsE2 induced ethylene responses among ecotypes ....	32
4.1.3 Callose deposition variation elicited by RsE1 and RsE2 .....	35
4.1.4 Geographic distribution of sensitive and insensitive ecotypes of RsE1 and RsE2.....	38
4.1.5 Diversification of sensitive and insensitive ecotypes is illustrated in the phylogenetic tree .....	40
<b>4.2 Single recessive gene controls RsE recognition .....</b>	<b>41</b>
<b>4.3 GWAS mapping.....</b>	<b>45</b>
<b>4.4 Genotyping by sequencing.....</b>	<b>51</b>
<b>4.5 Identification of the RsE2 receptor .....</b>	<b>56</b>
<b>4.6 The bioinformatics characterization of the Rlp32 gene .....</b>	<b>59</b>
<b>4.7 Protoplast transformation of a Rlp32 allele derived from sensitive ecotype ICE153 complements the phenotype in ecotype ICE73 .....</b>	<b>61</b>
<b>4.8 <i>N. benthamiana</i> gains RsE2 perception by transient expression of Rlp32.....</b>	<b>62</b>
<b>4.9 Stable transformation of Rlp32 in Arabidopsis insensitive ecotypes .....</b>	<b>64</b>
<b>4.10 Two elicitors RsE1 and RsE2 are identical .....</b>	<b>65</b>
<b>4.11 Interaction of RLP32 with other RLKs .....</b>	<b>67</b>
<b>5. Discussion .....</b>	<b>69</b>

---

<b>5.1. GWAS/Rad-seq offers a genomics-based tool for rapid receptor identification/isolation. ....</b>	<b>69</b>
<b>5.2. RLP32 is an LRR-RLP-type receptor.....</b>	<b>73</b>
<b>5.3. RLP32-mediated signalling.....</b>	<b>78</b>
<b>5.4. Biotechnological application of novel PRRs .....</b>	<b>80</b>
<b>6. References .....</b>	<b>83</b>
<b>7. Appendix.....</b>	<b>97</b>
<b>7.1 Supplementary figures and tables .....</b>	<b>97</b>
<b>7.2 Identification of novel PAMPs from <i>Pseudomonas syringae</i> pv tomato strain DC3000 .....</b>	<b>104</b>
7.2.1 Workflow for purification of novel PAMPs from <i>Pseudomonas syringae</i> pv tomato strain DC3000.....	104
7.2.2 Two active fractions were separated by step-wise ammonium sulfate precipitation .....	107
7.2.3 Identification of a series of candidate PAMPs by further purification of PS45.....	107
7.2.4 Mass spectrometer detects a single candidate from purified PS65 .....	108
7.2.5 PAMP candidates were validated by over-expression in <i>E.coli</i> ...	109
7.2.6 Peptides derived of PSPTO_3270 and PSPTO_1424 elicit ethylene responses in fls2/efr Arabidopsis .....	111

---

## Table directory

Table 2. 1 Summary of PAMPs and PRRs.....	5
Table 3. 1 List of buffer conditions for FPLC .....	16
Table 3. 2 List of T-DNA insertion alleles for the candidate genes .....	18
Table 4. 1 SCFE1 induced ethylene response among ecotypes .....	47
Table 4. 2 Phenotype score upon RsE2 treatment among ecotypes.....	49
Table 4. 3 The candidate SNPs that passed the threshold .....	51
Table 4. 4 The genomic position and LOD value from rQTL.....	54
Table 7. 1 Recombination breakpoint was identified based on genotyping between markers Chr3: 1321901 to 1587717 of individual plant P2A03. ....	97
Table 7. 2 Recombination breakpoint was identified based on genotyping between markers Chr3: 2206537 to 2674522 of individual plant P1H03. ....	98
Table 7. 3 Phenotype layout for RAD-seq library .....	99
Table 7. 4 Phenotype score upon RsE1 treatment among ecotypes.....	100
Table 7. 5 List of stable transgenic Rlp32 of Arabidopsis .....	101
Table 7. 6 PS45 candidates from Mass Spectrometry .....	108

## Table of figures

Figure 3. 1 Sequence processing for GBS.....	24
Figure 4. 1 Two active PAMP fractions were identified from <i>Ralstonia solanacearum</i> .....	31
Figure 4. 2 RsE1 sensitivity screening among ecotypes.....	34
Figure 4. 3 RsE2 sensitivity screening among ecotypes.....	34
Figure 4. 4 RsE1-induced callose deposition among five insensitive ecotypes	36
Figure 4. 5 RsE2-induced callose deposition among five insensitive ecotypes	37
Figure 4. 6 Distribution of ecotypes that are ethylene response insensitive to RsE1 (upper) and RsE2 (lower) .....	39
Figure 4. 7 Diversification of sensitivity to RsE1/RsE2 did not happen during the re-colonization of the species after the last glaciation.....	41
Figure 4. 8 The summary of allelism test .....	42
Figure 4. 9 RsE2 induced ethylene responses in reciprocal crosses of sensitive and insensitive ecotypes .....	43
Figure 4. 10 Neither heterosis nor necrosis was detected upon RsE2 treatment .....	43
Figure 4. 11 Phenotype histogram of F2 population from ICE153XICE73.....	45
Figure 4. 12 Manhattan plot of the top 10% of all p-value upon SCFE1 treatment .....	48
Figure 4. 13 Manhattan plot of the top 10% of all p-value upon RsE2 treatment .....	50
Figure 4. 14 rQTL mapping for RsE2-induced ethylene response in F2 mapping populations.....	53
Figure 4. 15 The diagram of 31 individual plants containing informative recombination events which define the left and right boundary of QTL .....	55
Figure 4. 16 RsE2 induced ethylene response in multiple T-DNA/transposon insertion alleles of candidate receptors.....	57
Figure 4. 17 The gene structure of Rlp32 and mutant alleles .....	58
Figure 4. 18 The qRT-PCR analysis of rlp32 gene expression in ecotype ICE73 and Col-0.....	59
Figure 4. 19 A phylogenetic tree of Rlp32 genes from 80 Arabidopsis ecotypes .....	60

Figure 4. 20 The expression of 35S::RLP32-GFP in protoplasts of insensitive ecotype ICE73 obtains the function of perception of the RsE2.....	62
Figure 4. 21 RsE2-induced ethylene response in 35S::RLP32-GFP transient expressed <i>N. benthamiana</i> .....	63
Figure 4. 22 RsE2 induced ethylene response in transgenic ICE73 and Wt-5 plants.....	65
Figure 4. 23 Comparison of ethylene response elicited by RsE1 and RsE2 in T-DNA insertion alleles of Rlp32.....	66
Figure 4. 24 RsE2 failed to induce ethylene responses in bak1-5/bkk1-1 double mutants.....	67
Figure 4. 25 Reduced ethylene response upon RsE2 treatment in two T-DNA insertion alleles of Sobir1 .....	68
Figure 7. 1 Manhattan plot of the top 10% of all p-value upon RsE1 treatment .....	102
Figure 7. 2 Perception of RsE2 in different plant families .....	103
Figure 7. 3 Scheme of PAMPs purification from <i>Pseudomonas syringae DC3000</i> .....	105
Figure 7. 4 Ethylene responses in fls2/efr Arabidopsis elicited by protein fractions through step-wise precipitating from crude extract of <i>Pseudomonas syringae DC3000</i> .....	107
Figure 7. 5 PS45 candidates (left) and PS65 candidates (right) were spread on silver stained Tricine SDS page gels.....	109
Figure 7. 6 Ethylene responses in fls2/efr double mutants elicited by candidate PAMPs from <i>DC3000</i> .....	111
Figure 7. 7 Peptides-induced ethylene responses in fls2/efr double mutant plants.....	113
Figure 7. 8 Peptides-induced ethylene responses in fls2/efr double mutant plants or ecotype ICE73 with optimized conditions.....	113
Figure 7. 9 Peptides synthesis illustration for PSPTO_3270.....	114
Figure 7. 10 Peptides synthesis illustration for PSPTO_0217.....	115
Figure 7. 11 Peptides synthesis illustration for PSPTO_1424.....	116
Figure 7. 12 Peptides from PSPTO_0217 (known as NRPII protein) could not induce ethylene responses in double-mutant plants .....	117



## Abbreviations

<b>aa</b>	amino acid
<b>CEBiP</b>	chitin oligosaccharide elicitor binding protein
<b>CRoPS</b>	complexity reduction of polymorphic sequences
<b>DAMP</b>	damage-associated molecular pattern
<b>EF-Tu</b>	elongation factor Tu
<b>EIX</b>	ethylene-inducing xylanase
<b>ETI</b>	effector-triggered immunity
<b>flg22</b>	peptide from flagellin
<b>GBS</b>	genotyping by sequencing
<b>GFP</b>	green fluorescent protein
<b>GlcNAc</b>	N-acetylglucosamine
<b>GWAS</b>	genome wide associated study
<b>LGM</b>	last glacial maximum
<b>LOD</b>	logarithm of the odds, a LOD score of 3 means the odds are a thousand to one in favor of genetic linkage
<b>LPS</b>	lipopolysaccharides
<b>LRR</b>	leucine rich repeat
<b>MDP</b>	muramyl dipeptide
<b>NF</b>	nodulation factor
<b>NGS</b>	next generation sequencing
<b>NILs</b>	near-isogenic-lines
<b>NLPs</b>	necrosis and ethylene-inducing peptide 1-like proteins

<b>OGA</b>	oligogalacturonic acid
<b>OMVs</b>	outer membrane vesicles
<b>PAMP</b>	pathogen-associated molecular pattern
<b>PEN</b>	crude extracts of <i>Penicillium chrysogenum</i>
<b>PG</b>	endopolygalacturonase
<b>PGN</b>	peptidoglycan
<b>PRR</b>	pattern recognition receptor
<b>PTI</b>	PAMP-triggered immunity
<b>QTL</b>	quantitative trait locus
<b>RAD-seq</b>	restriction site associated DNA tag sequencing
<b>RLK</b>	receptor like kinase protein
<b>RLP</b>	receptor like protein
<b>ROS</b>	reactive oxygen species
<b>RTK</b>	receptor tyrosine kinase protein
<b>SCFE1</b>	sclerotinia culture filtrate elicitor1

## 1. Acknowledgements

I would like to express my deepest appreciation to my supervisor, Professor Thorsten Nürnberger, whose enthusiasm and dedication to science salvaged me from my early “desperate” frustration: science means suffering! Now I regain the courage to re-search happily!

I would like to thank my committee members, Professor Georg Felix, Professor Claus Harter and Professor Claudia Oecking who serve as my committee and supply a great deal of constructive suggestions during my study and preparation of dissertation!

In addition, my cordially thanks to all the partners on this project, especially, Dr. Eric Melzer who is sharing project information with me, involves in all discussions and provides helps for FPLC troubleshooting; Dr. Weiguo Zhang who involves in discussions of mapping methods and protein purifications especially when I started this project; and Dr. Eunyoung Chae who introduce the new technology to me and provides precious seeds for this project. This project couldn't be accomplished without your involvements! “Thank you all”.

I would like to thank Dr. Andrea Gust, Dr. Brunner Frédéric, and Prof. Georg Felix for your constructive suggestions during my progress reports. Your brilliant ideas always stimulate me to think more!

I owe my deep gratitude to my other colleagues, those working in N3 group, N1 group, N2 group, N4 group and Felix group, as well as our greenhouse gardeners! Thanks for your friendship and your generous helps even when you had your hands full! Special thanks to Mrs. Liane Schön, who gives me a great help for correspondence during my thesis revising!

Last, but not the least, I thank my family for their cares and loves! Their understandings and supports are always the most precious treasures in my life!

## 2. Introduction

### 2.1. Plant innate immunity---PTI and ETI

Plants live in diverse ecological environments as well as with diverse microbial communities and the key for their survival is to deal with both challenges from these two sides, the abiotic stress from the environment and the biotic stress from microbial attacks. In the constant battle against microbial infection, plants have evolved an innate immune system in response to diverse and fast evolving microbial communities. The arms race and the co-evolution of both plant immune systems and microbial infection mechanisms have shaped two major forms of plant immunity. We have not fully explored such diversity yet, but from the limited examples we learned that plants have developed receptor systems to perceive a wide spectrum of molecules and to respond to the presence of microbial threats. On one end of the spectrum, plants utilize membrane-localized pattern recognition receptors (PRR) to recognize pathogen-associated molecular patterns (PAMP); this is referred to as PAMP-triggered immunity (PTI). PTI is a form of ancient and basal defense layer to deal with generic and/or host non-adapted pathogens. On the other end of the spectrum, host-adapted microbes evolved effectors to suppress PTI, while host co-evolved cytoplasmic NLR receptors (R genes) recognize effectors or effector-derived molecular to suppress and to bypass host defense responses. This is referred to as effector-triggered immunity (ETI) (Böhm et. al., 2014). Compared to the complex and diversified ETI system, the PTI system has more generic composition.

Considering the diverse environments and microbial communities which the different ecotypes of a given plant species have to encounter, plants have not only evolved a wide range of defense responses within one particular plant species; we now realize that they also evolved diverse recognition systems (receptors) among different ecotypes. We are now starting to see studies exploring the genetic diversity of pathogen recognitions in different ecotypes of a given plant species (Roukos, 2010; Clark, 2010; Dunning et al., 2007; Gómez Gómez et al., 1999; Zipfel et al., 2004; Vetter et al., 2012), and these studies will hold promise of better understanding of how plants have adapted to diverse

environments and have evolved different immune systems. Such knowledge will also provide us with tools to improve crop production and to control crop diseases.

Although the prime genetic model plant, *Arabidopsis* was not initially considered a good system for plant-pathogen interaction research due to the fact that frequently used ecotypes are not susceptible to several important pathogens. In the past decades researchers have made great progress on enabling it to be used in plant pathology studies and have harvested fruitful fundamental knowledge on the molecular basis of plant-microbe interaction (Nishimura and Dangl, 2010). However, we still have not fully utilized the genetic diversity within the species, especially the genetic diversity of pathogen recognition capacities among ecotypes. New genomic tools have started showing their power to utilize such resources. There are a limited number of PAMPs that have been identified in the past decades, and even fewer corresponding PRRs were isolated. On the ETI side, also a rather limited set of effector/receptors is known. The identification of additional PAMPs and their corresponding receptors as well as of effector/receptor pairs will undoubtedly benefit from the use of *Arabidopsis* ecotype resources. Now more than several thousands of such ecotypes are available in stock centers. Likewise, whole genome sequencing data for a thousand of such ecotypes have been made available recently (Cao et al., 2011), which provides good opportunities to discover the full spectrum of diversity in plant-pathogen interactions.

## **2.2. PAMPs and receptors**

### **2.2.1. A large variety of microbial patterns are recognized by plants**

PAMPs usually represent conserved microbial structures (Table 2.1). New types of PAMPs are likely to be discovered and it is also very likely that any types of conserved and exposed microbial molecules might have the potential to serve as PAMPs.

Flagellin protein is the principle component of the bacterial mobility organ flagellum. The epitope flg22, a conserved peptide on the N-terminus of flagellin, can be recognized by many plant species from dicots to monocots (Felix et al.,

1999; Takai et al., 2008). The recognition of flagellin by plants is a very ancient function and different specificity/sensitivity of recognitions exist among plant species. A short synthesized peptide flg15 displayed the same activity as flg22 in tomato, while it displayed 100-fold reduced activity in *Arabidopsis*, compared to flg22 (Bauer et al., 2001). Another flg15 originated from *E. coli* could be recognized by LeFLS2 (FLAGELLIN-SENSING-2) in tomato, but was not active in the other *Solanum* plants such as *N. benthamiana* (Robatzek et al., 2007). Flg22 seemed a weak elicitor to rice, while the full length flagellin protein originated from the rice-incompatible strain of bacteria *A. avenae* could elicit strong immunity responses, such as the hypersensitive response in rice through the receptor OsFLS2 (Takai et al., 2008). Contrary to the dogma that PTI does not involve the hypersensitive response, several studies have reported induced hypersensitive response by flagellin (Takai et al., 2008; Hao et al., 2014).

The elongation factor Tu (EF-Tu) is another example of a bacterial PAMP. It was disclosed by the identification of the N-acetylated 18 aa epitope (elf18), which elicited the classical PTI response in *Brassicaceae* plants (Kunze, 2004). Both EF-Tu and flagellin are highly abundant proteins in bacteria. Lacking a signal peptide, EF-Tu is transported to the bacterial surface by secreted outer membrane vesicles (OMVs), which contain many virulence factors (Nieves et al., 2010).

Peptidoglycan (PGN) is another bacterial PAMP. In contrast to the recognition of the muramyl dipeptide (MDP) fragment in invertebrates, the conserved glycan backbone is the PAMP unit active in plants (Gust et al., 2007). PGN has a similar backbone structure as fungal chitin, but non-identical recognition systems were found in plants (Gust et al., 2007; 2012; Shimizu et al., 2010).

Besides aforementioned PAMPs that are structural molecules required for microbial fitness and survival, ever-larger numbers of PAMPs are found among molecules interfering host defense (Thomma et al., 2011). For example, chitin is a structural molecule triggering PTI in plants. *Avr4* is another PAMP secreted by fungus *C. fulvum*. *Avr4* uses highly conserved cysteine knot structure to bind to chitin on the cell wall of fungi, therefore to prevent chitin's hydrolysis by plant chitinases and to avoid chitin's recognition by plants (van den Burg et al., 2006; Joosten et al., 1994). Nevertheless, un-camouflaged chitins on cell wall

are digested by chitinase and a set of LysM-related PRRs recognize the tiny amount of released chitins and triggered PTI (Shimizu et al., 2010). Tomato utilizes the PRR Cf-4 to recognize the *Avr4* and to trigger the hypersensitive response as well as PTI (Joosten et al., 1997). The second examples are PAMPs endopolygalacturonases (PGs), which are secreted by fungus *Botrytis cinerea* and can destroy the integrity of host cell walls by hydrolyzing the pectin (Zhang et al., 2014). Recently, a new PAMP called nlp20 was identified as a 20-amino acids peptide derived from necrosis and ethylene-inducing peptide 1 (Nep1)-like proteins (NLPs) that function in phytotoxin-induced host damages (Böhm et al., 2014).

Table 2. 1 Summary of PAMPs and PRRs

PAMPs	Micro-organism	Strains	Receptors	Plants harboring recognition system	Representative references
<i>flagellin</i>	bacteria	<i>Pseudomonas syringae</i> pv <i>tabaci</i>	FLS2	<i>Lycopersicon peruvianum</i> (a wild relative of tomato), tobacco, potato and Arabidopsis	Felix et al., 1999, Gómez-Gómez et al., 2000
elf18	bacteria	<i>E. coli</i> strain GI826 (FlhC), <i>R. solanacearum</i> , and <i>S. meliloti</i>	EFR	Arabidopsis and other <i>Brassicaceae</i>	Kunze et al., 2004
Peptidoglycans (PGNs)	bacteria	gram-negative and positive	AtLYM1/ LYM3, OsLYP4/LYP6, CERK1	Arabidopsis and rice	Willmann et al., 2011, Liu et al., 2012(a/b)
Lipopolysaccharides (LPS)	bacteria	<i>Burkholderia cepacia</i> , <i>Xanthomonas campestris</i> pv. <i>Campestris</i>	LORE	Arabidopsis	Coventry et al., 2001, Meyer et al., 2001, Ranf et al., 2015
eMAX	bacteria	<i>Xanthomonas axonopodis</i> pv <i>citri</i> strain 306 ( <i>Xac</i> )	ReMAX (RLP1)	Arabidopsis	Jehle et al., 2013
Avr2/4/5/9	fungi	<i>C. Fulvum</i>	Cf-2/-4/-5/-9	tomato	van den Burg et al., 2006
Ave1	fungi	<i>Verticillium</i> spp.	Ve1	tomato	Fradin et al., 2009
Penicillium chrysogenum (PEN)	fungi	<i>Penicillium chrysogenum</i>	unidentified	unidentified	Thüring et al., 2005
ethylene-inducing xylanase (EIX)	fungi	<i>Trichoderma viride</i>	<i>LeEix1</i> and <i>LeEix2</i>	tobacco and tomato	Ron and Avni, 2004
Chitin	fungi	unspecified	CERK1	tomato, rice and Arabidopsis	Felix et al., 1993, Shimizu et al., 2010
SCFE1	fungi	<i>S. sclerotiorum</i>	RLP30	Arabidopsis	Zhang et al., 2013
PGs	fungi	<i>Botrytis cinerea</i>	RLP42	Arabidopsis	Zhang et al., 2014
β-Glucan	oomycete	<i>Phytophthora megasperma</i>	GE-binding protein (GEBP)	soybean	Umemoto et al., 1997
Pep-13	oomycete	<i>Phytophthora sojae</i>	unidentified	parsley and potato	Nürnbergger et al. 1994, Brunner et al., 2002
elicitin	oomycete	<i>Phytophthora species</i>	ELR	potato	Du et al., 2015
nlp20	bacteria, fungi and oomycete	unspecified	RLP23	Arabidopsis	Albert and Böhm et al. 2015

In addition to these PAMPs, a few of endogenous signals, termed damage associated molecular patterns (DAMPs) could also act as elicitors to trigger immunity in plants, such as the peptide elicitors systemin and Pep1-5, the nucleotide elicitor ATP and saccharide elicitor oligogalacturonic acid (OGA) (Scheer et al., 2002; Tang et al., 2014; Choi et al., 2014; Tanaka, 2014; Decreux et al., 2006; Brutus et al., 2010).

In our study, we have used RsE1/RsE2 semi-purified elicitors from *Ralstonia solanacearum*, which can cause bacterial wilt in broad range of host plants (Melzer, 2013).

### 2.2.2. Pattern recognition receptors (PRRs)

Based on the studies of the known PRRs, it appears that plant use a common theme similar to that of the more studied animal system (Shiu and Bleecker, 2001), in which the coupling of the receptor and ligand triggers a cascade of signal pathways and subsequently invokes immune reactions. In plants, a group of genes encoding receptor-like kinase proteins (RLKs) are used for the perception of PAMPs in the pathogen interaction. RLKs are related to receptor tyrosine kinases (RTKs) in animals. Plant RLKs share similar structure with animal RTKs; they have a ligand-binding extracellular domain and a cytoplasmic kinase domain separated by a single membrane-spanning domain.

In addition to RLKs, a different, structurally related protein family has been identified to be involved in the perception of PAMPs. They are classified as receptor-like proteins (RLPs). They possess similar ligand-binding extracellular domains and a single membrane-spanning domain, but lack the cytoplasmic kinase domain (Wang et al., 2008). Due to the absence of a kinase domain, RLPs are thought to require interaction with other components of the signal cascade to invoke the immune response. RLPs are also implicated in plant development (Kruijt et al., 2005; Jones et al., 1994; Nadeau, 2002; Jeong et al., 1999).

As shown in the table 2.1, currently known PRRs already showed substantial diversity. In plants, RLKs is one of the largest gene families. In *Arabidopsis* there are more than 600 of its members encoded in the genome. In addition to



the large number, the RLKs are also one of the most variable gene families in *Arabidopsis* species (Cao et al., 2011). The critical structure feature of the RLKs that enables such diversity is the ligand-binding extracellular domain. A great deal of varieties of signal-recognizing domains and the combination of such domains make it possible for plants to perceive diverse biotic and abiotic signals. From the limited number of known PRRs, we already obtain partial picture of how such diversity has evolved to recognize different PAMPs from potential plant pathogens.

At least ten different structured domains are found in the extracellular ligand-binding domain of the RLK/RLP gene family. Among them, the leucine-rich repeat (LRR) motif and the lysine motif (LYM) are two motifs that are frequently present in the known PRRs.

#### 2.2.2.1. LRR-related (LRR-RLKs and LRR-RLPs) PRRs

The *Arabidopsis* LRR containing RLKs (LRR-RLKs) are the largest sub-family in the RLKs family with more than 200 genes. LRR-RLKs are also the most variable genes in the genome attributed by their repetitive nature of the LRR domains. Several LRR-RLKs gene have been identified as PRRs of bacteria-derived PAMPs, including FLS2 and EFR (ELONGATION FACTOR RECEPTOR) that bind the bacterial flagellin peptide flg22 or the bacterial elongation factor EF-Tu, respectively (Chinchilla et al., 2006; Zipfel et al., 2006). AtFLS2 and AtEFR belong to the LRR-RLK XII subfamily, and are made of 28 LRRs and 21 LRRs respectively (Shiu and Blecker, 2003). AtPEPR1/AtPEPR2 (PEP-RECEPTOR-1/2) are receptors of endogenous peptide AtPep1, a damage-associated molecular pattern (DAMP). The crystal structure of the AtPep1/AtPEPR1 complex revealed that the extracellular domain of AtPEPR1 is constituted of 27 LRRs, and that the ligand AtPep1 binds to AtPEPR1 LRR4 to LRR18, forming a pair of salt bridges between the conserved residues Asn23 of AtPep1 and Arg487 of AtPEPR1 (Tang et al., 2014). Similar to flg22-induced FLS2 activation, AtPep1 binding to AtPEPR1 initiated the heterodimerization of AtPEPR1 and the co-receptor BRI1-ASSOCIATED KINASE-1 (BAK1) (Sun et al., 2013; Tang et al., 2014). Most known LRR-RLKs in *Arabidopsis* are activated by forming heterodimers with the co-receptor AtBAK1, while in rice three LRR-RLKs, OsXA21, OsXA3 and OsFLS2 use a similar mechanism to

activate immunity by heterodimerizing with OsSERK2, an ortholog of BAK1 (Chen et al., 2014).

A different class of LRR-containing receptors involved in plant immunity is LRR-containing RLP (LRR-RLP). Unlike LRR-RLKs that contain a cytoplasmic kinase domain, LRR-RLPs contain only an extracellular LRR domain, juxtamembrane and transmembrane domains and a short cytoplasmic tail. LRR-RLP-type PRRs require the kinase domain of the co-receptor SUPPRESSOR OF BIR1-1 (SOBIR1) to activate immunity signaling. The Arabidopsis LRR-RLP-family harbors 57 members (Wang et al., 2008). Recent studies showed that a few members, such as RLP1, RLP23, RLP30 and RLP42, were all involved in microbe-associated molecular pattern perception (Jehle et al., 2013; Zhang et al., 2013; Zhang et al., 2014; Albert and Böhm et al., 2015). RLP1/REMAX, RLP30 and RLP42/RBPG1 have been reported to mediate resistance to fungal pathogens (Jehle et al., 2013; Zhang et al., 2013; Zhang et al., 2014). In tomato, LRR-RLPs, Cf-2, Cf-4, Cf-5 and Cf-9 recognize elicitor patterns from and mediate resistance to *C. fulvum* (Thomas et al., 1998). Eix2 and Ve-1 are the other tomato LRR-RLP-type PRRs for fungal xylanase and Ave-1 from *Verticillium spp.*, respectively (Ron and Avni, 2004; Bar et al., 2010; de Jonge et al., 2012). In wild potato, an LRR-RLP protein ELR was found to recognize a molecular pattern elicitor from *Phytophthora* and conferred resistance to *Phytophthora infestans* once transferred to cultivated potato (Du et al., 2015). A recent study found that RLP23 associated with SOBIR1 in ligand independent way but forming a RLP23-SOBIR1-BAK1 tripartite couplet indeed required the ligand binding to RLP23 in advance, which implied a general mechanism of elicitor perception for all LRR-RLP-type PRRs (Albert and Böhm et al. 2015).

There is a second class of LRR-RLKs that serves as co-receptors of PRRs (e.g. BAK1 and SOBIR1) (Fradin et al., 2009; Chinchilla et al., 2007; Liebrand et al., 2013). In a ligand-dependent manner, BAK1 interacts with multiple LRR-RLK type PRRs, such as FLS2, EFR and PEPR1/2, to initiate immune responses (Sun et al., 2013; Tang et al., 2014). BAK1 also interacts with the LRR-RLK BRASSINOSTEROID INSENSITIVE-1 (BRI1) to activate brassinosteroid signaling (Nam et al., 2002). The kinase domain of BAK1 uses un-coupled phosphorylating strategies to activate either development or defense signaling

pathway (Liebrand et al., 2013). The other LRR-RLK SOBIR1 associates with LRR-RLP type PRRs in a ligand-independent way (Liebrand et al., 2013; Albert and Böhm et al. 2015). Furthermore, a ligand binding to LRR-RLP/SOBIR1 complex is prerequisite for recruiting BAK1 to mediate downstream defense responses (Liebrand et al., 2013; Albert and Böhm et al. 2015). SOBIR1 is required by almost all LRR-RLP type immune receptors, such as RLP1, RLP23, RLP30 and RLP42 in Arabidopsis, and *Ve1*, *Cf-4* and *Eix-1/2* in tomato (Gust et al., 2014). SOBIR1 is not directly involved in LRR-RLK type PRR-mediated immune responses, however, the gene *Sobir1* is transcriptionally up-regulated upon perception of flg22 or EF-Tu by LRR-RLK type PRRs. (Liebrand et al., 2013).

#### 2.2.2.2. LysM-related receptors

Lysine motif-containing receptors, including OsCERK1/OsCEBiP, AtLYM1/LYM3, and OsLYP4/LYP6, can also be classified into two classes, the LysM-RKs with the cytoplasmic protein kinase domain and LysM-RPs without kinase domain. Its extracellular domain contains Lysine motifs that bind to N-acetylglucosamine (GlcNAc) containing ligands, which include fungal chitin, bacterial peptidoglycan and bacterial nodulation factors (NF) (Monaghan and Zipfel, 2012; Christiaan Greeff, 2012; Gust et al., 2012). They mediate resistance to both fungal and bacterial pathogens. Usually, ligand-binding induces the dimerization (or trimerization) of LysM receptors, which is different from the LRR-containing RLKs and RLPs where the ligand-binding induces not only conformational changes, but also heterodimerization of FLS2 with BAK1 or RLP/SOBIR1 with BAK1 (Liu et al., 2012b; Albert and Böhm et al. 2015). Another difference is that LysM-containing RLP signaling is independent of BAK1 (Shimizu et al., 2010; Willmann et al., 2011).

#### 2.2.2.3. Other types of PRRs

Plants have also evolved other types of receptors to perceive several damage-associated molecular patterns (DAMPs). Among the four known DAMP receptors, the systemin receptor SR160 and the Pep1-5 receptors PEPR1/PEPR2 belong to the aforementioned LRR-RLK-type receptor (Scheer et al., 2002; Tang et al., 2014). There are two additional types of PRRs: the

Lectin receptor kinase AtDORN1 recognizing the nucleotide elicitor ATP and the EGF-like domain-containing receptor kinase AtWAK1 for saccharide elicitor oligogalacturonic acid (OGA) (Choi et al., 2014; Tanaka, 2014; Decreux et al., 2006; Brutus et al., 2010). Both animals and plants use extracellular ATP as a DAMP signal. In animals, ATP perception is mediated by plasma membrane-localized purinergic receptors P2X/P2Y (Khakh and Burnstock, 2009). In Arabidopsis, damaged leaves release as high as  $\sim 40\mu\text{M}$  ATP at wounding sites, which is sufficient to trigger signaling considering the high affinity of AtDORN1 for ATP ( $K_d \sim 46\text{nM}$ ) (Tanaka, 2014). The elevated ATP could trigger the immune response and the expression of genes for cell wall healing while the pathogen could secrete proteins to deplete the elevated extracellular ATP at damage sites. These evidences suggested that the extracellular ATP is a *bona fide* DAMP signal (Tanaka, 2014).

Besides L-type lectin domain-contained RLKs that the PRR AtDORN1 belongs to, other two types of lectin-RLKs are contained in Arabidopsis: G-type (32 gene members in this subfamily) and C-type (represent by a single gene) (Bouwmeester et al., 2009; Choi et al., 2014). Former study disclosed that a G-type lectin receptor Pi-d2 in rice functions in resistance to fungal pathogen *Magnaporthe grisea* (Chen et al., 2006). A recent study found that a G-type RLK, S-domain (SD) -1 RLK LORE (lipooligosaccharide-specific reduced elicitation; also known as SD1-29), serves as a PRR to sense lipid A moiety and mediate lipopolysaccharide-induced (LPS-induced) immune responses, such as calcium and oxidative bursts (Ranf et al., 2015). The LORE-PRR consists of a signal peptide, an extracellular putative ligand-binding region, a transmembrane domain, cytoplasmic serine-threonine kinase domain and a carboxy-terminal tail (Ranf et al., 2015). The putative ligand-binding region contains an amino-terminal bulb-associated lectin domain, an S-locus glycoprotein or cysteine-rich epidermal growth factor domain and a plasminogen-apple-nematode motif, with latter two domains functioning in protein homodimerization (Ranf et al., 2015; Bouwmeester et al., 2009).

### 2.3. Approaches to identify and clone immune receptors

The most widely used approach to identify PRRs is map-based genetic cloning experiments. A few early-identified receptors XA21 and FLS2, as well as recently identified receptors EMAX, RLP30 and RLP42, are all examples of using such method (Song et al., 1995; Gómez-Gómez et al., 2000; Jehle et al., 2013; Zhang et al., 2013; Zhang et al., 2014). The other approach is the traditional biochemistry method, which was successfully used in one case only. A fragment of chitin oligosaccharide elicitor binding protein (CEBiP) was isolated by (GlcNAc)<sub>8</sub>-APEA high-affinity chromatography and identified by mass spectrometry (Kaku et al., 2006). However, the challenge of the biochemistry approach always lies with the little amounts of receptors present in plants.

The identification of plant accessions that are either incapable or capable to elicit PTI is important for the genetic mapping of PRRs. Early studies utilized artificial EMS-mutagenized seedlings to screen for mutants of elicitor perception (Gómez-Gómez et al., 2000). Thousand *Arabidopsis* ecotypes provide a great natural variation source containing particular accessions with PAMP perception deficiencies. For example, mutant plants incapable of sensing bacterial EMAX, the fungal SCFE1 elicitor or the fungal RBPG1 elicitor were separately identified in *Arabidopsis* natural ecotypes in several studies (Jehle et al., 2013; Zhang et al., 2013; Zhang et al., 2014). Natural variation for pathogen perception also exists in other plant species, e.g. tomato. In tomato, *C. fulvum* resistance genes Cf-2 and Cf-9 were contained in wild species *L. pimpinellifolium*, Cf-4 was found in *L. hirsutum* and Cf-5 was found in *L. esculentum* (Thomas et al., 1998). The NILs (near isogenic lines) were generated by introgressing four wild lines into *C. fulvum* susceptible line Money-maker (Cf-0) separately (Thomas et al., 1998). The natural variation for pathogen perception has provided great sources to generate mapping population by crossing different ecotypes.

The advance in genomics technology, such as next generation sequencing (NGS) has further simplified and speeded up gene cloning approaches. RAD-seq (restriction site associated DNA tag sequencing) was a recently developed GBS (genotyping by sequencing) method (Elshire et al., 2011; Davey et al.,

2011; Poland et al., 2012). Making use of the polymorphism of flanking sequences around the particular restriction site between two parental ecotypes, high-density genetic markers were generated by isolation processes. NGS made it possible to sequence those markers from the pooled and genetically segregated population. Combined with the QTL-mapping, the genetic markers could be associated to phenotypes. Different from the traditional mapping, the genetic markers and the phenotype scores could be achieved at the same step, therefore eliminating the slow and arduous steps for developing new markers for the causal site. RAD-seq-associated mapping has well balanced the two mapping requirements: high resolution genetic markers and increased numbers of segregated populations (Baird et al., 2008; Davey et al., 2011). A recent study using such technology has successfully identified that the incompatibility hot sites in hybrids of *Arabidopsis* are mostly the regions with tandem repeats of immunity receptors (Chae et al., 2014).

To apply GWAS (genome wide associated study) to identify PRRs in this study is another pioneering approach. GWAS was first used to associate SNPs to particular traits of disease in humans and was shown to be more effective than family-based linkage study (Klein et al., 2005; Manolio et al., 2009). In plants, GWAS was used for high-throughput screens for genetic associations of 107 adaptive important phenotypes in 95 ecotypes of *Arabidopsis* (Atwell et al., 2010). This study confirmed the capability of this technique to detect the major-effect gene loci and demonstrated how sample size, genetic architecture of traits, population structure as well as allele frequency affected the power of GWAS's application in plants (Atwell et al., 2010). Contrasting to human disease, *Arabidopsis* GWAS exhibits two advantages: first, uncomplicated genetic architecture of traits in plants leads to higher ratio of phenotypic variance to be explained by top associated SNPs; second, multiple phenotypes scoring could be controlled to reduce environmental effect and increase reproducibility (Aranzana et al., 2005; Atwell et al., 2010). In our study, we used prior-determined causal locus of SCFE1-triggered immunity to illustrate the capability of GWAS in finding PRR and further to use this technology to associate genetic variance to novel elicitor triggered phenotype variation.

## 2.4. The application of pathogen recognition systems in crop improvement

Improving disease resistance is crucial in crop breeding to avoid the loss of harvest/yield caused by severe infections of pathogens, which have produced devastating impacts in history. For example, the oomycete *Phytophthora infestans* gave rise to the late blight Irish potato famine, and the fungus *Cryphonectria parasitica* caused the epidemic of chestnut blight in the Eastern United States. Among a few strategies to improve plant disease resistance, PRR transfer was recently considered as a promising way to boost plant immunity in many cases. Interfamily expression of Arabidopsis EFR in solanaceous plants *N. benthamiana* and tomato generated broad-spectrum bacteria resistance (Lacombe et al., 2010). Transfer of Arabidopsis RLP23 into potato confers enhanced resistance to *P. infestans* (Albert and Böhm et al. 2015). Transfer of RLP ELR originated from wild potato into cultivated potato results in enhanced immunity to *P. infestans* as well (Du et al., 2015). A recent study on chimeric receptors made of Arabidopsis EFR and rice XA21 suggested that monocots and dicots can share immune signaling systems mediated by two evolutionary-distant receptors, which provides the rationale for applying PRR transfer beyond families (Holton et al., 2015). Conversely, conventional breeding is more suitable for PRR manipulation within species. The XA21 from wild rice species was transferred into cultivated rice through breeding (Song et al., 1995). Cf-2, Cf-4, Cf-5 and Cf-9 were introgressed from wild tomatoes into cultivar money-maker and confer resistance to different strains of *C. fulvum* (Thomas et al., 1998). Ectopic expression of AtDORN1 (LecRK-I.9), which recognizes wounding signal ATP in Arabidopsis, confers the enhanced *Phytophthora* resistance both in potato plants and in *N. benthamiana* (Bouwmeester et al., 2014; Choi et al., 2014).

In addition of PRRs transfer, stacking of resistance proteins mediating ETI is another engineered disease resistance strategy, which is thought to cope with rapidly mutating effector genes in pathogen populations. Therefore, it is thought to produce more sustainable resistance. Three wild-relative-potato R genes (*Rpi*), as a cassette, transferred into the susceptible cultivar Desiree conferred to transgenic plants resistance to *Phytophthora infestans* isolates containing

three *Avr* effectors (Zhu et al., 2011). With increased capability to recognize the major effectors, this strategy shows great potential for engineering durable crop resistance (Jones et al., 2014).

In order to identify novel receptors for transfer into crop plants, development of methods for fast isolation of diverse plant receptors in response to diverse microbial infection has to be achieved. Only with efficient new technologies we can accumulate enough knowledge that can help us to understand the complete picture of PAMP/PRR interaction and rather generally, the evolution and diversification of plant immune systems. Such knowledge is essential for breeding and genetic manipulation of crops to enhance their ability to fight against pathogen infections.

## **2.5. The scope of current thesis**

RsE1/RsE2 are partially purified PAMPs from the plant pathogen *Ralstonia solanaceum* (Melzer, 2013). The identification of RsE1/RsE2 receptors in *Arabidopsis* has been hampered by differentiating between weak and null responses upon elicitor treatments in natural *Arabidopsis* ecotypes. In this thesis, I explored the use of genomics tools, large-scale phenotyping approaches and large-scale genomic resources to facilitate the discovery of novel PRRs. The main work is genetic mapping and identification of a novel receptor for RsE1/RsE2 in *Arabidopsis* using two independent methods: GBS-assisted extreme phenotype mapping and GWAS mapping. Both methods have greatly improved the efficiency to associate PAMP perception to the causal genetic region in *Arabidopsis*. The application of extreme phenotype sampling has reduced the risk of false phenotypes among bi-parental segregated populations. The application of GWAS has also expanded the utilization of genetic populations from two divergent parents to unspecified hundreds of ecotypes, which suggested the great potential to associate PAMP perception systems to genetic regions in high-throughput way.

The identified receptor RLP32 has also advanced our understanding of how RLP-type PRRs initiate downstream signaling by making use of co-receptors. This study also improved our understanding how plants sense xylem pathogens such as *Ralstonia solanaceum* and provided possible ways to make use of this



receptor to engineer broad disease resistant in economically important crops in the future.

In the appendix, I have mainly described a biochemistry approach to isolate novel potential PAMPs from *Pseudomonas syringae* DC3000. Several peptides have been identified to elicit ethylene biosynthesis in Arabidopsis seedling leaves of the fls/efr double mutant. Thus, those peptides will represent novel triggers of PTI.

### 3. Materials and methods

#### 3.1 Protein biochemistry

##### 3.1.1 Buffer conditions for FPLC

All buffers are filtered by 0.22 $\mu$ M membrane under the vacuum condition and kept in 4°C.

Table 3. 1 List of buffer conditions for FPLC

purification strategy	chromatography column	buffer A	buffer B
<b>CEC</b>	Hitrap SP FF (5ml)	50mM MES, pH 5.2	50mM MES, 0.5M KCl, pH 5.2
<b>AEC</b>	Hitrap Q FF (5ml)	50mM Tris, pH 8.5	50mM Tris, 0.5M KCl, pH 8.5
<b>CEC</b>	Source 15S 4.6/100 PE	50mM MES, pH 5.2	50mM MES, 0.5M KCl, pH 5.2
<b>AEC</b>	Source 15Q 4.6/100 PE	20mM 1,3-Diaminopropan, pH 11.1	20mM 1,3-Diaminopropan, 0.5M KCl, pH 11.1
<b>Gel filtration</b>	HiLoad™ 16/600 Superdex 75 prep grade	50mM MES, 150mM KCl, pH 6.5	none
<b>IMAC</b>	HisTrap FF, 1ml	0-20mM Imidazol, 50mM Tris, 50mM NaCl, pH 8.1	500mM Imidazol, 50mM Tris, 50mM NaCl, pH 8.1
<b>IMAC</b>	HiTrap Chelating HP, 1ml (Co <sup>2+</sup> )	0-20mM Imidazol, 50mM Tris, 50mM NaCl, pH 8.1	500mM Imidazol, 50mM Tris, 50mM NaCl, pH 8.1

##### 3.1.2 Partial purification of PAMP RsE2 from *Ralstonia solanacearum*

*Ralstonia solanacearum* was kindly provided by Dr. Eric Melzer and cultivated in Kelmans Medium for 28°C over 36~48 hours on shaker. To isolate elicitor from *Ralstonia solanacearum*, 5L cell culture was heated to boiling then cooled down on ice bath. Then the whole-cell culture was divided into small volumes and centrifuged at 5000g for 15 minutes. The ammoniumsulfate was added into the supernatant until 90% saturation to precipitate the whole proteins. The precipitated proteins then were re-dissolved in water. This crude extract can be stored in -20°C for long-term use. To isolate the PAMP RsE2 from crude extract, we followed the strategy which was described in Dr. Eric Melzer's thesis. The crude extract was first dialysed in 50mM MES buffer, PH 5.2. The equilibrated crude extract was run through the cation exchange HiTrap™SP FF (GE Healthcare) column in Äkta explorer system in a buffers containing the

following: the buffer A (50mM MES PH 5.2) and the buffer B (50mM MES, 0.5M KCl, PH5.2). All binding proteins were eluted, pooled together and dialysed in 50mM PH8.5 Tris buffer. This dialysed elicitor containing solution was loaded into HiTrap<sup>TM</sup>Q FF (GE Healthcare) column to perform anion exchange chromatography with the buffer A (50mM Tris PH8.5) and the buffer B (50mM Tris, 0.5M KCl, PH8.5). The flow-through from anion exchange chromatography was dialysed again in 50mM MES buffer (PH 5.2), and at the last step, this RsE2 containing solution was loaded on the Source 15S 4.6/100 PE cation exchange column again for fine protein separation at a loading speed of 1ml/min, followed by gradient elution. The fractions were checked for the elicitor activity by inducing ethylene response in *Arabidopsis*. Those fractions that produce high ethylene response were pooled together and normalized the quantity among the induced responses in insensitive ecotype ICE73 and sensitive ecotype ICE153. The partially purified RsE2 was used in other biological assay.

### 3.2 Plant materials and growth conditions

A total of 126 *Arabidopsis thaliana* were used in this study. Among them, 86 *Arabidopsis* ecotypes were kindly provided by Dr. Jun Cao from Weigel's lab at MPI Tuebingen, the other 40 ecotypes were kindly provided by Weiguo Zhang and Dr. Andrea Gust from the lab collection. The seeds were soaked in 0.1% Agarose for 5 days in cold-room for stratification before sowing. After 10 days, germinated seedlings were transferred into square pots, six plants per pot. The plants were under the standard short-day greenroom condition. Leaves from 16~25 leaf-stage plants were cut for ethylene measurement. Half of F1 population seeds for allelism test were kindly provided by Dr. Eunyoung Chae from Weigel's lab at MPI Tuebingen. The other half of F1 populations was generated by crossing those ecotypes reciprocally in order to obviate the maternal effect that could blur the allelism-test phenotype. For those ecotypes were nick, the crosses were conducted by following the procedure described by NASC([http://arabidopsis.info/InfoPages?template=crossing;web\\_section=arabidopsis](http://arabidopsis.info/InfoPages?template=crossing;web_section=arabidopsis)). Those late flowering ecotypes were sprayed with 100µM GM3 to promote the flowering, some of them for example, Dog-4 and ICE21 were flowering after the GM3 treatment, the remaining ecotypes such as Leo-1 and

ICE33 were treated with 4°C cold for 6 weeks, and flowered after cold treatment eventually. Seeds of F2 population from ICE153 by ICE73 are kindly provided also by Dr. Eunyoung Chae. The leaves from 600 F2 plants were harvested in four continuous days and prepared for phenotype screening.

T-DNA insertion lines are obtained from either NASC or Dr. Thomma Lab, and were grown under standard greenhouse condition (Table 3.2). The leaf harvesting and phenotype screening were done as mentioned above.

Table 3. 2 List of T-DNA insertion alleles for the candidate genes

Candidates	Loci.	alleles	source
<b>Rlp31</b>	AT3G05370	SALK_058586 (RLP31-1)	Thomma
		SALK_094160 (RLP31-2)	Thomma
		GT_5_84055	N162867
		SM_3_16776	N104462
		SM_3_23072	N111326
		SM_3_33809	N120520
		SAIL_388_H01	N817885
<b>Rlp32</b>	AT3G05650	FLAG_588C11 (RLP32-1)	Thomma
		SM_3_33092	N119803
		SALK_137467C	N657024
		SM_3_33695	N120406
		SM_3_15851	N106446
<b>Rlp33</b>	AT3G05660	FLAG_048F06 (RLP33-1)	Thomma
		SALK_087631 (RLP33-2)	Thomma
		SM_3_20358	N105659
<b>LRR gene</b>	AT3G05990	SALK_143696	N643696
		SALK_203784C	N692234
<b>R gene</b>	AT3G07040	SALK_146601C	N660645
		SAIL_918_H07	N879828

### 3.3 Bio-assay

#### 3.3.1 Ethylene assay

Arabidopsis plants used for ET (ethylene) measurement were grown in the growth chamber under the short-day condition. At the stage of 18-20 leaves, leaves were cut into small pieces of 3mm×4mm each and floated on the autoclaved water at room temperature overnight. Three pieces were transferred into one glass tube with 400µl autoclaved water. Then the elicitors RsE2, Pen (Thuerig et al., 2005) and SCFE1 (Zhang et al., 2013) was added into the tube

then sealed by rubber cap immediately. After 4 hours' incubation, ET was determined by chromatography using Shimadzu GC-14A combined with C-R4A chromatopac integrator (Felix et al., 1999).

### 3.3.2 Callose assay

Three individual leaves from 5~6 weeks old *Arabidopsis* plants were infiltrated by elicitor RsE2, and incubated for 8 hours. The leaves were cut off, fixed in solution containing 1% glutaraldehyde, 5mM citric acid and 90mM Na<sub>2</sub>HPO<sub>4</sub> (PH 7.4) overnight. The leaf tissues were cleared and dehydrated with 100% ethanol for 1~2 days and transferred to fresh ethanol a few times until the leaf tissues went to pale colour. Displaced in 100% ethanol then with 50% ethanol for 30 min, the leaf tissues then were equilibrated with 67mM K<sub>2</sub>HPO<sub>4</sub> (PH 12) for 30 min. The callose deposits in leaf tissues were stained with fresh staining solution containing 0.1% aniline blue, 67mM K<sub>2</sub>HPO<sub>4</sub> (PH 12) for one hour at room temperature. Stained leaf tissue was transferred onto object slides, mounted with 70% glycerol/30% staining solution. The callose deposition was examined by UV epifluorescence microscope (Felix et al., 1999; Veit et al., 2001; Sohn et al., 2007).

## 3.4 GBS based QTL

### 3.4.1 *Arabidopsis* genomic DNA isolation for F2 populations

Genomic DNA isolation was done as described by Cao Jun and was modified to fit 96-well DNA extraction by Dr. Eunyoung Chae (Cao et al., 2011). 386 leaf samples were collected in four Auto-tube Racks (Roth, EC05.1) containing a steel bead per well and put in -80°C. The frozen leaves were grinded with Qiagen shredder. The powder was re-suspended in 500µL CTAB (100mM Tris-HCl pH7.5, 1% CTAB, 700mM NaCl, 10mM EDTA pH7.5, 1% β-ME) using auto multi-channel pipette and incubated at 65°C for 30min, then the samples were cooled for 5 minutes at RT. Adding 350µL Chloroform:Isoamylalcohol (24:1) into each well using manual multi-channel pipette, the plates were sealed with caps and inverted several times. The plates were then spanned for 4000rpm - 5000rpm for 10 minutes. The upper layer (400µL) was transferred to a new plates containing equal volume of isopropanol using manual multi-channel

pipette. The solution was mixed gently and spanned 4000-5000 rpm for 10 minutes. DNA pellet was washed in 75% EtOH, and then re-suspended in DNase free water (containing RNaseA 10µg/ml).

To reduce the degradation of DNA caused by multiple freezing-melting cycles, the fresh DNA was normalized immediately by gel electrophoresis. The quantity of DNA in each well should be around 15ng/µL. Normalized DNA wells were randomly selected to quantify DNA by Qubit Fluorometer (Life Technology) again. 192 DNA samples from the plants with preferred phenotype were selected and re-located in two new 96-well plates. All DNA plates were kept in -20°C.

### 3.4.2 PstI-MseI GBS

Double enzyme restriction digestion was used to generate a DNA library consisting of barcoded 192 segregated F2 populations for sequencing by illumina system. The method was described by Poland (Poland et al., 2012) and by Eunyoung Chae (Chae et al., 2014).

#### Anneal Adapters

To make barcoded adapter 1,

1. Single-stranded adapter oligos in 96-well format were suspended to 100µM 1X elution buffer (10mM Tris-Cl, pH 8.0-8.5).
2. make 100µL of 10µM double stranded adapter:  
10µL each single stranded oligo (100µM)  
10µL 10X adapter buffer (500mM NaCl, 100mM Tris-Cl)  
70µL H<sub>2</sub>O  
Heat to 95°C and cool at a rate of 1°C/min to 30°C. Hold at 4°C.
3. Dilute adapters 3:10 to ~3µM and quantify using Qubit kit.
4. Normalize each well to ~0.1µM.

To make MseI common reverse Y-adapter (adapter 2) in single tube, the same strategy was used to get the double stranded adapter with the concentration 10µM.

In 96-well format, the working adapter stock was prepared by mixing 20 $\mu$ L Barcoded Adapter 1 (0.1 $\mu$ M), 30 $\mu$ L MseI Adapter 2 (10 $\mu$ M) with 50 $\mu$ L 1X adapter buffer (500mM NaCl, 100mM Tris-Cl) and spin it down.

Two restriction enzymes digestion

Preparing Restriction reaction:

<u>Plate</u>	<u>Sample</u>	<u>Content</u>
220 $\mu$ L	2.0 $\mu$ L	10XNEB buffer 4
44 $\mu$ L	0.4 $\mu$ L	PstI-HF (20,000 U/ $\mu$ L)
88 $\mu$ L	0.8 $\mu$ L	MseI (10,000 U/ $\mu$ L)
	25.8 $\mu$ L	gDNA(normalized to 15ng/ $\mu$ L)

The plate was mixed well and 37°C for 2 hours; 80°C for 20min; hold at 8°C.

Ligation

Preparing Ligation Master Mix:

<u>Plate</u>	<u>Sample</u>	<u>Content</u>
115.5 $\mu$ L	1.05 $\mu$ L	10XNEB buffer 4
440 $\mu$ L	4.0 $\mu$ L	ATP (10mM)
55 $\mu$ L	0.5 $\mu$ L	T4 DNA ligase (400,000 U/ $\mu$ L)

Ligation reaction:

30 $\mu$ L digestion solution

5 $\mu$ L Adapters (working adapter stock)

5.55 $\mu$ L Ligation Master Mix

Mix all above together and incubate at 22°C for 2 hours; 65°C for 20 min; hold at 8°C.

Multiplexing of samples

5 $\mu$ L of ligation products from two plates (192 samples) were pooled. 4x200 $\mu$ L samples were cleaned using QIAquick PCR Purification Kit. 200 $\mu$ L sample and 1000 $\mu$ L buffer PB were combined in one tube. 600 $\mu$ L mixture was added into column and spanned down, dispose the flow-through and the second 600 $\mu$ L mixture was added into column and spanned again, dispose the flow-through. The mixture was the washed in the column as described by the kits protocol

and re-suspended in 60 $\mu$ L. The final mixture were combination of the four clean-ups in total 240 $\mu$ L per library.

#### Amplification

PCR reaction Mix:

8  $\mu$ L DNA template

6.5 $\mu$ L H<sub>2</sub>O

1 $\mu$ L 10 $\mu$ M Illumina Primers PE forward

1 $\mu$ L 10 $\mu$ M Illumina Primers PE reverse

5 $\mu$ L 5x buffer

3 $\mu$ L dNTPs (2mM)

0.5 $\mu$ L phusion

Pre-PCR reaction for promising condition by 25cycle, 18 cycle and 12cycle under the program:

95°C 30sec;

95°C 30sec;

65°C 20sec;

72°C 10sec; (cycle 8, 12 or 16)

72°C 5min;

4°C forever.

The amount of the PCR products was estimated on the gel to select less cycle numbers if possible. Repeat PCR by 8 reactions and pool the products and clean up using QIAquick PCR Purification Kit. Re-suspend in 30 $\mu$ L Elution Buffer.

#### Library size selection

30 $\mu$ L amplified products were mixed with 10 $\mu$ L loading buffer. 7 $\mu$ L LMW (low molecular weight) was mixed with 3 $\mu$ L loading buffer. They were loaded on 2% Agarose gel and run at 120V for 60 minutes. 350-500bp fractions were excised and purified with QIAquick gel Purification Kit. 30 $\mu$ L EB was used to re-suspend the library. The Products were evaluated on ABI 3730xl DNA Analyzer (Applied Biosystems, Genome Center of MPI tuebingen).

#### Sequencing

The library containing 192 plants was indexed by RAD method using PstI and MseI. After quality and quantity control by Bioanalyzer, this library was



sequenced on Illumina HiSeq2000 using single-end 101bp sequencing protocol (The sequencing was conducted at Genome Center of MPI-Tuebingen by Dr. Christa Lanz).

### 3.4.3 Sequence Processing

This sequencing data analysis was done by Dr. Sang-Tae Kim and Dr. Eunyong Chae at MPI-Tuebingen (Figure 3.1). Sequencing reads data from Illumina was imported into SHORE with maximum 2 mis-matches of barcodes. Burrows-Wheeler Aligner (BWA) software was used to map short sequence reads to the reference genomes. SHORE consensus was applied to find variant and reference calls in each individual sample. A genome matrix with high quality SNPs calls and reference calls was established. The data goes through final filtering before QTL mapping. The potential marker positions were extracted by comparing the variable positions between parental sequences. In this study, genome sequences of ICE153 and ICE73 are got from 80 accession genome re-sequencing project (Cao et al., 2011). Markers with at least 80% genotyped were selected for analysis, allowing 20% missing data per marker. Heterozygous calls were obtained based on a criterion of 0.4-0.6 concordance and 3 support values. 192 F2 individuals from ICE153 x ICE73 were arranged to a library. After data processing, it was estimated that the average sequence coverage is about 36.43 with the upper limit 106.4 and the lower limit 1.078. About 16,972 markers were predicted by analyzing the parental genomic potential markers. About 901 markers were generated by RAD processing and marker filtering.

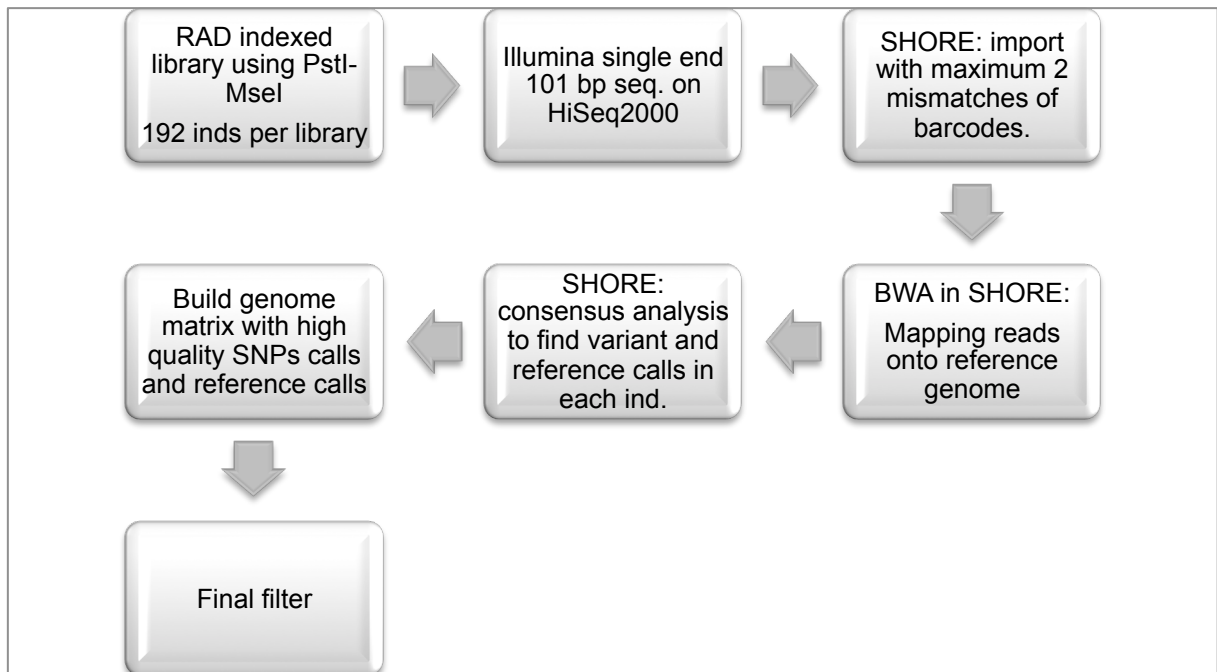


Figure 3. 1 Sequence processing for GBS

#### 3.4.4 rQTL mapping

192 F2 individuals from ICE153 x ICE73 cross were assigned the phenotype (method was described as above) based on the RsE2 induced ethylene response. Raw data see appendix Table 7.3.

901 markers were used to map the mutant phenotype by running R program. (Conducted by Dr. Eunyoung Chae)

rQTL script was used as following:

```

cross <- read.cross(format=c("csv"),
file="ICE153ICE73.0.8p.3.7.S5.GT.headQTLtrim2.csv", na.strings=c("-", "NA"),
genotypes=c("A", "H", "B"), alleles=c("A", "B"), estimate.map=FALSE)
summary(cross)
cross<-
calc.genoprob(cross,step=0,off.end=0,error.prob=0.001,map.function=c("kosambi"), stepwidth=c("fixed"))
ICE153ICE73binarytrait.em<-scanone(cross,pheno.col=1,model=c("normal"),
method=c("em"), addcovar=NULL, intcovar=NULL,
weights=NULL,use=c("all.obs"))
  
```

```

ICE153ICE73qtrait.em<-scanone(cross,pheno.col=1,model=c("normal"),
method=c("em"), addcovar=NULL, intcovar=NULL,
weights=NULL,use=c("all.obs"))
summary(ICE153ICE73qtrait.em,thr=3)
permo<-scanone(cross,method="em",n.perm=1000)
summary(permo,alpha=c(0.05,0.10))
plot(ICE153ICE73qtrait.em)
abline(h=3.61, col="blue" )
write.table(ICE153ICE73binarytrait.em, file="/<path>/ICE153ICE173qtrait.txt",
sep="\t")
write.table(ICE153ICE73trait2.em, file="/<path>/ ICE153ICE173trait1.txt",
sep="\t")

```

### 3.5 Software and Web tools

GWAS: <https://easygwa.tuebingen.mpg.de/>  
Sequence analysis: <http://www.ncbi.nlm.nih.gov/>  
Arabidopsis genome sequences:  
<http://signal.salk.edu/atg1001/3.0/gebrowser.php>  
T-DNA insertion position checking:  
<http://signal.salk.edu/cgi-bin/tdnaexpress>  
Primers design: <http://gmdd.shgmo.org/primer3/?seqid=47>  
Sequence alignment: CLC main workbench 6  
QTL mapping: rQTL  
Statistic: R program

### 3.6 Molecular biology

#### 3.6.1 qRT-PCR validation

The RNA was isolated from ecotype Col-0 and ICE73 leave tissues using GeneJET Plant RNA Purification Kit (Thermo scientific). 5µg RNA was incubated in 70°C for 10 minutes, then on ice to be cooled down, mixed with the RT mix. Reverse transcription condition was 42°C, 90 minutes then 70°C, 5 minute. rlp32 gene specific primers were designed to amplify a 100-200 bp amplicon from the cDNA to perform quantitative real-time PCR analysis. qRT-

PCR was conducted with iQTM5 Multicolor Real-Time PCR Detection System (Bio-Rad) using Maxima SYBR Green/Fluorescein qPCR Master Mix (Thermo scientific) and the PCR dissociation temperature was set to 58°C. Data analysis was performed according to Swanson-Wagner et al., 2006. The gene EF1 $\alpha$  (At1g07920/30/40) served as a reference gene for normalization and quantitative analysis.

The primers were used in qRT-PCR as following:

EF1 $\alpha$  F: 5' TCACATCAACATTGTGGTCATTGG 3' Tm 63.50

EF1 $\alpha$  R: 5' TTGATCTGGTCAAGAGCCTACAG 3' Tm 59.36

RLP32f2 5' TTTCAAGGACAACCCTGGAC 3' Tm 59.94

RLP32r2 5' GAGGGTTGTAAGTGGCCAAA 3' Tm 59.97

### 3.6.2 Primers for genotyping T-DNA lines

The Spm transposon specific primer Spm32 (5'GAATAAGAGCGTCCATTTTAGAGTG 3' Tm 62.5), the rlp32 gene specific primer R1406 (5' CAGATTGAGTAGGGAAAGGGG 3'Tm 59.94) and the rlp32 gene specific primer L367 (5' AATTGTTCAAACCGGTTGTG 3' Tm 59.75) were used to genotype the line of SM\_3\_33092.

T-DNA left boundary primer LBb1.3 (5' ATTTTGCCGATTTTCGGAAC 3' Tm 52.4), the rlp32 gene specific primer L5 (5' CGGAATTGAAGACGTTCGTT 3' Tm 60.11) and the rlp32 gene specific primer R994 (5' TCACTGTTATTCGCCCATGA 3' Tm 60.07) were used to genotype the line of Salk\_137467C.

### 3.6.3 Cloning and Protoplast transformation

The rlp32 gene sequences were cloned from the genomic DNA with PCR. The four sequences were amplified as following.

description	primer L	primer R
sequence containing the ATG and stop codon	P153ATG	P153stop
sequence containing the promoter region and no stop codon	P153promoter	P153non-stop
sequence containing the promoter region and stop codon	P153promoter	P153stop
sequence containing the ATG and no stop codon	P153ATG	P153non-stop

P153ATG: 5'ATG AAA GAC TCT TGG AAC TCA ACG AG 3'

P153 promoter: 5' CGG AAT TGA AGA CGT TCG TT 3'

P153 stop: 5' TTA TTG CTT TCT CCT CAA TCT TTT TTC ATG TGC 3'

P153 non-stop: 5' TTG CTT TCT CCT CAA TCT TTT TTC ATG TGC 3'

The PCR products were cloned into entry vector by using pCR<sup>®</sup>8/GW/TOPO<sup>®</sup> TA Cloning<sup>®</sup> Kit (Invitrogen). LR reaction was performed by following the protocol of Gateway<sup>®</sup> LR Clonase<sup>™</sup> II Enzyme Mix. Doner vectors were digested by restriction enzyme Apal. The linear DNA was used to increase the efficiency of LR reaction. A series of pGWB vectors (Nakagawa et al.) and pB7FWG2 vector (Karimi et al., 2002; 2007) were used as destination vectors. The constructed vectors were transformed into GV3101 agrobacterium under the resistant control of rifampicin, gentamycin and antibiotics characterized by destination vector. pGWB vectors are resistant to kanamycin whereas pB7FWG2 contains spectinomycin selection marker. Electroporation was used to generate high efficient *A. tumefaciens* transformation.

Protoplast transformation was conducted in insensitive ecotype ICE73. The preparation of protoplast from Arabidopsis leaves was following the description by Yoo (Yoo et al., 2007). ICE73 were planted in growth benches under standard short-day conditions, and without any bio- or non-bio stresses. After 5 weeks, the well-expanded leaves were selected and were sliced into ~0.5mm in size. The leave pieces were transferred into enzyme solution, followed by vacuum infiltration and digestion in dark for 3 hours. The protoplasts were released and filtered through nylon mesh into 12ml cell culture tubes on ice. After a few times of re-suspension and washing, the concentration of protoplast was determined by haemocytometer under microscope. The working concentration was set to  $2 \times 10^5$  pp/ml for transformation. The protoplasts were added into plasmid DNAs from the construct of RLP32-pGWB and the construct

of FRK1 promoter-driven luciferase. The co-transformation is mediated by 1.1 x pp volume of PEG solution (40% w/v PEG4000, 0.2 M mannitol, 100 mM NaCl, 100 mM CaCl<sub>2</sub>) and incubated at RT for 10 min. The transformation was terminated by 4 x pp volume of W5 (2 mM MES with pH 5.7, 154 mM NaCl, 125 mM CaCl<sub>2</sub>, 5 mM KCl). W5 was displaced by 1 x pp volume of WI (4 mM MES with pH 5.7, 0.5 M mannitol and 20 mM KCl) after centrifuge. Transformed protoplasts were kept in dark at RT for overnight before examining luciferase assay. 100µL protoplasts were transferred into a 96-well microtiter plate for luminescence measurement (Mithras LB 940, Berthold technologies). 200µM luciferin was added into protoplasts. The entire mixture was treated with H<sub>2</sub>O, 0.25µM flg22 and normalized RsE2, respectively and kept in dark. The luciferase activity was measured every hour during 8 hours treatments.

#### 3.6.4 Transient expression in *N. benthamiana*

*A. tumefaciens* with expression construct and with P19 construct (kanamycin resistant) were grown separately in 5ml LB with antibiotics for 1 or 2 days at 28°C. The two tubes of medium were centrifuged 5min at 4500 rpm at room temperature to collect the *A. tumefaciens* pellets. The two pellets were re-suspended in 10mM MgCl<sub>2</sub> with O.D<sub>600nm</sub> value equal to 1. Both cell suspension solutions were treated with 150µM acetosyringone for 2-3 hours at RT. Meanwhile the *N. benthamiana* plants were irrigated to promote stomata opening. 1ml cell suspension containing expression construct and 1ml P19 cell suspension (or 2ml P19 cell suspension as control) were mixed with 4ml 10mM MgCl<sub>2</sub>. Smooth leaves were infiltrated with mixture of suspension. After 1 or 2 days infiltration, RsE2- or PEN- induced ethylene responses were measured using infiltrated leaves. Transient expression of RLP32-GFP fusion gene was checked for fluoresces by microscopy.

#### 3.6.5 Arabidopsis transformation and selection

Four ecotypes: ICE21, Dog-4, ICE73 and ICE153 were selected to over-express the RLP32 (alleles from Col-0 or ICE153) driven by 35S promoter or native promoter from ICE153. The transformation was conducted using dipping protocol. 5ml LB culture with *Agrobacterium* GV3101 containing the destination construct was shaken over night at 28°C. The entire cell culture was transferred

into 500ml LB medium and shaken again over night at 28°C. The cell culture was spin down at 5000 rpm for 10 minutes. The pellet was re-suspended in dipping solution (25g sucrose, 250µl Tween 20 in 500ml H<sub>2</sub>O) with O.D<sub>600nm</sub> value about 0.8. The suspension was treated with 0.02% Silwet-77 before dipping. After dipping, the pots containing the flowering Arabidopsis plants were kept in humid condition over night.

## 4. Results

### 4.1 Natural variation within *Arabidopsis* ecotypes for RsE2 sensitivity

#### 4.1.1 Use of a double mutant system to identify the RsE2 receptor

The flagellin and elongation factor Tu (EF-Tu) are PAMPs that are found in virtually all bacteria. The flagellin is the major structural protein and is responsible for shape and motility of the flagellum of bacteria. An active peptide, flg22, was first identified from a highly conserved N-terminal domain of flagellin to elicit the early immunity response in *Arabidopsis* through the FLS2 receptor (Bauer et al., 2001; Gómez-Gómez et al., 1999). A wide range of eubacteria from proteobacteria to firmicutes contains the active flagellin, although inactive peptides were also found in some proteobacteria such as *A. tumefaciens* and *Rhizobium meliloti* (Felix et al., 1999). Strikingly, a recent study showed that an active flg22 was contained in uncultivable intracellular bacterium, *Candidatus Liberibacter solanacearum* (Lso), a pathogen responsible for zebra chip disease in potato (Hao et al., 2014). EF-Tu is another abundant protein in bacteria and has been shown to serve as PAMP. Both flagellin and EF-Tu elicit the same set of gene transcription and similar defense responses.

To avoid re-purification of flagellin and EF-Tu from *Ralstonia solanacearum*, we have used *Arabidopsis* double mutants fls2/efr, which are insensitive to both PAMPs. Early work showed that the leaf pieces from fls2/efr double mutants could be elicited to produce ethylene by crude extracts of *Ralstonia solanacearum* (Melzer, 2013). This suggested that the crude extract contains additional elicitors other than flagellin and EF-Tu. We named the putative elicitor the *Ralstonia solanacearum* Elicitor (RsE).



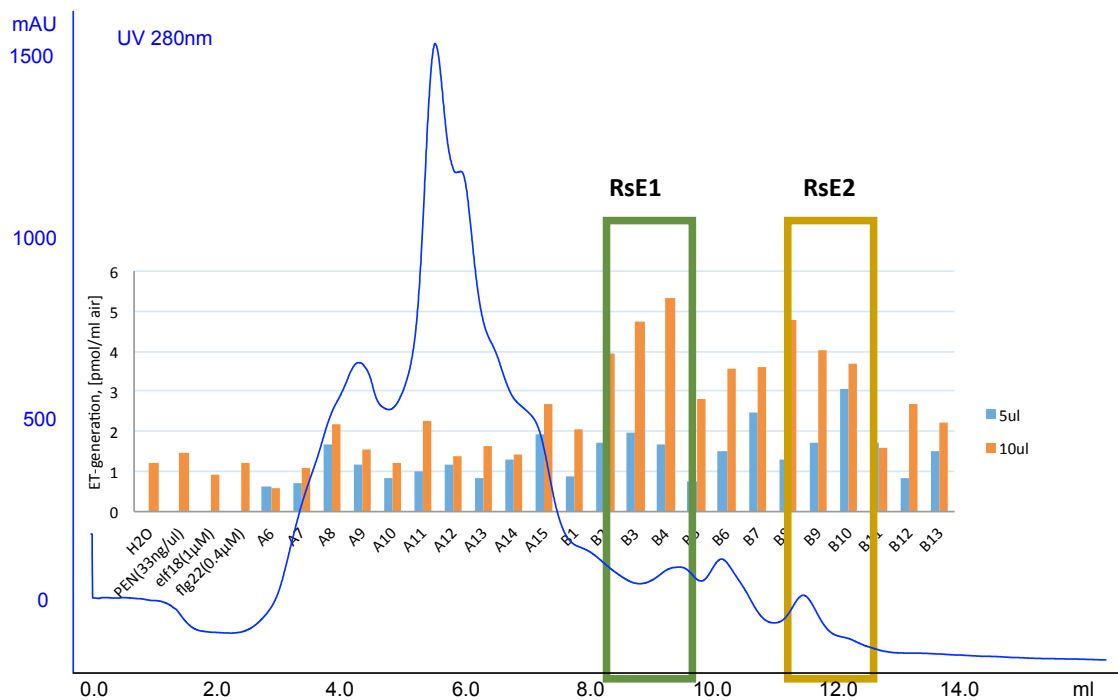


Figure 4. 1 Two active PAMP fractions were identified from *Ralstonia solanacearum*

Blue curve represents elution profile from Source cation exchange column (absorption at 280nm). Ethylene responses elicited by fractions from A6 to B13 with 5 $\mu$ l and 10 $\mu$ l respectively were measured in fls2/efr Arabidopsis plants. The fractions from B2 to B4 were pooled into elicitor RsE1 (green box); the fractions from B8 to B10 were pooled into elicitor RsE2 (yellow box).

In order to isolate and identify RsE, a series of chromatography-based fraction screening methods was established (Melzer, 2013). This purification started with cultivation of *Ralstonia solanacearum* in Kelmans Medium for two days. The cell culture (~5L) was first heated to boiling then cooled down in ice bath. The most of un-dissolved substances were removed by centrifuging and the supernatants were added into ammoniumsulfate reaching up to 90% saturation to precipitate proteins. Those proteins are called crude extract, which could elicit early immunity responses in fls2/efr double mutants. This crude extract was further purified by cation exchange chromatography (HiTrapTMSP FF, GE Healthcare), anion exchange chromatography (HiTrapTMQ FF, GE Healthcare) and cation source column (Source 15S 4.6/100 PE, GE Healthcare). After each chromatography, the ethylene elicitable fractions were pooled together and went through the next chromatography. At last, two active fractions were isolated from *Ralstonia solanacearum*, the fraction that appeared first and

elicited the ethylene response is named RsE1 (Figure 4.1) and the second fraction eliciting the ethylene production is named RsE2.

Characterization of RsE1 and RsE2 verified that both of them could elicit the early immunity response such as ethylene, callose apposition, extracellular alkalization, MAPK activation, oxidative burst and defense gene transcription (Melzer, 2013). Their activities are sensitive to endo-proteinases GluC and AspN. Furthermore, proteinase K could abolish their activities at all. As RsEs triggered early immunity in mutants, we were certain that we had found novel proteinaceous PAMPs. PAMP activities again suggested that we identified one or two novel PAMPs that are different from flagellin and EF-Tu.

#### 4.1.2 RsE1 and RsE2 induced ethylene responses among ecotypes

The next question after isolation of RsE1 and RsE2 is how plants sense them? The search for the RsE1- and RsE2-insensitive plants is the key to figure out the genetic features underlying mechanism. Previous studies have used such natural plant immunity deficiencies to clone plant immunity genes. *Ws-0* is an ecotype of *Arabidopsis*, which was found insensitive to flagellin due to an early stop codon in kinase domain, which belongs to a RLK encoded by the *fls2* allele (Bauer et al., 2001; Zipfel, 2006). Another ecotype *Sha* failed to recognize eMAX, a MAMP derived from xanthomonads due to a deletion in receptor gene *Rlp1* (Jehle et al., 2013). Three ecotypes, *Bak-2*, *ICE111* and *Lerik1-3*, out of 56 ecotypes screened were insensitive to MAMP SCFE1 in my study, which suggested that a ratio of 1/20 could be reached to acquire the mutants in natural ecotypes screening.

To find RsE1 and RsE2 perception-deficient plants, we have used ethylene assay, a quantitative, easy to handle, highly repetitive immunity marker assay (Zhang, 2013; Melzer, 2013), to screen the ethylene production for over a hundred ecotypes of *Arabidopsis* upon treatment with RsE1 or RsE2. Leaves from each ecotype were cut into small pieces and incubated in distilled water overnight before they were treated with RsE1 or RsE2. The induced ethylene responses could be measured by gas chromatography (Shimadzu GC-14A combined with C-R4A chromatopac integrator). The *fls2/efr* double mutant and *Col-0* were included in each assay from day to day to serve as controls. The

---

second elicitor, Pen, flg22, elf18 or SCFE1 (Zhang et al., 2013) was also included as control to indicate the responsiveness of leaves in general.

A collection of 102 ecotypes, which represent highly geographic and ecological diversities, was assessed for ethylene responses upon RsE1 and RsE2 treatment. Among the 102 ecotypes, 32 ecotypes are from the lab's collection; the other 70 ecotypes are from the MPI 80 genomes project (Cao et al., 2011). All ecotypes displayed substantial variation for both elicitors RsE1 and RsE2. We identified five ecotypes, Wt-5, ICE33, Dog-4, ICE21 and ICE73, which showed weak ethylene responses induced by RsE1 (Figure 4.2); while two ecotypes Leo-1 and Bak-2 consistently displayed the strong capability of ethylene induction by RsE1. Similarly, RsE2 elicited weak ethylene responses in ecotype Mr-0, Yeg-1, Dog-4, ICE21 and ICE73 (Figure 4.3); and strong ethylene responses in ecotype ICE153 and Istisu-1. Three ecotypes Dog-4, ICE21 and ICE73 shared the similar weak phenotype triggered by RsE1 and RsE2, and four additional ecotypes Wt-5, ICE33, Mr-0 and Yeg-1 displayed specifically insensitivity to RsE1 or RsE2.

Large variation of the RsE1 and RsE2 elicited ethylene responses among ecotypes suggested that extensive genetic variation related to elicitor perceptions exists in nature. As RsE1 and RsE2 shared the similar profiles of ethylene assay among ecotype collection, we were aware of the possibility that RsE1 and RsE2 might contain the same active elicitors.

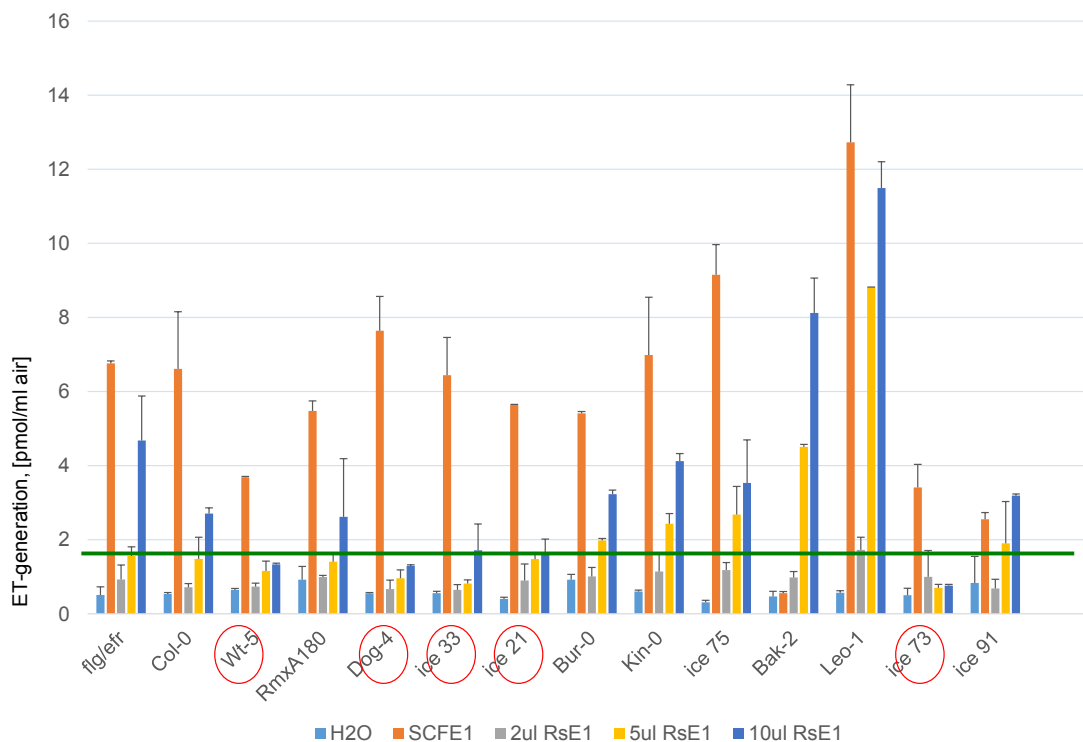


Figure 4. 2 RsE1 sensitivity screening among ecotypes

The ethylene responses elicited by RsE1 were measured among ecotypes. The five insensitive ecotypes are Wt-5, Dog-4, ICE33, ICE21 and ICE73; the highly sensitive ecotypes are Bak-2 and Leo-1. The error bars indicate standard deviations of two individual plants.

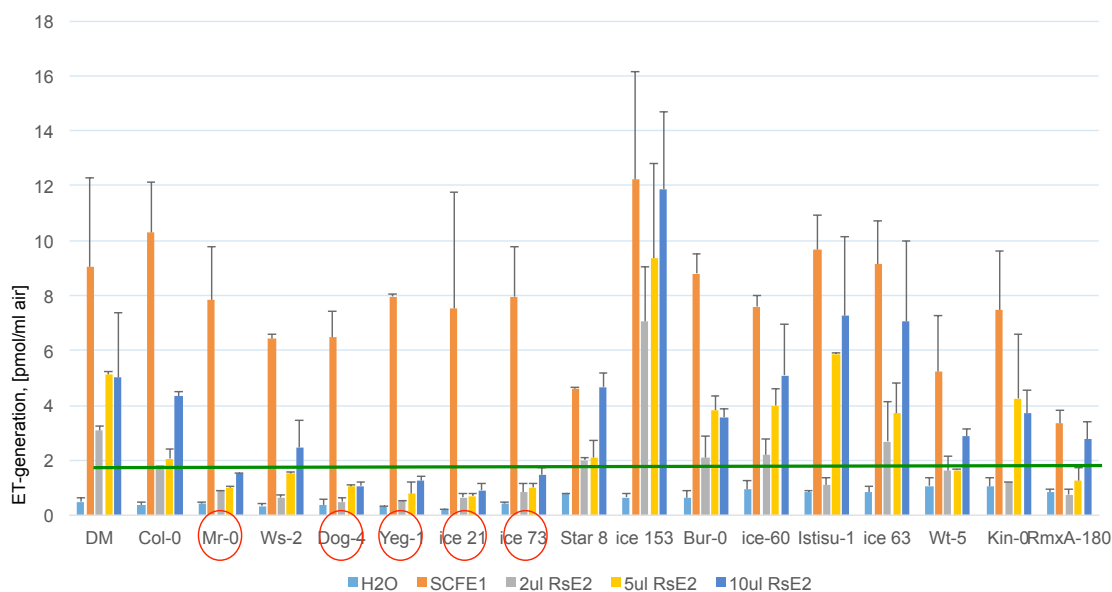


Figure 4. 3 RsE2 sensitivity screening among ecotypes

The ethylene responses elicited by RsE2 were measured among ecotypes. The five insensitive ecotypes are Mr-0, Dog-4, Yeg-1, ICE21 and ICE73; the highly sensitive ecotypes are ICE153 and Instisu-1. The error bars indicate standard deviations of two individual plants.

#### 4.1.3 Callose deposition variation elicited by RsE1 and RsE2

As typical PAMPs, RsE1 and RsE2 could trigger immunity-associated responses, such as ethylene, ROS, callose apposition and MAPK activation in *fls2/efr* double mutants (Melzer, 2013). Since we screened ethylene responses to acquire some insensitive ecotypes, we were also interested in their performances in other immunity assays triggered by RsE1 or RsE2, for example, in callose deposition.

Here, we compared this early response triggered by elicitors RsE1 and RsE2 between five insensitive ecotypes and two sensitive ecotypes. Both insensitive ecotypes and sensitive ecotypes were infiltrated with RsE1, RsE2 or buffer control in three replicates. Four RsE1-insensitive ecotypes displayed no significantly enhanced callose deposition when compared to buffer controls. Only one exception, ICE73, displayed a highly induced callose deposition. One of RsE1 sensitive ecotype (Leo-1) showed strongly induced callose. On the contrary, Bak-2 could not induce callose better than the buffer control (Figure 4.4). Parallel to RsE1, three RsE2-insensitive ecotypes displayed the non-enhanced callose deposition as well; the callose deposition was not obvious compared to buffer infiltration. However, two RsE2-insensitive ecotypes Mr-0 and ICE73 showed induced callose deposition compared to buffer control. Two RsE2 sensitive ecotypes ICE153 and Institu-1 made enhanced callose deposition compared to buffer control (Figure 4.5).

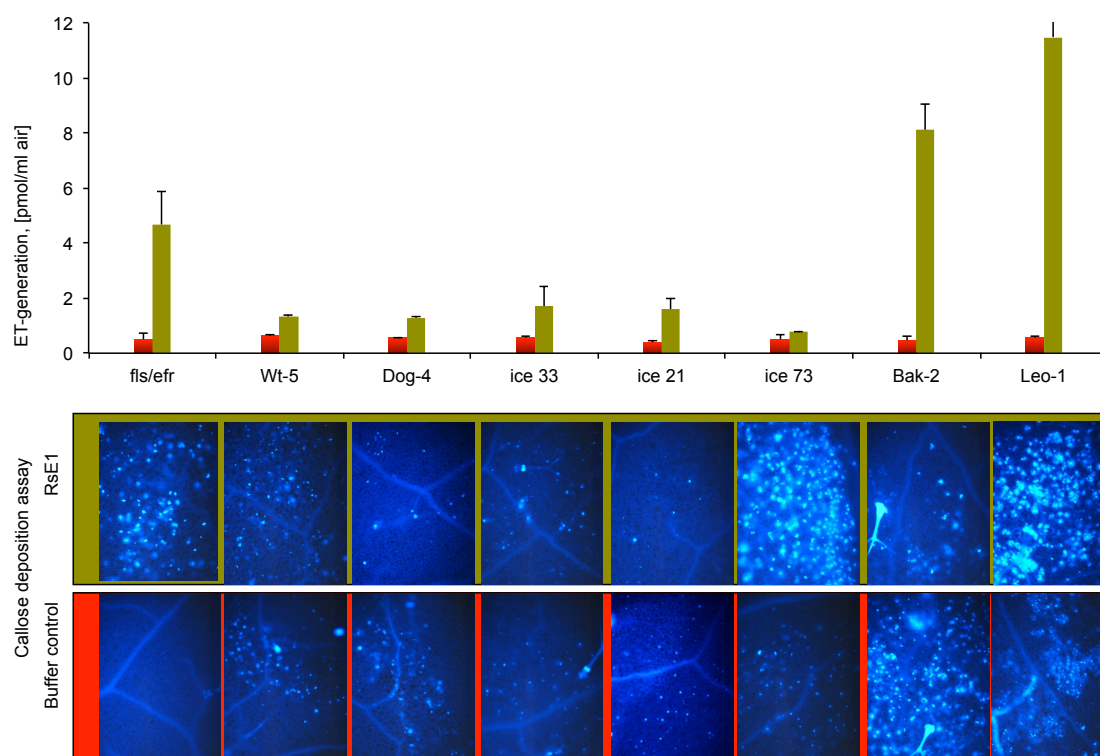


Figure 4. 4 RsE1-induced callose deposition among five insensitive ecotypes

Upper panel: five ecotypes (Wt-5, Dog-4, ICE33, ICE21 and ICE73) produce lower amounts of ethylene than the fls2/efr double mutants, although two ecotypes (Bak-2 and Leo-1) produce higher amounts of ethylene upon RsE1 (green) than the fls2/efr double mutants. The buffer controls were labeled as red. The error bars indicate standard deviations of two individual plants. Lower panel: All above ecotypes and fls2/efr double mutants were examined for callose depositions after 8 hours infiltration of RsE1 and buffer control. The images represent the average callose depositions of three individual plants treated with RsE1 (green background) and of three individual plants treated with buffer (red background).

Therefore, RsE1 and RsE2 could elicit the callose deposition in Arabidopsis and the responses were variable among ecotypes. Furthermore, in most ecotypes with extreme phenotype in ethylene assay also displayed the similar capability of callose deposition, however two ecotypes, Mr-0 and ICE73, which could produce weak ethylene response but strong callose response. Therefore, the phenotypes elicited by RsE1 and RsE2 may not be absolutely consistent with ethylene response. The recent studies suggested that callose deposition in response to flg22 requires callose synthase Arabidopsis Powdery Mildew Resistant 4 (PMR4) and this process also depends on RbohD (Nishimura et al., 2003; Vogel et al., 2000; Luna et al., 2010; Malinovsky, 2014). Although we are not sure how similar between RsE2- and flg22-elicited callose depositions, one

concept should be the same: additional callose synthases and corresponding signaling proteins are involved. Thus, the variation of callose deposition in ecotypes reflected not only the genetic variation of receptor for RsE2 but also the genetic variation of callose deposition required enzymes. On the other hand, RsE1 and RsE2 are half purified complexes whereas both contain the same active elicitor, which means that they could have some unknown substances causing slightly different immunity responses in plants.

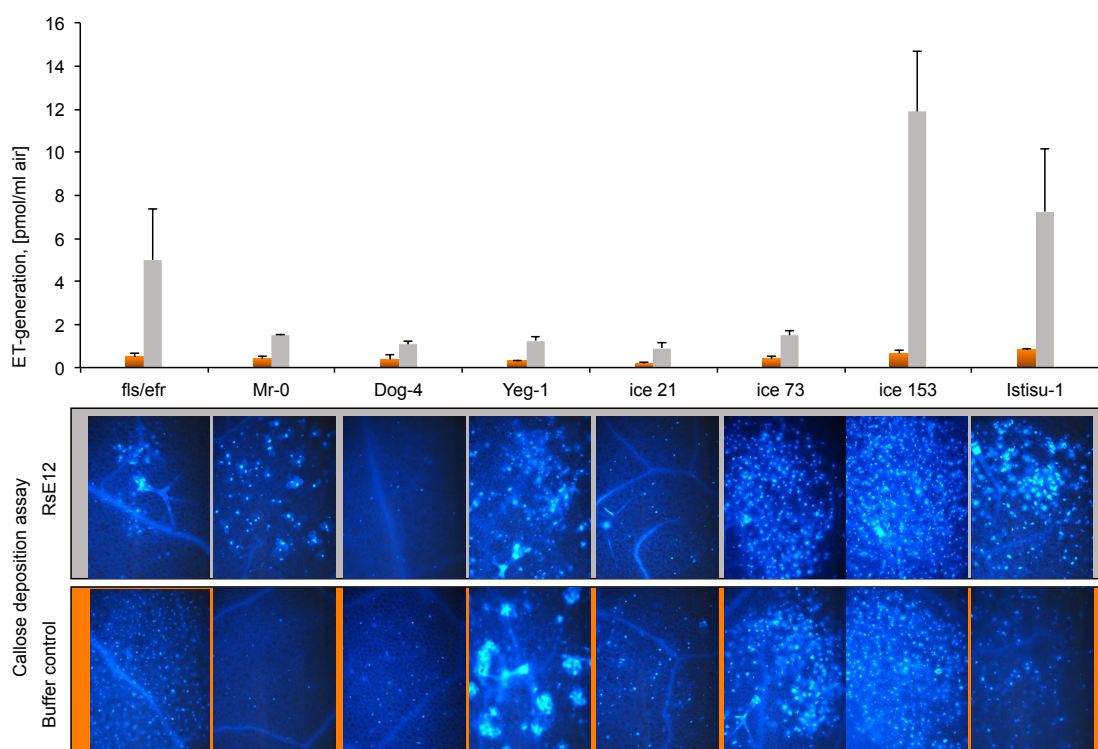


Figure 4. 5 RsE2-induced callose deposition among five insensitive ecotypes

Upper panel: five ecotypes (Mr-0, Dog-4, Yeg-1, ICE21 and ICE73) produce lower amounts of ethylene than the fls2/efr double mutants, although two ecotypes (ICE153 and Istisu-1) produce higher amounts of ethylene upon RsE2 (grey) than the fls2/efr double mutants. The buffer controls were labeled as orange. The error bars indicate standard deviations of two individual plants. Lower panel: All above ecotypes and fls2/efr double mutants were examined for callose depositions after 8 hours infiltration of RsE2 and buffer control. The images represent the average callose depositions of three individual plants treated with RsE2 (grey background) and of three individual plants treated with buffer (orange background).

#### 4.1.4 Geographic distribution of sensitive and insensitive ecotypes of RsE1 and RsE2

RsE1 and RsE2 are PAMPs from *Ralstonia solanacearum*, which is a pathogen predominating in tropical, subtropical, and some warm temperate regions bounded by 45N and 45S latitudes where rainfall averages above 100 cm/year (39 inch/year). Although understanding of why *Ralstonia solanacearum* is dependent on the climate remains to be elucidated, there are a few common environmental conditions, such as the average growing season exceeds 6 months, the average winter temperatures are not below 10°C (50°F), the average summer temperatures are not below 21°C (70°F) and the average yearly temperature does not exceed 23°C (72°F) (<http://extension.psu.edu/pests/plant-diseases/all-fact-sheets/ralstonia>) reported to favor the epidemic of this pathogen in many crops.

Five RsE1/RsE2-insensitive ecotypes from a collection of 102 ecotypes implied that the distribution of RsE1/RsE2-insensitive alleles in nature might be affected by environmental factors.

To investigate this hypothesis, we checked the geographic distribution of those ecotypes. We plotted the geographic location of extreme insensitive and extreme sensitive ecotypes of RsE1 and RsE2 in Google Earth (Figure 4.6). Insensitive ecotypes are scattered quite widely and unexceptionally they are accompanied by some extreme sensitive ecotypes. There appear to be no obvious geographical preferences for insensitive ecotypes.



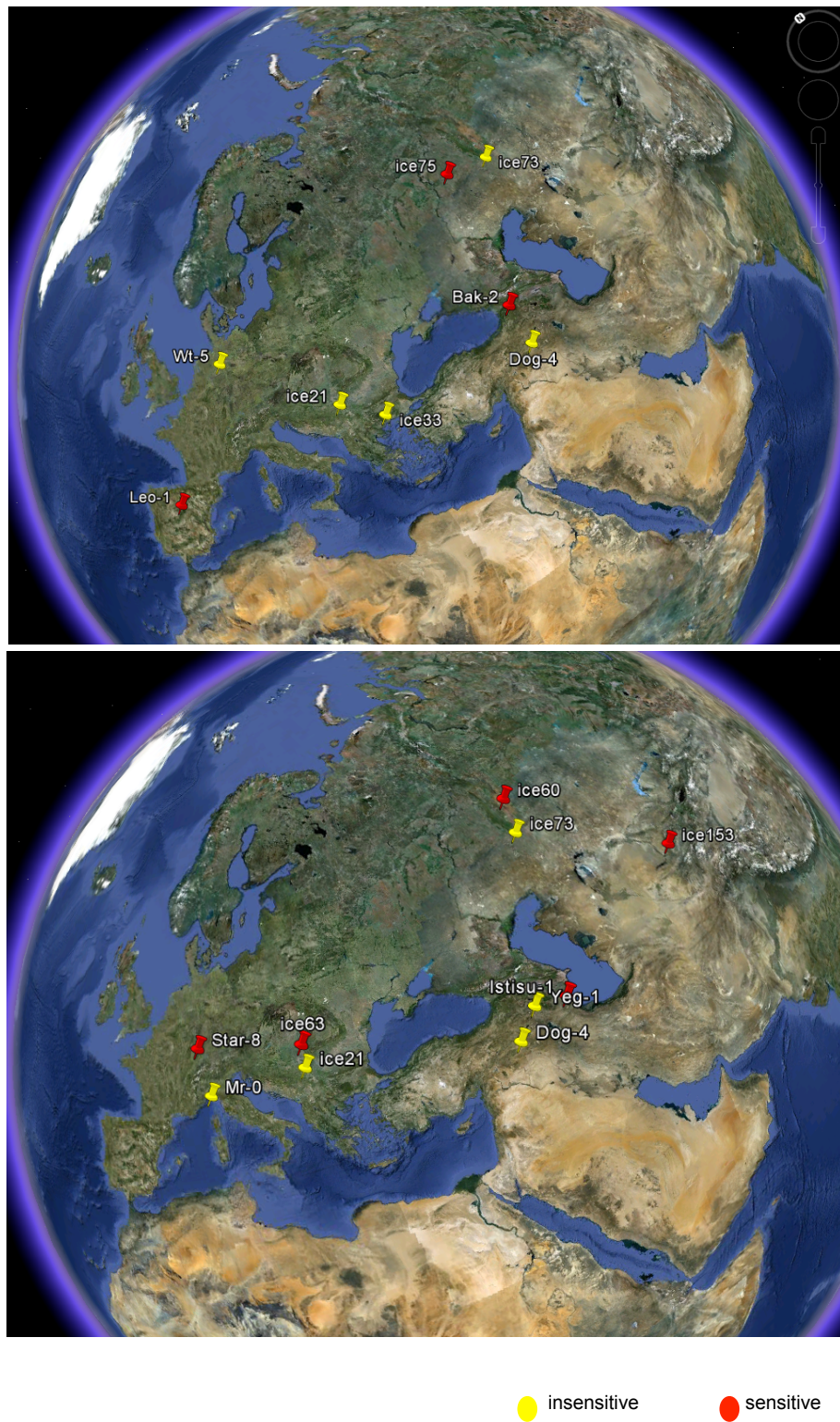


Figure 4. 6 Distribution of ecotypes that are ethylene response insensitive to RsE1 (upper) and RsE2 (lower)

Insensitive ecotypes (yellow) and sensitive ecotypes (red) were geographically labeled on Google earth.

#### 4.1.5 Diversification of sensitive and insensitive ecotypes is illustrated in the phylogenetic tree

Using ecotypes with extreme phenotype alone is not enough to infer the environmental effects. However, the sequence divergence of sensitive and insensitive ecotypes can be illustrated better using larger size ecotype collections.

80 ecotype genomes were selected to study the trends of sequence divergence of sensitive and insensitive ecotypes. The highly RsE1-sensitive ecotypes or RsE2-sensitive ecotypes were marked as red color and insensitive ecotypes to RsE1 or RsE2 were labeled as yellow color (Figure 4.7). The insensitive ecotypes appear mainly in the region of Caucasus and Eastern Europe and Russia and none of them are found in the area of south Italy, Spain or N. Africa. Since the *Ralstonia solanacearum* favor the warm region, which are close to equator, our study suggested that in the region, which has unfavorable environment for *Ralstonia solanacearum*, some ecotypes could survive healthy even without the recognition capability of pathogen of *Ralstonia solanacearum*. Considering the recent re-colonization of Arabidopsis species after the last glacial maxima the relatively limited distribution of insensitive ecotypes also suggested that this divergence of sensitive and insensitive ecotypes happened rather recently.

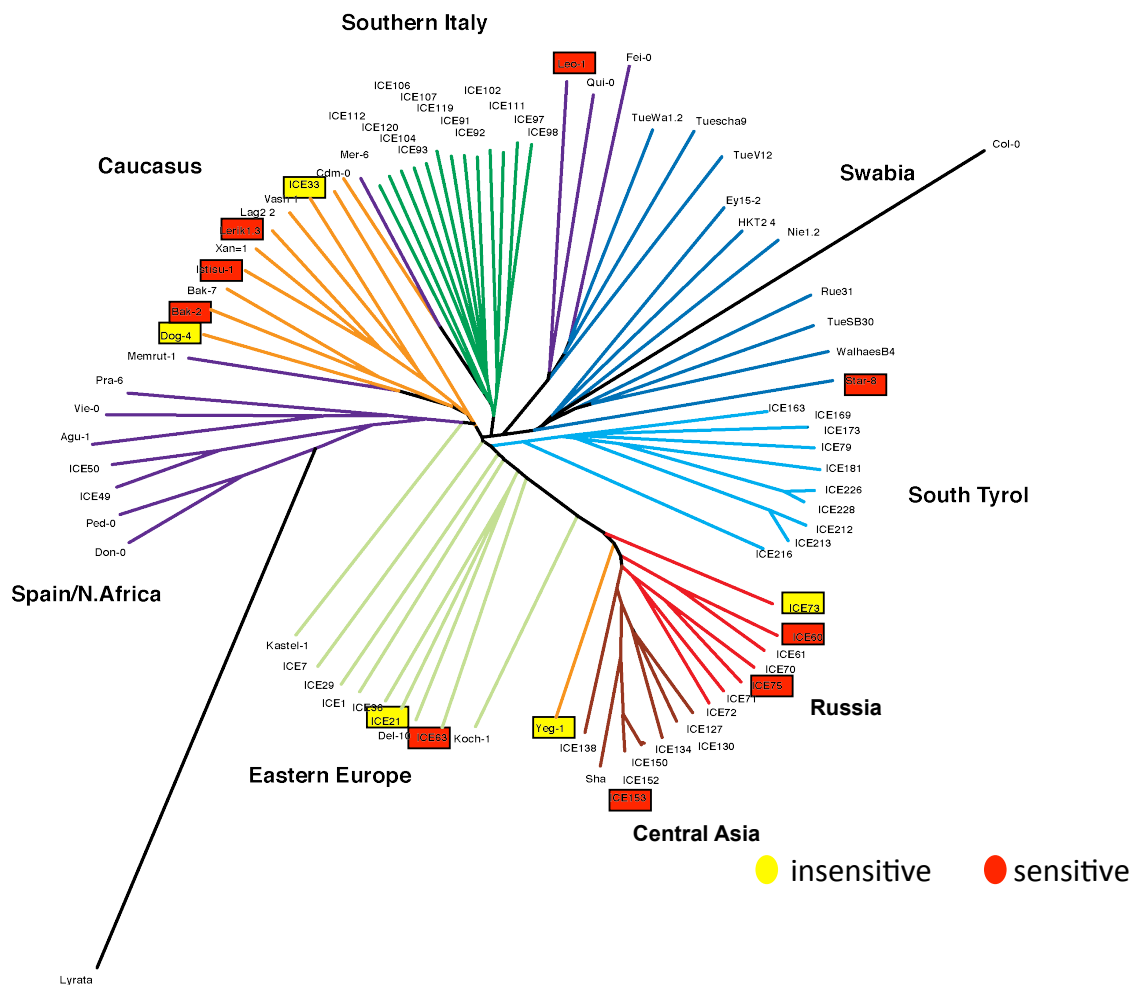


Figure 4. 7 Diversification of sensitivity to RsE1/RsE2 did not happen during the re-colonization of the species after the last glaciation

80 ecotype genomes were used to generate the phylogenetic tree. RsE1/RsE2-insensitive ecotypes were labeled as yellow; RsE1/RsE2 very sensitive ecotypes were labeled as red. The insensitive ecotypes appear mainly in the region of Caucasus and Eastern Europe and Russia; and none of them are found in the area of Southern Italy, Spain/N. Africa.

## 4.2 Single recessive gene controls RsE recognition

The natural variation of innate immunity is reflected in our study with the variable ethylene response elicited by RsE1 and RsE2 among different ecotypes. We screened over a hundred ecotypes and found that five ecotypes, ICE73, Wt-5, ICE33, ICE21 and Dog-4 were insensitive to RsE1; and five ecotypes, ICE73, ICE21, Dog-4, Yeg-1 and Mr-0 were insensitive to RsE2. We were interested to use this information to address questions such as: Does the phenotype variation infer to some extent of genetic association? And are the phenotypes that are elicited by RsE1/RsE2 heritable?

We recruited genetics approaches to dissect the underlying genetic behaviors. First of all, five insensitive ecotypes were crossed reciprocally to each other as pollen donor and pollen receiver to obviate the maternal effect (Figure 4.8). The ethylene responses from three individual F1 plants from such crosses were averaged and compared to F1 from crosses between sensitive and insensitive ecotypes. All F1 from reciprocal crosses among five insensitive ecotypes to RsE1 were also insensitive to RsE1 comparing to the F1 from crosses between sensitive and insensitive ecotypes to RsE1; all F1 plants from crosses among five insensitive ecotypes to RsE2 are also insensitive to RsE2 comparing to the F1 from crosses between sensitive and insensitive ecotypes to RsE2 (Figure 4.9). Since the progeny showed the insensitive phenotype as well as both of insensitive parents and the insensitive phenotype was not complemented by crossing, all five insensitive ecotypes to RsE1 are allelic, so were the five insensitive ecotypes to RsE2. Ecotypes ICE73, ICE21 and Dog-4 showed insensitivity to both RsE1 and RsE2 and they were allelic to Wt-5 and ICE33 upon RsE1 treatment and allelic to Yeg-1 and Mr-0 upon RsE2 treatment. Our study suggested that RsE1 and RsE2 fractions contained the same elicitor. However, due to the impurity of fractions, RsE1 and RsE2 could perform slightly different.

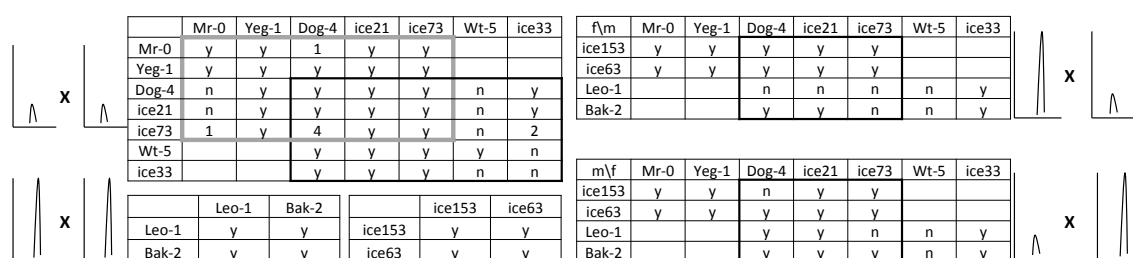


Figure 4. 8 The summary of allelism test

Upper left: reciprocal crosses between insensitive ecotypes;

Upper right: insensitive ecotypes as male cross to sensitive ecotypes;

Lower left: reciprocal crosses between sensitive ecotypes;

Lower right: sensitive ecotypes as male cross to insensitive ecotypes.

“y” means normal amount of seeds were generated; “n” means failed cross; “1”, “2” or “4” means the number of seeds harvested.

Following the allelism test, we examined the inheritance of very sensitive phenotype by crossing insensitive ecotypes to sensitive ecotypes; all progeny exhibited a complemented phenotype by showing an ethylene response.

Crosses between those sensitive ecotypes produced neither genetic heterosis effect nor genetic necrosis effect (Figure 4.10). They displayed the additive effect; the extent of ethylene responses shown by progenies fell into the range of two sensitive parents.

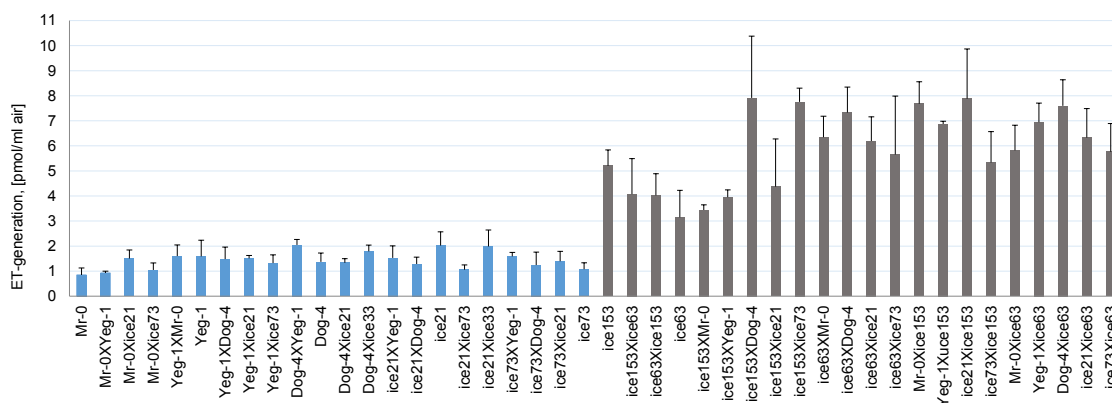


Figure 4. 9 RsE2 induced ethylene responses in reciprocal crosses of sensitive and insensitive ecotypes

Allelism tests were done by crossing insensitive ecotypes from each other. Progenies from all reciprocal crosses were insensitive to RsE2 (blue columns). Meanwhile, insensitive ecotypes were reciprocally crossed with sensitive ecotypes. All progenies from such crosses are sensitive to RsE2 (grey columns). The error bar indicates standard deviation of three replications.

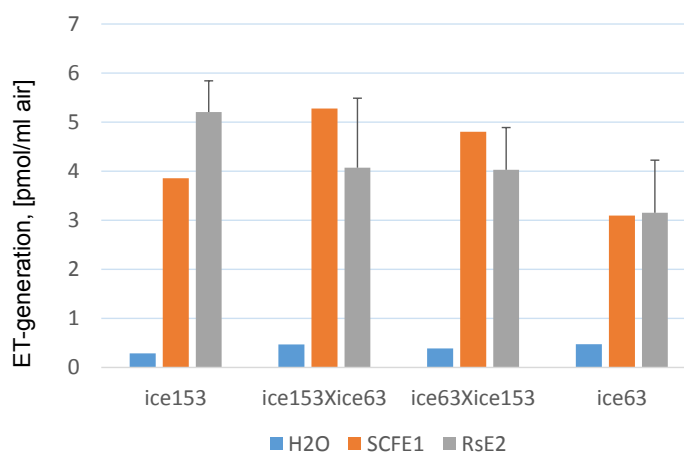


Figure 4. 10 Neither heterosis nor necrosis was detected upon RsE2 treatment

The progenies from crossing sensitive ecotypes ICE153 and ICE63 are neither more sensitive to both parents nor more insensitive to both parents, which suggest that no genetic heterosis or necrosis exists for RsE2 induced ethylene trait. The error bar indicates standard deviation of three replications.

Considering the allelism test described above and the fact that all F1 plants from the crosses between insensitive ecotypes and sensitive ecotypes showed complementary sensitive phenotype, we hypothesized that the insensitive

ethylene response phenotype is most likely to be controlled by a single recessive gene in Arabidopsis.

In order to confirm the inheritance of the phenotype triggered by RsE2, we developed F2 segregation populations by crossing insensitive ecotype ICE73 and sensitive ecotype ICE153. Based on ethylene response screening, ICE73 was the ecotype that consistently exhibited the lowest response in our study. The F1 generation from ICE153 X ICE73 crosses reached to high responses with significant distinction from ICE73 and ICE153 parents. We developed the F2 generation by self-crossing the F1 of ICE153 X ICE73 cross and expected segregated phenotype with a 1:3 ratio due to a single recessive gene. 400 F2 plants were screened for the ethylene response during four consecutive days (Figure 4.11). To confirm that the segregation of insensitive from sensitive happened in a random way instead of weird or skewed batch-dependent way, we plotted the histogram of ethylene response phenotype in four consecutive days. Comparing to the whole dataset of phenotype, the data from each day displays the similar segregation pattern. To further analyze the segregation of populations, 92 insensitive plants vs. 303 sensitive plants with the cut-off value 1.6 for ethylene response represents a statistics Chi-square test value 0.615, which is far smaller than 3.84 and strongly supported that the F2 population from ICE153 X ICE73 cross is segregated as a Mendelian single recessive trait.

Our genetic analysis verified that insensitive phenotype elicited by RsE1/RsE2 is heritable in Arabidopsis; moreover, a single recessive gene is most likely responsible for it. Allelism test also suggested RsE1 and RsE2 contain the same active elicitor in the two fractions since the three insensitive ecotypes to both RsE1 and RsE2 are allelic to the other two RsE1 insensitive ecotypes and two distinct RsE2 insensitive ecotypes respectively. The impurity of RsE1 and RsE2 could partly explain the slight difference of ethylene response triggered by RsE1 and RsE2.

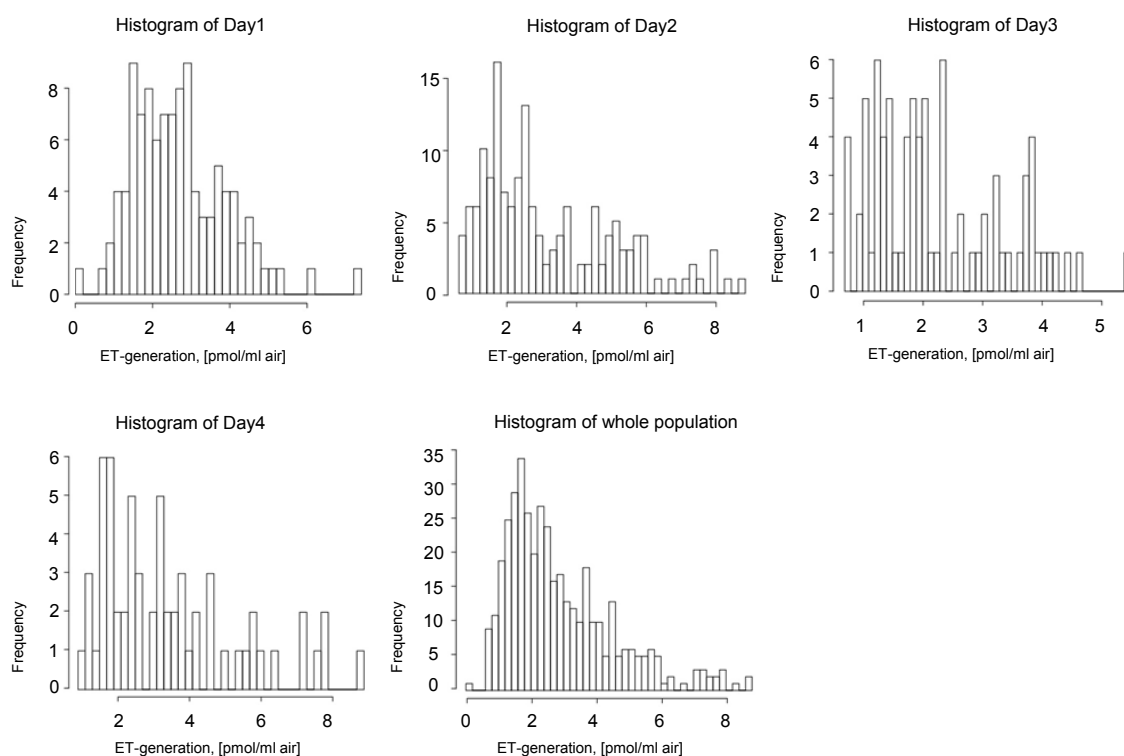


Figure 4. 11 Phenotype histogram of F2 population from ICE153XICE73

Four hundreds F2 individuals were screened for RsE2 sensitivities on four consecutive days. Phenotype histogram from each day shows no deviation from the whole population.

### 4.3 GWAS mapping

*Arabidopsis thaliana* contains a large amount of genetic diversity that can be explored in plant pathogen response studies (Gómez Gómez et al., 1999; Zipfel et al., 2004; Vetter et al., 2012; Jehle et al., 2013; Zhang et al., 2013). After LGM (last glacial maximum), *Arabidopsis thaliana* has re-colonized across the Eurasian continent, which covers various climate conditions. Each ecotype of *Arabidopsis thaliana* represents unique genetics adaptation to the local geological and ecological conditions in the past ten thousand years. As a consequence, *Arabidopsis thaliana* species harbors a great deal of natural variation of response to different types of plant pathogens in ecotypes. Several pathogen response genes have been cloned using traditional bi-parental-mapping based cloning approach utilizing the existing genetic diversity in different ecotypes. With advance of sequencing technology, we now have access to a large collection of those ecotypes with their entire genomes sequenced. Genome wide association studies (GWAS) has been shown to be



a direct and efficient way to explore the natural variation in *Arabidopsis* ecotypes and to identify genetic features associated with the phenotypic variations.

We used a collection of recently published *Arabidopsis thaliana* populations to study their responses to elicitor RsE2. The collection contains 40 ecotypes from lab collection and 80 ecotypes from eight populations across Eurasia, which is a good representation of the diverse geological and ecological conditions of the continent. Seeds of the 120 ecotypes were germinated under standard greenhouse short day condition. Leaves of 4 week-old plants were used for scoring the elicitor-induced responses, for example, ethylene biosynthesis.

To corroborate the rationality of GWAS in the background of pathogen perception of plant, we generated an ethylene response data set elicited by SCFE1, which is a well-studied elicitor and can be recognized by RLP30 in *Arabidopsis* (Zhang et al., 2013) (Table 4.1). GWAS was carried out on the website easyGWAS (<https://easygwas.tuebingen.mpg.de>). There are about forty candidates with a Bonferroni threshold 0.05 (Figure 4.12). One of them was noticed to be At3g05160, whose site is proximate to our known receptor RLP30 (At3g05360).

To improve the power of the method, we expanded to a larger accession collection during RsE2-induced ethylene response screening. Table 4.2 shows the phenotype score results. GWAS was carried out on the website easyGWAS (<https://easygwas.tuebingen.mpg.de>). All phenotype scores were considered as continuous variation type and were log<sub>10</sub> transformed. The 80 genome sequences in TAIR9 annotation were selected as genotype input (Cao et al., 2011). EMMAX was chosen as GWAS algorithm. The threshold of 0.05 minor allele frequencies was used. SNP candidate with a Bonferroni threshold of 0.05 was selected (Figure 4.13; Table 4.3).

From this GWAS study, the candidate SNPs suggested four genomic regions are highly associated to RsE2 triggered ethylene response. One is on chromosome 2, two are on chromosome 3 and one is on chromosome 5.



Table 4. 1 SCFE1 induced ethylene response among ecotypes

accession	score	accession	score	accession	score
Bak-2	1	ICE 112	3	Bak-7	4
Gu-0	1	ICE 138	3	cdm-0	4
ICE 111	1	ICE 212	3	Del-10	4
Lerik1-3	1	ICE 216	3	ICE 106	4
Bur-0	2	ICE 50	3	ICE 120	4
Dog-4	2	ICE 60	3	ICE 127	4
Gy-0	2	ICE 97	3	ICE 153	4
ICE 228	2	ICE-1	3	ICE 163	4
ICE 33	2	ICE-49	3	ICE 173	4
Nemrut	2	ICE150	3	ICE 181	4
Pu2-23	2	ICE63	3	ICE 213	4
Reu-1	2	ICE71	3	ICE 226	4
RmxA180	2	ICE75	3	ICE 29	4
vod-1	2	Koch-1	3	ICE 61	4
Ws-2	2	Nie1-2	3	ICE 7	4
Wt-5	2	Ped-0	3	ICE-152	4
Agu-1	3	Pua-10	3	Kastel-1	4
Col-0	3	Sha	3	Leo-1	4
Ey1.5-2	3	Tsu-1	3	NFA-8	4
Fab-2	3	TüSB30-3	3	Rü3.1+31	4
Fei-0	3	Ty-0	3	Star-8	4
HKT2-4	3	Vash-1	3	Strand-1	4
ICE 102	3	Wal-HäsB-4	3	Xan-1	4
ICE 104	3	Ws-0	3	Yeq-1	4

Note: the original ethylene production was normalized into score value by using Col-0 (score value is 3) and insensitive ecotypes Bak-2, ICE111 and Lerik1-3 (score value is 1) as control.

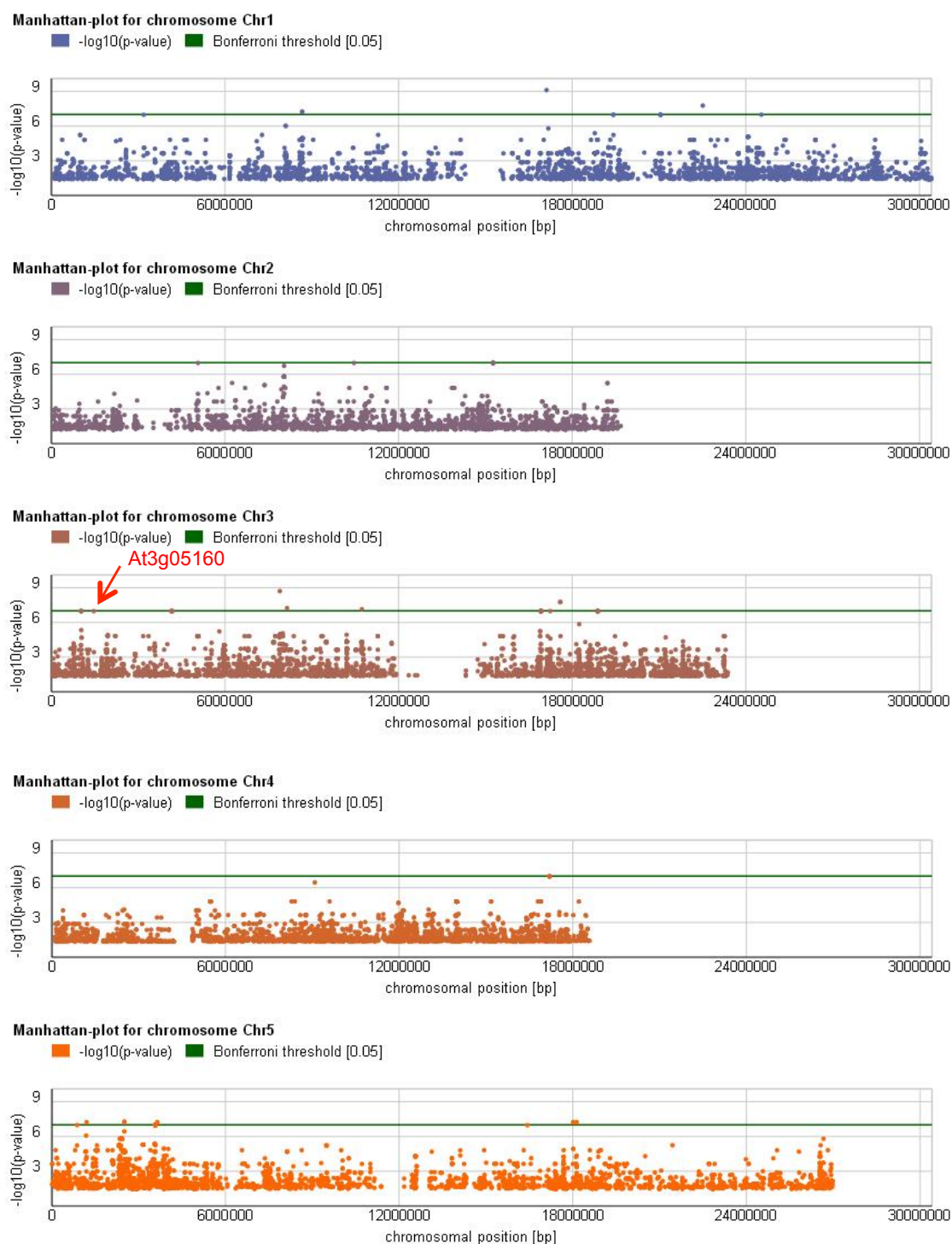


Figure 4. 12 Manhattan plot of the top 10% of all p-value upon SCFE1 treatment

The x-axis shows genomic coordinates, and the y-axis shows negative logarithm of the associated P-value for each SNPs. Horizontal green lines represent the thresholds for Bonferroni significance. About 40 SNPs above green lines indicate their significant association with SCFE1-triggered ethylene response. One of SNPs (indicated by red arrow) is within a 20kb vicinity of receptor RLP30 (At3g05360).

Table 4. 2 Phenotype score upon RsE2 treatment among ecotypes

accession	score	accession	score	accession	score
Agu-1	3	ICE 216	2	Nemrut	4
Bak-2	4	ICE 226	2	Nie1-2	2
Bak-7	3	ICE 228	2	Ped-0	2
Bur-0	3	ICE 29	3	Pra-6	3
cdm-0	3	ICE 33	1	PRS-10	3
Col-0	3	ICE 36	2	Pu2-23	2
Del-10	3	ICE 50	3	Qui-0	3
Dog-4	1	ICE 60	4	Ra-0	2
Edi-0	3	ICE 61	3	RmxA180	2
Ey1.5-2	3	ICE 7	3	Rü3.1+31	2
Fab-2	3	ICE 70	4	Sha	2
Fei-0	3	ICE 72	2	sorbo	3
Got-22	4	ICE 73	1	sq-8	2
Gy-0	3	ICE 79	3	Star-8	4
HKT2-4	3	ICE 91	4	Strand-1	4
ICE 102	3	ICE 93	4	Tn2-1	3
ICE 104	3	ICE 97	2	TüSB30-3	2
ICE 106	3	ICE 98	3	Tü-Scha-9	4
ICE 111	4	ICE-1	4	Tü-v-13	2
ICE 112	3	ICE150	3	Tü-wal-2	3
ICE 119	4	ICE-152	4	Ty-0	4
ICE 120	3	ICE-49	3	ull-2-3	2
ICE 127	4	ICE63	4	Vash-1	3
ICE 130	2	ICE71	4	Vie-0	3
ICE 134	3	ICE75	4	vod-1	2
ICE 138	3	Istisu-1	4	Wal-HäsB-4	4
ICE 153	4	Kastel-1	4	Ws-0	2
ICE 163	3	kin-0	3	Ws-2	2
ICE 169	3	Koch-1	4	Wt-5	1
ICE 173	2	KZ-9	3	Xan-1	3
ICE 181	3	Lag2-2	2	Yeg-1	1
ICE 21	1	Leo-1	4	zu-9	3
ICE 212	2	Lerik1-3	4		
ICE 213	3	Mr-0	1		

Note: the original ethylene production was normalized into score value by using Col-0 (score value is 3), insensitive ecotypes Dog-4, ICE21, Mr-0, Yeg-1, ICE73 (score value is 1) and sensitive ecotypes Istisu-1 and ICE153 (score value is 4) as control.

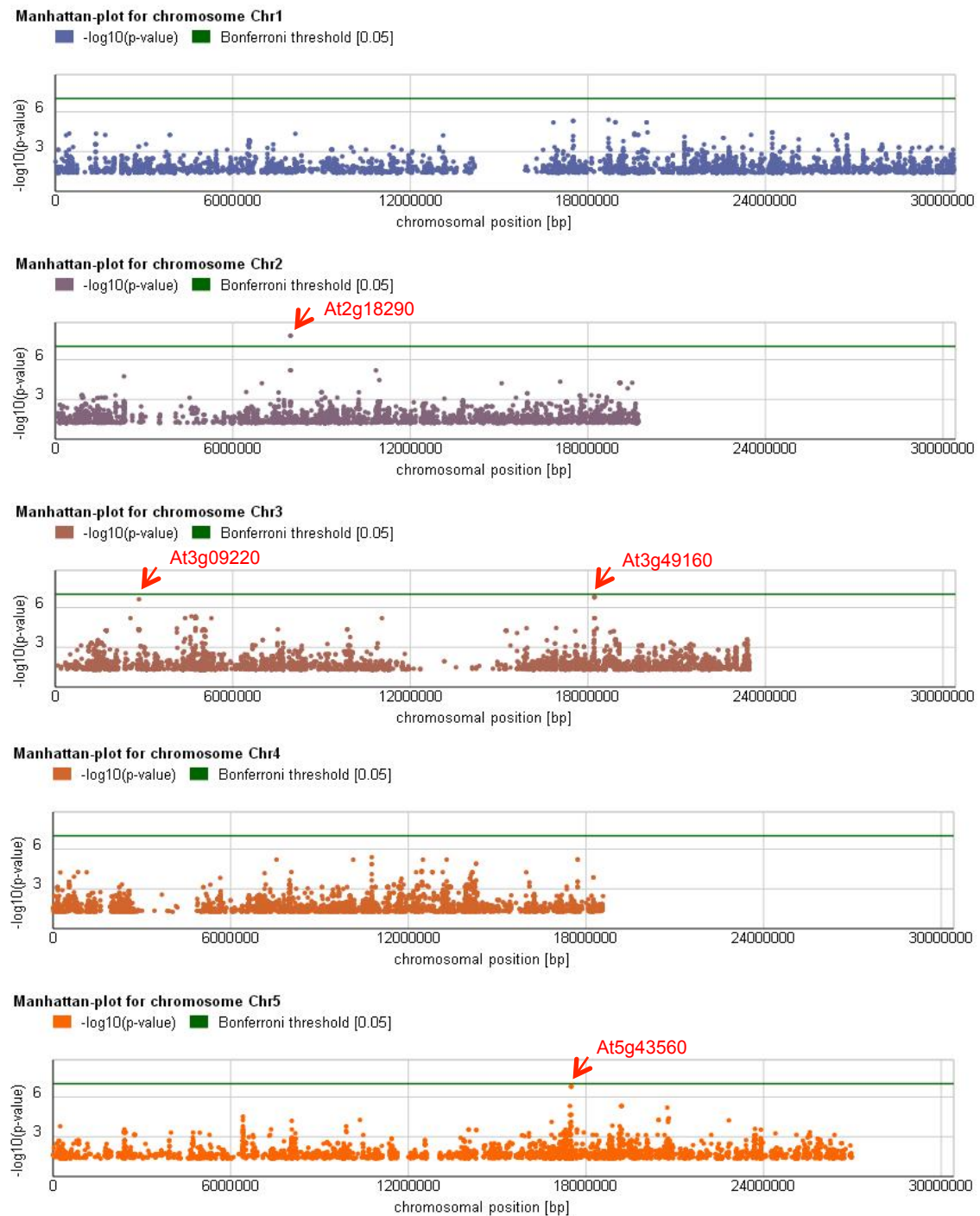


Figure 4. 13 Manhattan plot of the top 10% of all p-value upon RsE2 treatment

The x-axis shows genomic coordinates, and the y-axis shows negative logarithm of the associated P-value for each SNPs. Horizontal green lines represent the thresholds for Bonferroni significance. The four significantly associated SNPs were labeled with red arrows.

Table 4. 3 The candidate SNPs that passed the threshold

Chr	Position	Gene
Chr2	7949906	AT2G18290
	7949983	
Chr5	17502350	AT5G43560
	17502351	
	17505189	
Chr3	18223389	AT3G49160
	18223271	
	18222715	
Chr3	2828853	AT3G09220

#### 4.4 Genotyping by sequencing

Combining the knowledge that most of PRRs are derived from RLKs and RLPs, GWAS method is a convenient tool to quickly establish the potential genetic association with the elicitor-induced early immunity response by going through the RLKs and RLPs in candidate regions in the genome. However, given the quite low frequency of the insensitive ethylene response accessions (for example, one per twenty accessions upon RsE2 treatment) and a very limited integrated SNPs dataset in current web-based GWAS tool (for example, only 76 accessions among 100 phenotype-screened accessions were included in query dataset on EasyGWA), it is hard to precisely map the receptor.

We have showed a segregation ratio of 1:3 for ethylene responses among the F2 population, which was established by crossing insensitive ecotype ICE73 and sensitive ecotype ICE153 then by self-crossing. This F2 population provides a reliable source for genetic mapping. The next-generation-sequencing (NGS) technology associated mapping can efficiently salvage us from tedious bench work and provide us with low cost alternative approaches such as bulked segregate analysis and RAD-seq associated QTL analysis.

Genotyping by sequencing (GBS) is a fast developing approach, which can generate high density and high quality polymorphism data at relative low cost. This concept was first addressed as AFLP-based CROPS (Complexity

Reduction of Polymorphic Sequences) to detect about 1200 polymorphism markers successfully in maize genomes with highly repetitive DNA or low polymorphism between two lines of B73 and Mo17 (van Orsouw et al., 2007). RAD-seq has two advantages: determining marker density by selected restriction enzymes; and identifying candidate boundary by checking recombination breakpoints (Baird et al., 2008). This technology showed even flexible complexity-reduction capability (Poland et al., 2012; Stolle and Moritz, 2013), by including methylation-sensitive enzymes which enhances the chance of discovered markers locating in genic regions of the genome. Taking into account the three major advantages: high-resolution markers, visible recombination boundary and known bi-parents genome sequences, we decided to map the RsE2-insensitive allele by RAD-seq associated QTL.

Individual DNA samples from 384 F2 populations were isolated; followed by normalizing the quantities of DNA samples to be roughly equal. 192 DNA samples were selected and re-located into two 96-well format plates, which contained 84 samples from insensitive phenotypes ( $\leq 1.6$ ) and 108 samples from sensitive phenotypes ( $\geq 2.0$ ). We excluded those DNA samples from ambiguous phenotypes (1.7-2.0). 192 barcode adaptors were incorporated into individual DNA samples. The RAD library (Table 7.3) was single-end sequenced for 101bp on HiSeq2000 to acquire average coverage about 36.43 times (with maximum coverage 106.4 and minimum coverage 1.078), and to produce totally 16,973 potential markers. The coverage is higher than the estimation of 25.9 based on bi-parental genomic sequences double digested by PstI/MseI. Allowing 20% missing genotypes, 901 markers from 16,973 potential markers were selected to do QTL mapping.

At a LOD threshold 0.05, we detected only one major QTL peak which locates on the beginning of chromosome 3. Comparing to QTL trait model (ethylene response is continuous way), the binary trait model (ethylene response assigned to 1, insensitive and 0, sensitive) generates even stronger significant association with LOD value of 25 and lower background LOD value. A region from Chr3:20373 to Chr3:6582498 represented by LOD value above 10 is suggested to be highly associated with the RsE2 induced ethylene response

(Figure 4.14). One of the GWAS significant SNPs, Chr3:2828853 falls into this region (Table 4.4).

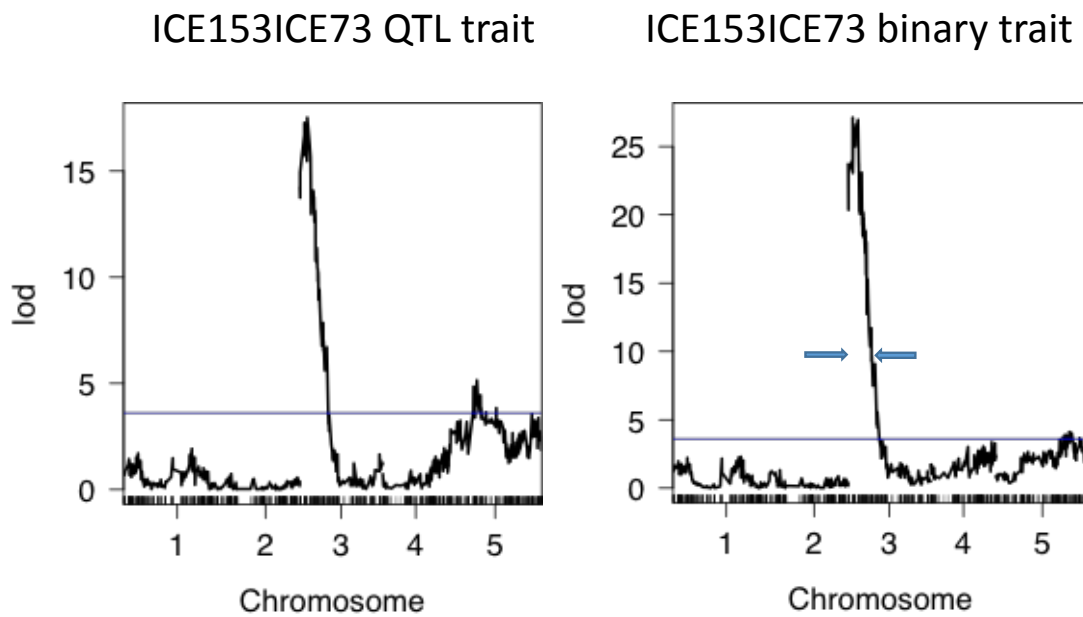


Figure 4. 14 rQTL mapping for RsE2-induced ethylene response in F2 mapping populations

LOD scores from full genome scan across five chromosomes of Arabidopsis using QTL trait and binary trait model for RsE2-elicited ethylene response score. Solid horizontal blue line represents that the genome-wise  $\alpha$  equals to 0.05 LOD thresholds, which defines significant QTLs based on 1,000 permutations. The blue arrow indicates a region with LOD value above 10.

Table 4. 4 The genomic position and LOD value from rQTL

Chr	position	LOD	Chr	position	LOD
2	18857542	0,3023032	3	3984300	19,2518605
2	18858222	0,65408905	3	4005543	20,3408255
2	18860115	0,63912253	3	4114238	18,4808285
2	19500124	0,36913299	3	4238450	18,4739649
2	19511097	0,16177605	3	4303467	20,1206988
2	19560723	0,35482815	3	4326887	19,2398194
3	20373	23,7161535	3	4415268	19,7751107
3	96618	20,3589304	3	4426951	18,3413229
3	97041	22,1412548	3	4458826	19,3354048
3	99998	22,2494445	3	4786003	17,1964815
3	100022	21,9456481	3	4786104	18,1941321
3	100053	23,1077577	3	4942846	18,8041414
3	1282003	24,0596519	3	5066042	15,7032338
3	1286337	27,1186078	3	5091471	15,594859
3	1286394	24,1720452	3	5168516	18,0124631
3	1321901	23,0619188	3	5225970	16,686886
3	1432648	26,1204765	3	5268500	12,7434904
3	1546715	26,6332744	3	5533254	15,2878901
3	1784868	25,4141172	3	5666710	13,7562499
3	1784883	25,4103308	3	5666736	13,7562499
3	1784886	25,4107724	3	5940140	11,5326217
3	2012983	25,010172	3	6169544	10,4838362
3	2063924	25,7413858	3	6169557	10,3794269
3	2097697	25,9038471	3	6208231	11,0247178
3	2795414	26,9539864	3	6582498	11,699298
3	3004962	23,5326429	3	6612203	9,29420715
3	3012844	23,7849338	3	6612208	9,29407201
3	3012876	23,7849338	3	6612223	9,29437913
3	3178197	20,2673228	3	6612255	9,49974994
3	3248222	20,8794091	3	6660685	9,38376536
3	3326972	20,0666037	3	6702174	9,64217411
3	3348485	20,8196009	3	6801332	9,0135602
3	3419062	20,4317097	3	7009733	7,48710839
3	3833444	23,0828747	3	7437740	9,07698364
3	3960217	19,6388366	3	7617984	8,83989564

Note: Grey indicates genomic positions with LOD value above 10, which is based on rQTL binary trait mapping.

A big advantage of RAD-seq is that it identifies the recombination breakpoints by looking through the genotypes of markers along the candidate QTL region. The bi-parental genotypes are A and B, which represent the RsE2 sensitive ecotype ICE153 and RsE2-insensitive ecotype ICE73, respectively. The heterozygous calls (genotype H) were determined by 0.3-0.7 concordance and at least 5 support values. RsE2-insensitive plants were expected to associate to QTL region represented by most of markers with genotype B. But in some cases, we found the genotype of markers are jumping from B to H, which suggests a recombination breakpoint between two adjacent markers. Similarly, RsE2-sensitive plants are expected to associate to genotype A or H in the QTL region. When the recombination happens, the genotype of markers is changing from H to B. Identifying the recombination breakpoints could effectively narrow down the QTL region. To further check the genotyping among QTL-included



region from Chr3:20373 to Chr3:8019376, we identified 31 informative recombination events among 192 F2 populations (Figure 4.15). Three of them define the left boundary although other 28 events define a very broad right boundary, which is reasonable since the left boundary of QTL is almost the end of Chromosome and rare recombination events occur in such narrow chromosome region. 5 recombination events support a conclusion that RsE2 elicited immunity response is genetically determined by a region from Chr3:1321901 to Chr3:2795414. So far, the QTL mapping and recombination breakpoints recognizing are based on 901 filtered markers. Considering the large GBS data (16,973 potential markers), we checked the genotype of all potential markers nested in the region of Chr3:1321901 to Chr3:2795414 for each of five individual plants which define this narrowed QTL. The plant P2A03 (Table 7.1) and P1H03 (Table 7.2) contain the markers that define a nested QTL region around 1.1Mb from Chr3:1399533 to Chr3:2485009.

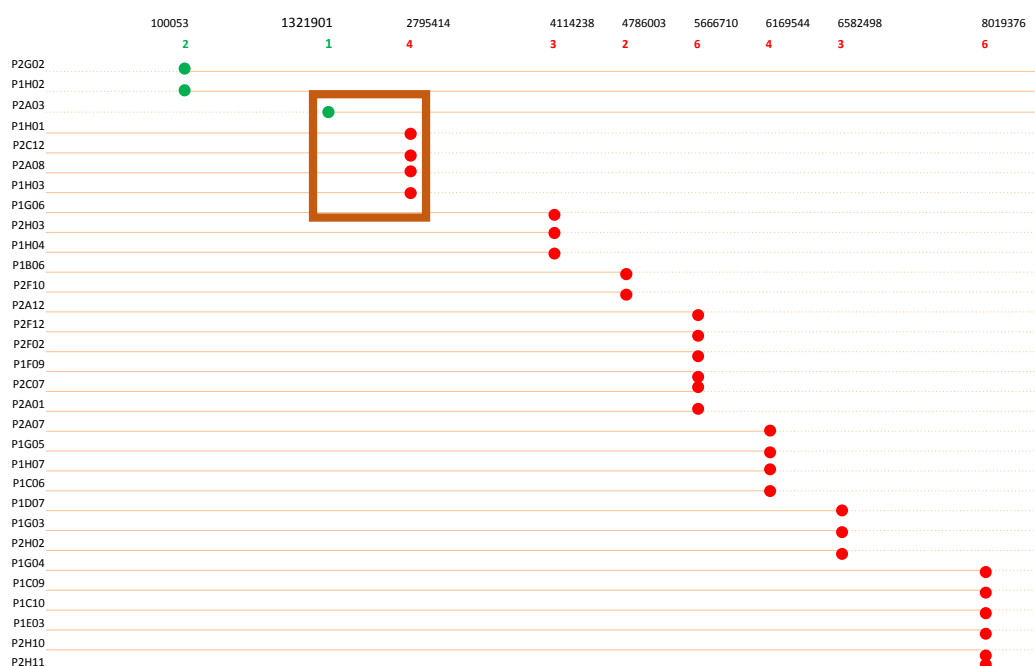


Figure 4. 15 The diagram of 31 individual plants containing informative recombination events which define the left and right boundary of QTL

Left codes indicate 31 individual F2 plants; the genomic positions on chromosome 3 are labeled above. Green numbers indicate summarized frequency of recombination events happened at left boundary within F2 population; red numbers indicate summarized frequency of recombination events happened at right boundary within F2 population. Brown box represents the rQTL-mapping region that is associated with the RsE2 induced ethylene response.

Strikingly, the rQTL region identified from a bi-parental segregation population using GBS overlaps with one of four regions identified from a species historical population using GWAS. This region, around 1.1Mb from Chr3:1399533 to Chr3:2485009, is most likely to harbor the RsE2 receptor.

#### 4.5 Identification of the RsE2 receptor

Most of PRRs identified in plants so far belong to the protein families RLKs and RLPs. Therefore, >300 RLKs (Shiu and Bleecker, 2001) and 57 RLPs (Wang et al., 2008) from *Arabidopsis* are potential candidates for RsE2 perception. The 1.1Mb QTL region from Chr3:1399533 to Chr3:2485009 contains 339 genes in *Arabidopsis* reference genome. There are four RLPs clustered into two groups, Rlp30 (At3g05360) and Rlp31 (At3g05370); Rlp32 (At3g05650) and Rlp33 (At3g05660), one LRR containing protein (At3g05990) and one disease related R protein (At3g07040) (Table 3.2), all of the candidates were predicted to be trans-membrane proteins. RLP30 is a receptor for specific perception of *Sclerotinia Culture Filtrate Elicitor1* (SCFE1) from the necrotrophic fungal pathogen *Sclerotinia sclerotiorum*. rlp30 mutant ecotype Bak2 can perceive the elicitor RsE2 in very sensitive way, which suggests another protein instead of RLP30 is functionally implicated recognizing the elicitor RsE2.

We used forward genetic methods to verify the genuine RsE receptor candidate. Multiple alleles of either T-DNA insertion or transposon insertion (SIGnAL; <http://signal.salk.edu>) for genes Rlp31 (At3g05370), Rlp32 (At3g05650), Rlp33 (At3g05660), LRR containing gene (At3g05990) and disease related R gene (At3g07040) were examined for RsE2-elicited ethylene response. Four mutant alleles of Rlp32, including SM\_3\_33092, SALK\_137467C, SM\_3\_33695 and SM\_3\_15851 (Figure 4.16), showed insensitive phenotype similar to ICE73 upon RsE2 treatment, compared to the mild response in Col-0 and the sensitive response in ICE153. All other alleles related to Rlp31, Rlp33, LRR protein and R protein showed normal ethylene production when treated with RsE2 (Figure 4.16). This forward genetic study suggests that the Rlp32 is associated with the function of RsE2 perception.

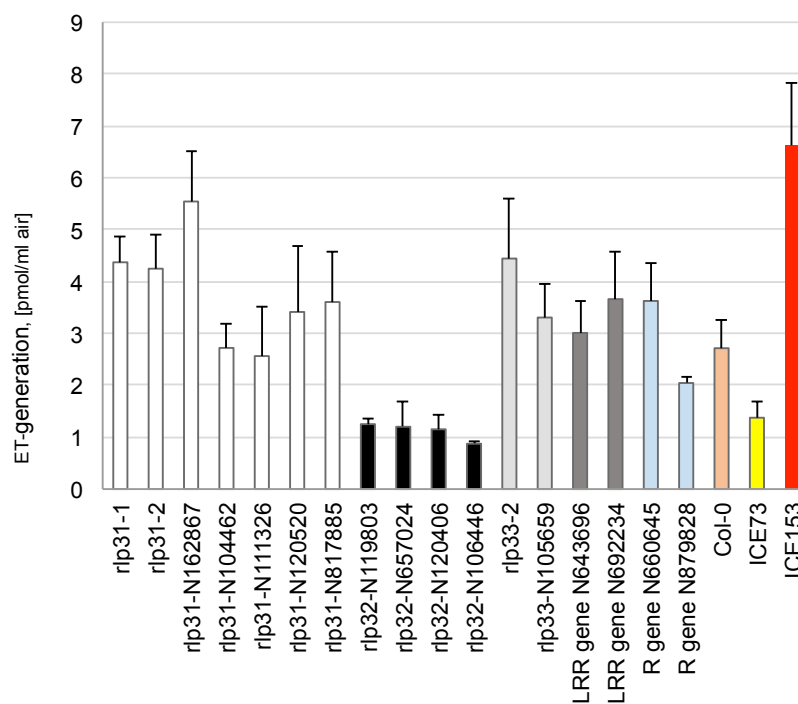
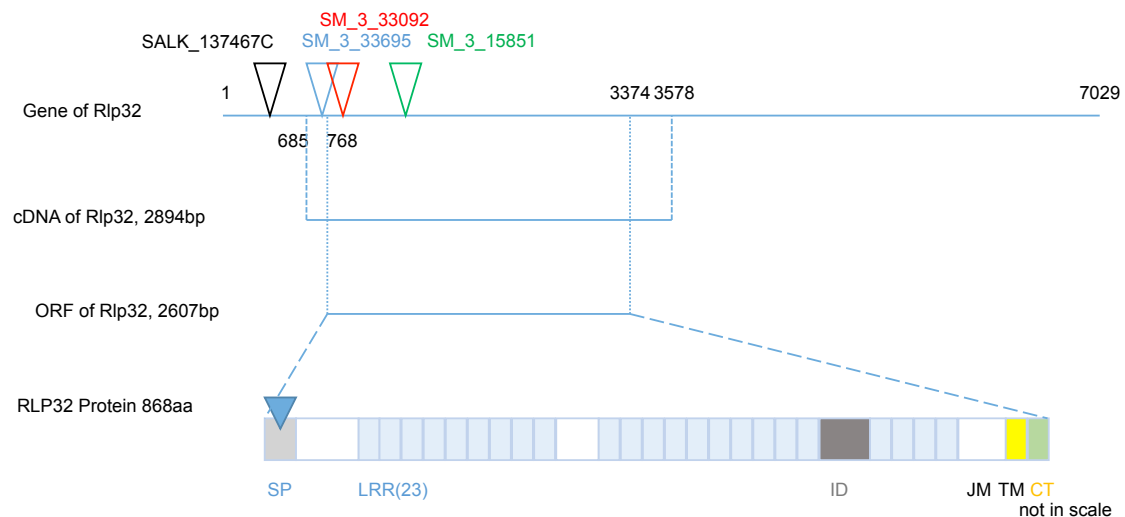


Figure 4. 16 RsE2 induced ethylene response in multiple T-DNA/transposon insertion alleles of candidate receptors

Alleles of rlp31, rlp32, rlp33, LRR gene and R gene are represented by white, black, light grey, dark grey and light blue, respectively. Controls Col-0, insensitive ecotype ICE73 and very sensitive ecotype ICE153 are represented with orange, yellow and red, respectively. The error bars indicate standard deviations of three individual plants.

The Rlp32 gene has a length of 7029bp in the Arabidopsis Col-0 reference genome flanked with large intergenic regions. The full length of cDNA is 2894bp with 5'UTR, 3'UTR and one single exon. Flanking fragment sequencing validated the four T-DNA or transposon insertion sites and they are 408bp upstream of start codon in SALK\_137467C, 2bp upstream of start codon in SM\_3\_33695, 12bp downstream of start codon in SM\_3\_33092 and 487bp downstream of start codon in SM\_3\_15851 (Figure 4.17). Similar to most members of the receptor-like protein family, the Rlp32 translated into a protein of 868 amino acids, started with a signal peptide (SP) domain, continued by 23 repetitive LRR structures separated by island domain (ID), followed by a juxtamembrane (JM) domain, transmembrane (TM) domain and attached to a cytoplasmic tail (CT) domain at the end. Because of the absence of endoplasmic kinase domain, signal transduction by RLP32 is likely to require other factors (proteins) interacting with RLP32.



Name of alleles	NASC catalog	Primer	Primer	position based on web data	validated position
SALK_137467C	N657024	L5,L83	R994,R1249	408bp upstream of start codon	verified by sequencing
SM_3_33092	N119803	L367	R1406	12bp downstream of start codon	verified by sequencing
SM_3_33695	N120406	L76	R1186	2bp upstream of start codon	verified by sequencing
SM_3_15851	N106446	L528	R1697	491bp downstream of start codon	487bp downstream of ATG

Figure 4. 17 The gene structure of Rlp32 and mutant alleles

The Col-0 allele of Rlp32 has 7029bp in full length. cDNA of Rlp32 is constituted of 5'UTR, 3'UTR and one single exon, which encodes 868aa RLP32 protein. Similar to most of receptor like protein, RLP32 has no endoplasmic kinase domain and contains a signal peptide (SP), 23 leucine rich repeats (LRR) isolated by island domain (ID), juxtamembrane domain (JM), transmembrane domain (TM) and cytoplasmic tail (CT). Colorful transparent triangles indicate the genomic insertion positions of four T-DNA/transposon insertion alleles, which were validated by PCR-based sequencing.

With the uncovering of the gene controlling RsE2 perception, what type of mutation in Rlp32 led to the insensitive ecotypes in nature raised our interest. The DNA polymorphism in Rlp32 among 80 ecotypes suggests a high diversity on the coding and intergenic region. By checking the gene sequences of the five insensitive ecotypes, we found a few amino acid substitutions present in almost all insensitive ecotypes. Additionally, we detected an early stop codon that appeared in Rlp32 of ecotype Dog-4 and a truncated promoter region of Rlp32 in ecotype ICE73. A qRT-PCR was executed to determine the transcription level of Rlp32 in Col-0 and ICE73, with the reference gene EF-1Alpha. About 0.15 fold change of transcription of Rlp32 was detected in ecotype ICE73 in contrast to Col-0 (Figure 4.18), which suggests that the RsE2-elicited low level ethylene response in ecotype ICE73 is associated with the low level transcription of Rlp32 due to incomplete promoter.

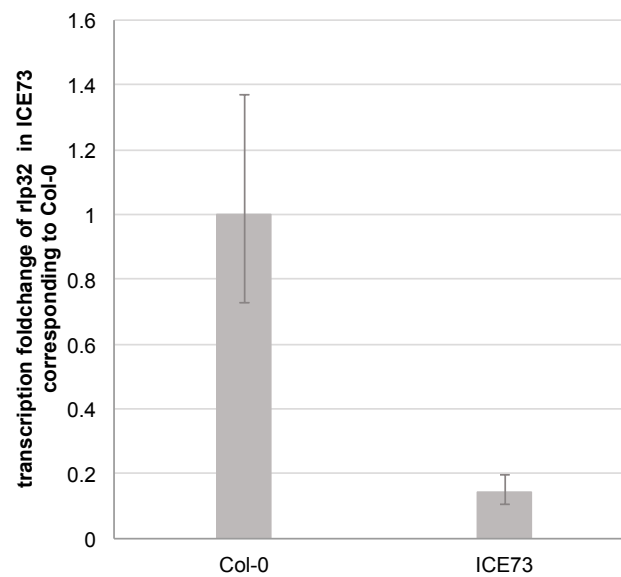


Figure 4. 18 The qRT-PCR analysis of rlp32 gene expression in ecotype ICE73 and Col-0

The transcription of Rlp32 in ecotype ICE73 is around 0.15 fold change of that in Col-0, with EF-1alpha as reference gene.

An RLP32 protein was identified as RsE2 receptor from 1.1Mb region of chromosome 3. Four T-DNA/transposon alleles of Rlp32 displayed a reduced capability of RsE2 perception. The insensitive ecotype ICE73 was found to harbor reduced gene Rlp32 transcription due to a truncated promoter. Together, these evidences suggested that the Rlp32-encoded receptor like protein is responsible for Arabidopsis to recognize the RsE2 elicitor.

#### 4.6 The bioinformatics characterization of the Rlp32 gene

The Rlp32 gene displays substantial diversity in the coding sequence among 80 Arabidopsis ecotypes. It contains 95 SNP positions in its 2.9kb sequences ([http://gbrowse.weigelworld.org/fgb2/gbrowse/ath\\_reseq\\_mpicao2010/](http://gbrowse.weigelworld.org/fgb2/gbrowse/ath_reseq_mpicao2010/)). A phylogenetic tree of Rlp32 gene from 80 ecotypes was generated in CLC workbench using neighbor-joining method (Figure 4.19).

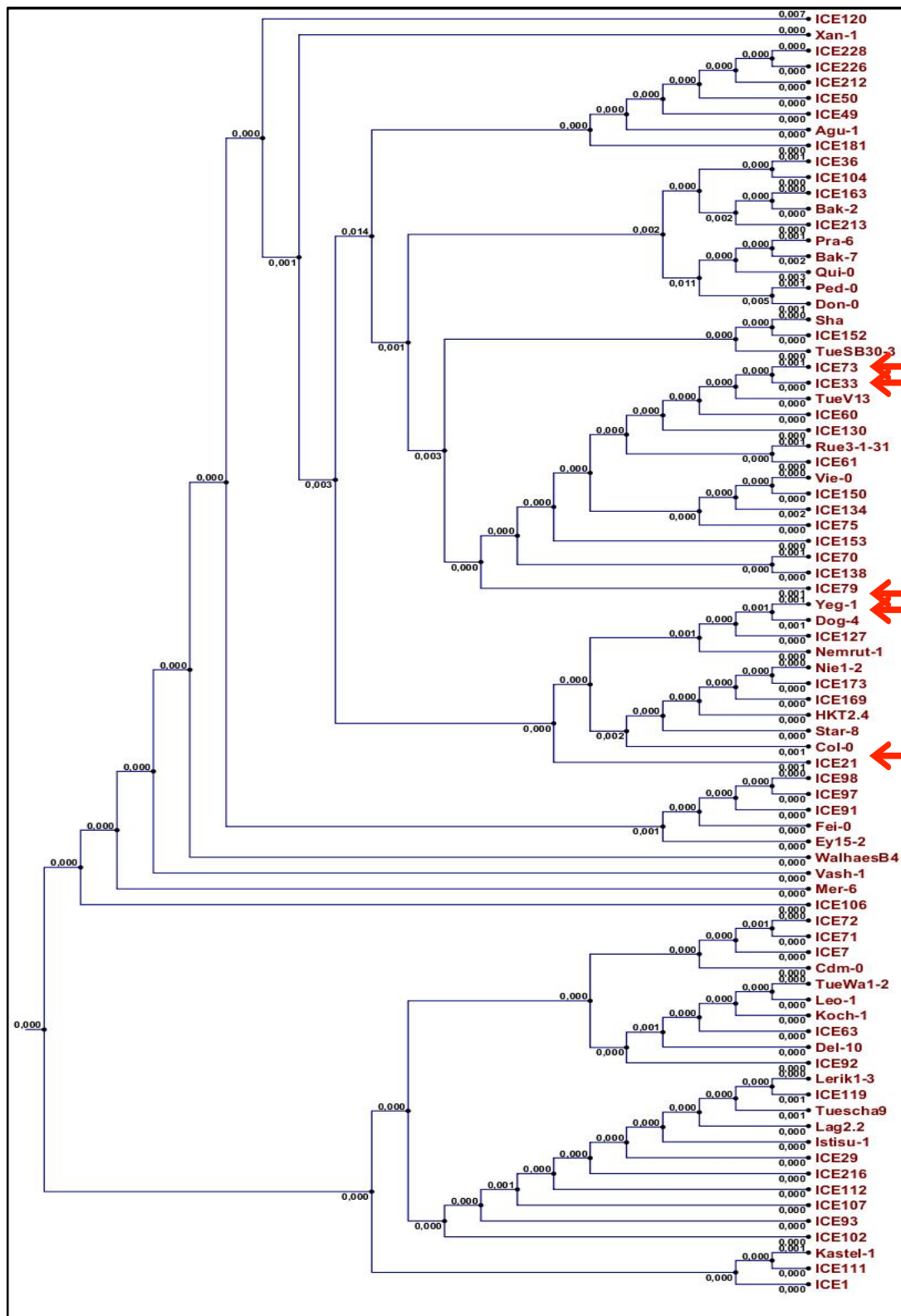


Figure 4. 19 A phylogenetic tree of Rlp32 genes from 80 Arabidopsis ecotypes

A phylogenetic tree of Rlp32 genes from 80 Arabidopsis ecotypes was built using neighbor-joining method. Insensitive ecotype ICE73 and ICE33 are grouped together, so are insensitive ecotype Dog-4 and Yeg-1. This suggested that grouped two insensitive ecotypes might share the similar genetic lesions.

We noticed that Rlp32 alleles from ICE73 (Russia) and ICE33 (Caucasus) have shorter distance, so are Rlp32 alleles of Dog-4 (Caucasus) and Yeg-1 (Caucasus) (Figure 4.19), which might suggest that two grouped RsE2-insensitive alleles are due to the similar genetic defect, and three independent events lead to the existence of insensitive alleles among 80 Arabidopsis ecotypes. To locate the exact sequence underlying RsE2 perception differences will benefit the identification of the key amino acids that have effects on RLP32 function.

#### **4.7 Protoplast transformation of a Rlp32 allele derived from sensitive ecotype ICE153 complements the phenotype in ecotype ICE73**

To confirm the specific recognition of elicitor RsE2 by RLP32, the Rlp32 allele from ICE153 was constructed into a vector pGWB5, which contains a 35S promoter and a C-terminal fused GFP; this expression vector was co-transfected with a construct containing FRK1 promoter driven luciferase into protoplasts isolated from RsE2-insensitive ecotype ICE73. FRK1 (*FLG22-INDUCED RECEPTOR-LIKE KINASE 1*; At2g19190) encodes a LRR receptor kinase which is induced to transcribe when plant innate immunity is activated by PAMPs. Several previous studies using transient expression of firefly luciferase reporter gene (*LUC*) driven by FRK1 promoter in mesophyll protoplasts successfully detected the luciferase activity upon elicitation (Kovtun et al., 2000; Asai et al., 2002; Yoo et al., 2007; Jehle et al., 2013). In our study, transformed protoplasts were elicited by RsE2, flg22 and H<sub>2</sub>O, respectively. After over-expressing RLP32-GFP protein in RsE2-insensitive ecotype ICE73, the protoplasts acquired improved capability to sense the RsE2 as compared to GFP-controls. The luciferase activity induced by RsE2 perception reaches 2-fold changes in two hours corresponding to un-elicited time point, the similar effect as flg22 perception induced luciferase activity (Figure 4.20). Therefore, transformation of the RLP32 allele from a sensitive ecotype ICE153 in protoplasts of insensitive ecotype ICE73 could complement the insensitive phenotype in ICE73 upon RsE2 elicitation.

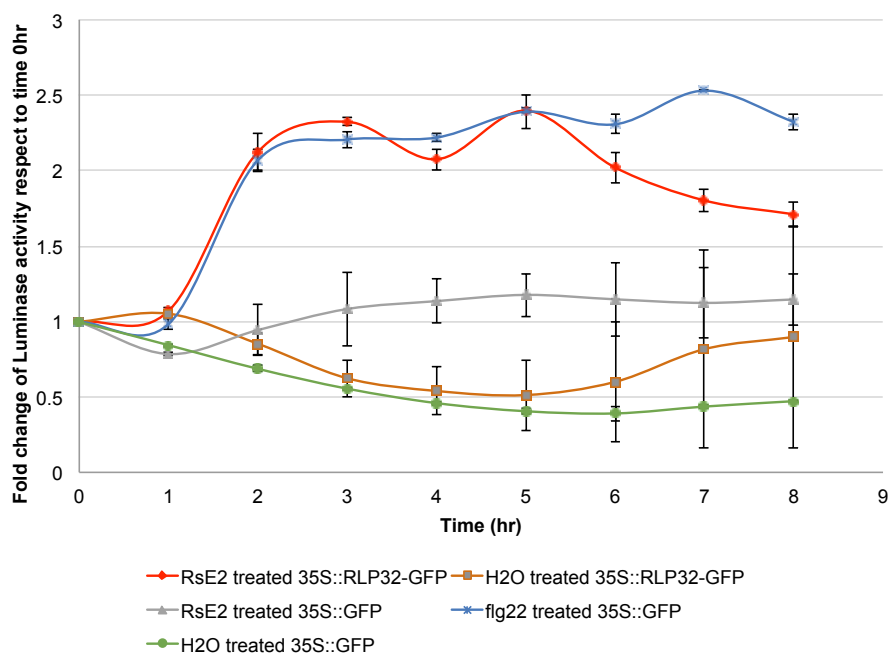


Figure 4. 20 The expression of 35S::RLP32-GFP in protoplasts of insensitive ecotype ICE73 obtains the function of perception of the RsE2

The construct 35S::RLP32-GFP or the construct 35S::GFP was co-transformed into protoplasts of insensitive ecotype ICE73 with the construct pFRK1\_Luc. The transformed protoplasts were elicited to express luciferase upon treatment of RsE2, flg22 or H<sub>2</sub>O respectively. The protoplasts of insensitive ecotype ICE73 after transformed with 35S::RLP32-GFP could produce higher fold change of Luminescence activity upon treatment of RsE2 than the protoplasts transformed with 35S::GFP. The fold change of Luminescence activity elicited by RsE2 is similar to flg22.

The protoplast transformation confirmed that RsE2 elicitor is recognized by Arabidopsis via the RLP32 receptor system. In addition, protoplast transformation illustrated that RsE2 could elicit the transcription of an immunity marker gene, although the receptor RLP32 was identified originally by a defect in ethylene production. Altogether, protoplast transformation verified that RsE2 sensitivity is restored in an insensitive ecotype upon RLP32 expression.

#### 4.8 *N. benthamiana* gains RsE2 perception by transient expression of Rlp32.

The long-term goal of studying PRRs in plants is to improve plant disease resistance through genetic modification of plants. Transformation of the PAMP receptor RLP32 supplies a pathway to enhance the immunity of susceptible plants to certain pathogens. An ortholog of Rlp32 in *N. benthamiana* shares only about 35% identity with Rlp32 in Arabidopsis. We showed that when leaf



slices from *N. benthamiana* are treated with elicitor RsE2, they can not produce the ethylene response at detectable levels. This experiment confirmed that *N. benthamiana* could not efficiently perceive the elicitor RsE2 using the native endogenous RLP receptors. We then used the *N. benthamiana* system to prove the concept of improving immunity ability by engineering plants.

We generated transient expression in *N. benthamiana* using the construct, Rlp32-pB7FWG2, which contains a 35S promoter and GFP tag at the C terminus. *N. benthamiana* was infiltrated with *Agrobacterium* GV3101 containing Rlp32-pB7FWG2 construct which was a modified method by co-transforming of p19 (Albert et al., 2010; Voinnet et al., 2003), which suppressed gene silencing due to over-expression. Two days after infiltration, GFP fluorescence was observed in plasma membranes of *N. benthamiana* under epi-fluorescence microscopy, which suggested a transient expression of RLP32-GFP fusion protein. The same infiltrated leaves were cut for ethylene assay; about 10 times ethylene production was detected upon RsE2 treatment comparing to single transformation of the p19 control. Transformation of Rlp32 alone instead of co-transformation with other co-receptors was enough to help *N. benthamiana* to perceive the elicitor RsE2 (Figure 4.21).

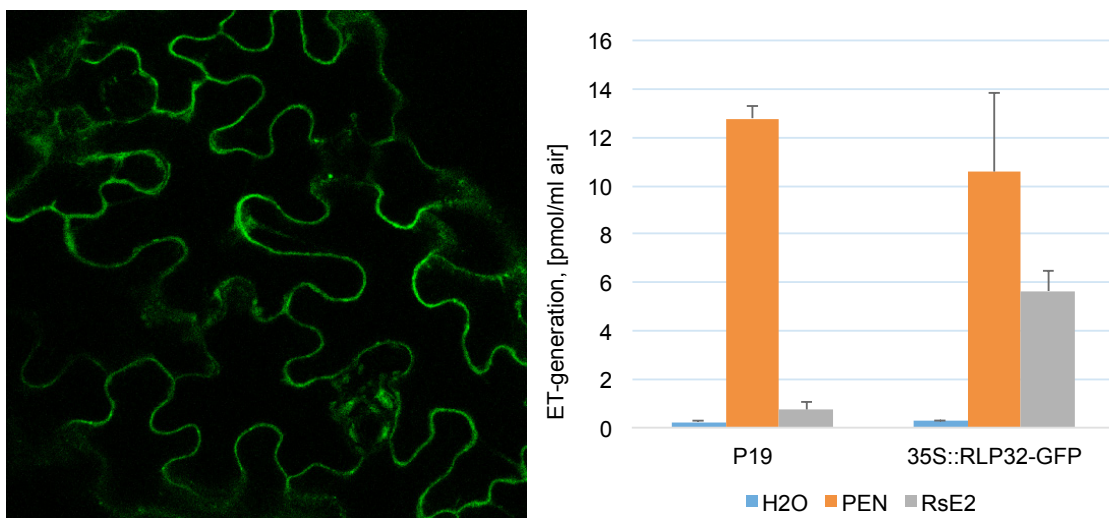


Figure 4. 21 RsE2-induced ethylene response in 35S::RLP32-GFP transiently expressed *N. benthamiana*

GFP tagged RLP32 protein was detected on the plasma membrane by epi-fluorescence microscopy two days after transformation (left). The leaf tissue from transiently expressing of RLP32-GFP can produce ethylene upon elicitor RsE2 treatment, whereas the leaf tissue from transiently expressing of P19 (control vector) cannot.

Transient expression of RLP32 in *N. benthamiana* suggested a successful case to restore an immune response in one of the host plants of *R. solanacearum*. In order to improve the resistance to *R. solanacearum* in approximately two hundreds host species, such as tomato, potato, ginger, banana, eggplants, tobacco, sweet pepper and olive, further disease symptoms still need to be scored to corroborate the value of its application in agriculture. This transient expression experiment also confirmed the subcellular location of RLP32 at the plasma membrane.

#### **4.9 Stable transformation of Rlp32 in Arabidopsis insensitive ecotypes**

RLP32 was confirmed to be the receptor of elicitor RsE2 through transient expression experiments; however, we still need to confirm that Rlp32 could genetically complement the insensitive phenotype in Arabidopsis. In addition, how the RLP32 perceives RsE2 and elicit immunity responses is not fully understood. To develop stable Rlp32 transformants in Arabidopsis is necessary to explore the function of the receptor.

An effort was made to get stable rlp32 transgenic lines for insensitive and sensitive ecotypes. First, we constructed the rlp32 allele from Col-0 into the CaMV 35S promoter and GFP tagged vector and transformed it into insensitive ecotype ICE73 and Wt-5. The T<sub>0</sub> seedlings were selected with Basta. All T<sub>0</sub> transgenic plants display no morphological difference with ecotype ICE73 or Wt-5, although the leaves from most of them recovered the capability to elicit ethylene responses significantly. The capacity of ethylene biosynthesis in T<sub>0</sub> of ICE73 upon RsE2 treatment was similar to that in the sensitive ecotype ICE153. The capacity of ethylene biosynthesis in T<sub>0</sub> of Wt-5 could reach at least that in the ecotype Col-0 (Figure 4.22).

The other transgenic plants (Table 7.5) using Rlp32 endogenous promoter from ecotype ICE153 were generated to explore the transcription regulation of this allele and we used GFP tagged protein to better understand the subcellular localization of Rlp32. The information of gene regulation and subcellular localization is potentially useful for the application of RLP32-mediated recognition system in the future.

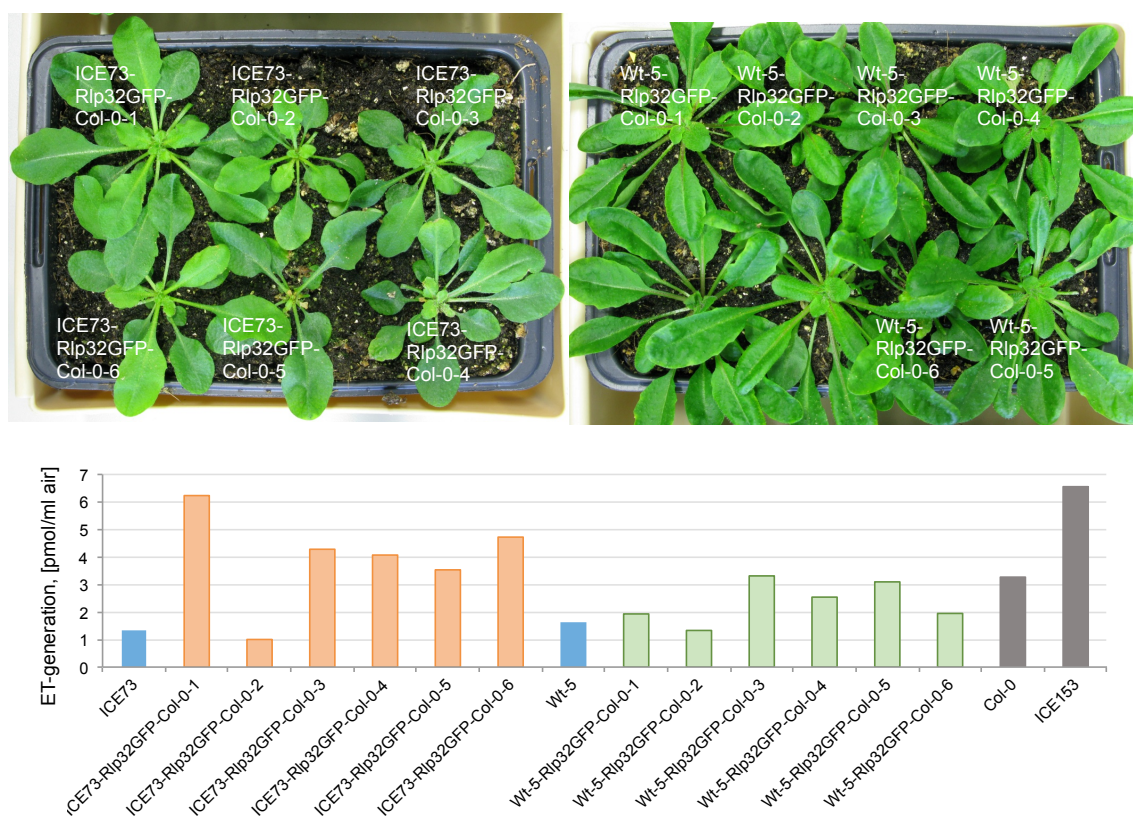


Figure 4. 22 RsE2 induced ethylene response in transgenic ICE73 and Wt-5 plants

The transgenic plants selected by Basta spraying were examined for the ethylene production elicited by RsE2 (lower panel). Upper left: transgenic ICE73; upper right: transgenic Wt-5. The screening was done by single measurement. Non-transgenic ecotypes ICE73, Wt-5, Col-0 and ICE153 are controls.

#### 4.10 Two elicitors RsE1 and RsE2 are identical

Two separated active fractions, RsE1 and RsE2, were purified from the crude extract of *Ralstonia solanacearum* (see chapter 4.1.1 and 4.1.2). The genetic allelism test showed that five insensitive ecotypes upon RsE1 treatment were allelic to each other and five insensitive ecotypes upon RsE2 treatment were allelic to each other. Because three common insensitive ecotypes upon RsE1 as well as RsE2 were allelic to each other, we hypothesized that RsE1 and RsE2 preparations contain the identical major elicitor. Furthermore, we used RsE2 to screen the ethylene responses in genetic populations and we confirmed that RLP32 is the receptor of RsE2. However, whether RLP32 could also perceive RsE1 was still to be shown.

To explore this, RsE1-induced ethylene response was compared to RsE2-induced ethylene response in two *rlp32* mutant alleles N119803-3 and N657024-1. Similar to RsE1- and RsE2-insensitive ecotype ICE73, the two mutants exhibited the same lack of ethylene biosynthesis when treated with either RsE1 or RsE2 (Upper panel of Figure 4.23). In addition, an observation of combined effect of ethylene responses elicited by both RsE1 and RsE2 (Lower panel of Figure 4.23) also suggested that there is a major elicitor contained in both RsE1 and RsE2.

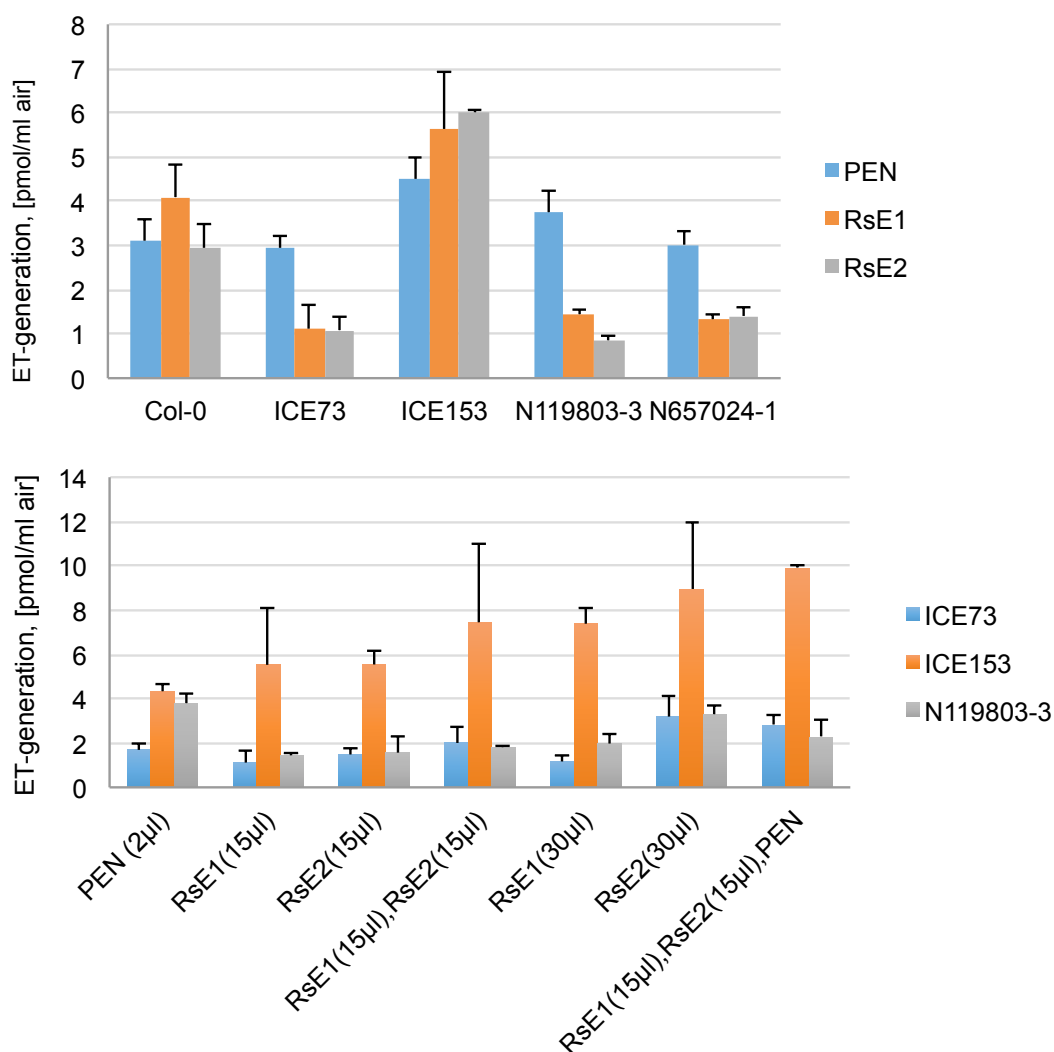


Figure 4. 23 Comparison of ethylene response elicited by RsE1 and RsE2 in T-DNA insertion alleles of Rlp32

Upper panel: Elicitors RsE1 and RsE2 induce identical ethylene response in two independent *rlp32* alleles, N119803-3 and N657024-1, as well as in insensitive ecotype ICE73; Lower panel: ethylene responses induced by different combinations of RsE1, RsE2 and PEN. The ethylene response induced by combining both RsE1 and RsE2 is not higher than the responses induced by double amount of single elicitors.

Together with the fact that RsE1 could elicit ethylene response in Rlp32 transiently expressing *N. benthamiana* (correspondence with Dr. Melzer), it is most likely that RsE1 and RsE2 preparations contain identical elicitors and both could be perceived by the receptor RLP32.

#### 4.11 Interaction of RLP32 with other RLKs

We examined RsE2-induced ethylene responses in different alleles of BAK1 or BKK1. RsE2-induced ethylene response was reduced in single mutant *bak1-5* and *bkk1-1*. Furthermore, the response was even lower in the double mutant of *bak1/bkk1* than in any of the single mutants (Figure 4.24). RsE2-induced weak/non immunity response in the double mutant was also reflected in other early immunity assay, such as callose deposition, which was conducted by Dr. Melzer (Melzer, 2013). Our study suggested that RLP32 is most likely dependent on Bak1 to mediate RsE-induced immune signaling.

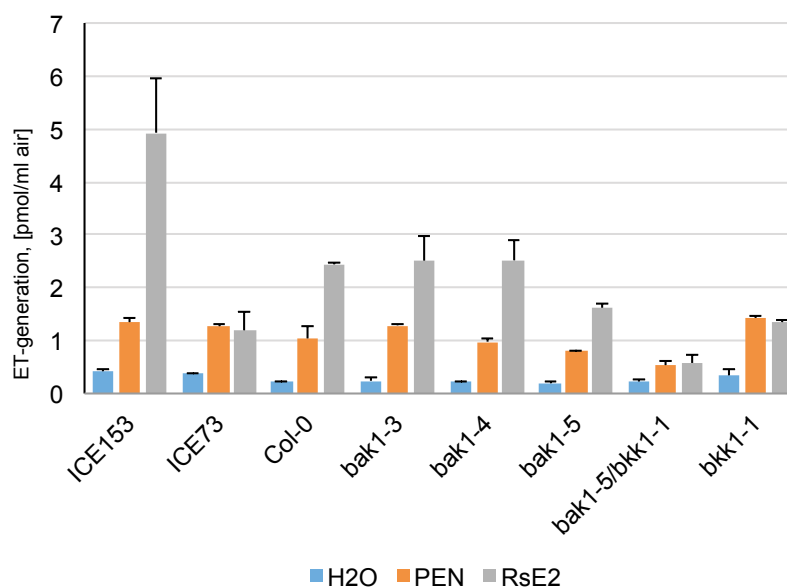


Figure 4. 24 RsE2 failed to induce ethylene responses in *bak1-5/bkk1-1* double mutants.

Three *bak1* mutant alleles, *bak1-5/bkk1-1* double mutant and *bkk1-1* were examined for their ethylene responses upon RsE2 treatment. Compared to the *Col-0* and *ICE153*, *bak1-5/bkk1-1* double mutants could not be elicited by RsE2 in ethylene assay (33ng/ $\mu$ l PEN and H<sub>2</sub>O are controls).

Sobir1 is another co-receptor of most RLPs, such as RLP30, RLP1 and RLP42 (Zhang, 2013; Jehle et al., 2013; Zhang et al., 2014). Col-0 shows weak ethylene response upon RsE2 treatment in our experiment, we hypothesize that Col-0 contains a weak Rlp32 allele and over-expression of Rlp32 in transgenic Arabidopsis may serve as a way to study interaction of RLP32 and co-receptors. In our current study, we have shown that two individual alleles of sobir1 produced reduced ethylene response upon RsE2 treatment compared to Col-0. In contrast to insensitive ecotype ICE73, however, the sobir1 mutant can still sense the RsE2 (Figure 4.25), which might be due to impurity of RsE2 preparations.

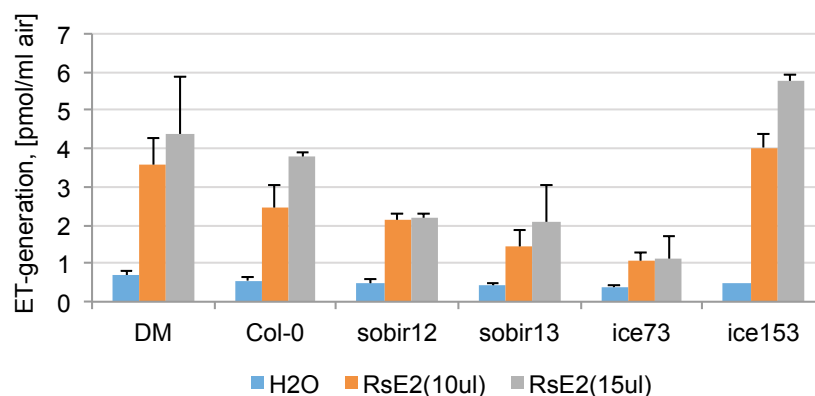


Figure 4. 25 Reduced ethylene response upon RsE2 treatment in two T-DNA insertion alleles of Sobir1

sobir12 and sobir13, two T-DNA insertion alleles, show reduced ethylene responses upon RsE2 treatment compared to Col-0 and fis2/efr double mutants.

Surprisingly, RLP32 transformation alone is enough to sense the elicitor RsE2, which suggested a different recognition mechanism from RLP30, which were functional only when co-transformed with co-receptor Sobir1. One explanation could be that the orthologous of Sobir1 in *N. benthamiana* cooperates with RLP32 well but not with RLP30.

## 5. Discussion

### 5.1. GWAS/Rad-seq offers a genomics-based tool for rapid receptor identification/isolation.

Tracing the history of PAMP receptor identification over the last twenty years, it is not hard to find that two major routes have always been followed in plant pathogen receptor research. The first receptor XA21 in rice (Song et al., 1995) was cloned using a traditional map-based genetics approach: the genetic locus was first mapped in near-isogenic-lines (NILs), then the BAC libraries were screened to find candidate genes. This was done without genome sequence data available and both development of NILs and the screening of BAC were very tedious and time consuming. A different, biochemistry-based route was used to clone a chitin oligosaccharide elicitor binding protein (CEBiP) (Kaku et al., 2006). CEBiP was isolated from the plasma membrane of suspension-cultured rice cell by (GlcNAc)<sub>8</sub>-APEA high-affinity chromatography, then cloned by PCR screening of a rice cDNA library for the coding sequence of N-terminal seven amino acid residues of CEBiP (Kaku et al., 2006). In addition to these two routes, certain “educated guesses” are also helpful to narrow down receptor candidate lists. For example, EFR was cloned by screening elf18-triggered growth inhibition among the seedlings of the mutant collection of 28 LRR-RLKs, which were postulated to contain the receptor of elf18 due to their similarity to FLS2 and transcriptional inducibility by both flg22 and elf18 (Zipfel et al., 2006). Similarly, because rice CEBiP has two LysM domains for chitin elicitor perception and no intracellular domain, it was hypothesized that other LysM containing receptor-like proteins were required for elicitor perception and intracellular signal transduction as well (Miya et al., 2007). Therefore, mutants of three LysM containing RLKs were screened for loss of chitin-inducible ROS reactions upon N-acetylchitooctase (GlcNAc)<sub>8</sub> treatment, and among them OsCERK1 was identified for chitin elicitor signaling and immune activation in rice as a consequence (Miya et al., 2007). Several PGN receptors, including AtLYM1, AtLYM3, AtCERK1, OsLYP4 and OsLYP6, were all assumed to be involved in PGN perception based on their LysM domain classification and their

localization at the plasma membrane and were verified by molecular biochemistry later on (Willmann et al., 2011; Liu et al., 2012a).

Recently, the use of bi-parental mapping and the use of reference genome sequences have revolutionized the identification of any protein of interest. In a bi-parental mapping study, recombination events that happened during the F2 population generation process were surveyed and the correlation between phenotype distribution in F2 population and the recombination events was used to calculate the location of the phenotype-causing genetic feature. It is critical to select and develop appropriate parents so that they have heritable and distinct phenotypes in their progenies and that they are genetically distant enough to find adequate markers to track the recombination breakpoints. The cloning of the flagellin receptor FLS2 reflected the application of combined forward genetics and bi-parental mapping in early research. Three *fls2* mutant plants were detected from 80,000 EMS seedlings upon flg22 treatment (Gómez-Gómez et al, 2000). The mapping population was established by crossing *fls2* mutant (with La-er background) to Col-0 and a well-developed marker system CAPS (Co-dominant Amplified Polymorphic Sequence) was used to identify the associated locus as FLS2 (Gómez-Gómez et al, 2000; Konieczny and Ausubel, 1993). Recent successful applications of bi-parental mapping focused on sorting the immunity function of RLPs in Arabidopsis. Instead of using EMS mutant screenings, a thousand Arabidopsis ecotypes provided a great variation source containing particular PAMP perception deficiency. The receptor of bacterial elicitor EMAX was mapped to Chr1 of Arabidopsis by two sets of RILs constituted of EMAX-insensitive ecotype Sha and one of other sensitive ecotypes Bay-0 or Ler and this receptor was verified to be RLP1 (Jehle et al., 2013). The perception of fungal elicitor SCFE1 was mapped to Chr3 of Arabidopsis by RILs between SCFE-insensitive ecotype Lov-1 and SCFE1-sensitive ecotype Col-0 and was annotated to be RLP30 (Zhang et al., 2013). Similarly, RLP42, the receptor of fungal elicitor RBPG1, was cloned by mapping the RILs between Br-0 and Col-0 using correlative polymorphism markers (Zhang et al., 2014). Benefiting from the wide existence of natural variation for PAMP perception in Arabidopsis, we have also detected RsE2-insensitive ecotypes that allowed us to generate bi-parental mapping populations. While the bi-parental mapping approach has proven to be effective in isolation of



receptor genes, the mapping population development (for example, the RILs with one of the parents has to be elicitor-insensitive) and marker development are relatively time-consuming and they have been the bottleneck for rapid gene identification.

Recently, several advances in genomics technologies, such as next generation sequencing (NGS), extreme phenotype mapping and genotyping-by-sequencing (GBS), have further simplified and speeded up gene cloning approaches. For example, Lectin receptor kinase I.9, the plant receptor for extracellular ATP was identified by map-based cloning and genome sequencing of two ATP-insensitive EMS alleles, *dorn1-1* and *dorn1-2* (Choi et al., 2014). While dealing with more complicated bi-parental populations, the use of NGS and GBS essentially eliminate the separate steps for marker development, the markers were identified and scored in the same step while the extreme phenotype pooling strategy simplified mapping population production and sampling steps. Taking advantage of NGS and GBS, we are the first one to apply this technology to map a PAMP receptor in plants. In our study, we took a particular RAD-seq based GBS method which allowed us to produce ~900 restriction site-associated DNA markers in a non-reference bi-parental population and to screen the genotypes of 192 individuals all together, which has avoided the traditional processes for marker selection and repetitive testing in order to walk to the mapping locus from both directions. On the other hand, a non-reference allele was used in our study and has improved the precision of phenotype segregation scores because Col-0 is not phenotypically significantly different from insensitive ecotype ICE73. We have screened 400 F2 populations totally, and we have sequenced 92 insensitive individuals and 100 top-sensitive individuals. Extreme phenotype selection increased the statistic power of QTL mapping with LOD values of 15~20 for an associated genomic region. The other advantage of RAD-seq lies in the identification of the recombination break boundaries of phenotype-associated genomic regions. Other recent GBS mapping methods, such as, BSA (bulk segregation analysis) identified SNP markers associated to the phenotype but failed to precisely define a region (Schneeberger et al., 2009). In our study, we have not only identified a genomic region associated to RsE2 perception but also defined the recombination boundary using the markers falling into the QTL region by examining 31

informative individuals. Another advantage worth to mention is the endurance of phenotype mistakes since the genomic association to phenotype was supported by statistical analyses in our GBS-based QTL. Traditional PCR polymorphism marker-based mapping is highly influenced by phenotype determination of segregated populations. The false phenotype determination together with false positive and/or false negative PCR results could mislead to wrong candidate genomic regions. In our study, we have detected by GBS that among 84 insensitive individuals phenotyped by biochemistry assays (ethylene production in response to RsE2 treatment), only one individual (with the phenotype score close to sensitive/insensitive cut-off value 1.6) was mistakenly attributed into insensitive group since all the markers within QTL region in this individual indicated its origin of sensitive parent ICE153. Our study suggested that a 1% mistake ratio of phenotype determination has not produced the adverse effect on mapping because we had enough markers with good sequencing coverage to statistically discriminate false and right phenotypes.

One limitation of the bi-parental mapping approach is the limited diversity in the pathogen response among common lab accessions. For example, there are only a few dozens of common *Arabidopsis* lab accessions available and often they do not show differences in their response to a particular pathogen infection. An ideal solution to overcome this limitation would be to survey response phenotypes of a large collection of diverse accessions and statistically correlate their genetic features across their genome to their phenotype and directly exploit the loci that associate with the phenotype. GWAS is the direct exemplification of such an idea, and now has been proven successful in many cases in plant research (Atwell et al., 2010 and Aranzana et al., 2005). The other advantages of GWAS include that historically accumulated recombination is scored and no crosses are needed and, secondly, that genotype information is usually already available in public databases. The application of GWAS has speeded up our process to identify the recognition system for the RsE2 elicitor by simply acquiring multiple accessions' phenotype upon RsE2 treatment. In our study, we have performed GWAS among three different populations for three elicitors. Our results showed that large populations provided better chances to narrow down receptor candidates. We have examined GWAS for 52 ecotypes upon fungal elicitor SCFE1-treatment, for 76 ecotypes upon RsE2

treatment and for 86 ecotypes upon RsE1-treatment (Table 7.4 and Figure 7.1), and our GWAS assays revealed significantly associated peaks in three treatments (40, 4 and 2 respectively). From our study, we postulated that if we are using 200 highly diversified ecotypes for GWAS, we might reduce the non-specific association and associate the phenotype directly to a causal genetic region in one step. Although this hypothesis needs to be tested in future studies, our pioneer study indicated the possibility of applying GWAS in immunity and implied the potential application of GWAS for efficient high-throughput identification of PAMP receptor systems.

GWAS is an efficient tool to map the genetic regions responsible for elicitor perception, which is the first step in elicitor-triggered immunity. It is not clear whether it is also powerful enough to detect co-receptors in one single experiment. To find some hints, we checked all significant GWAS hits from three elicitor experiments, and unfortunately, BAK1- and SOBIR1-representing loci were not on the list or even not on the vicinity of those hits. A closer look at genomic regions surrounding the two genes showed extraordinarily conserved gene sequences among 80 Arabidopsis genomes. This result suggested that GWAS is useful to detect rapidly evolving PAMP receptors, but not co-receptors that mediate multiple functions and appear to be highly conserved. The genetic diversity of PAMP receptors revealed by GWAS highlights substantial evolutionary divergence within the species Arabidopsis to sense microbes.

## **5.2. RLP32 is an LRR-RLP-type receptor.**

An efficient genetic tool will undoubtedly accelerate the mapping process, but we could not ignore the pre-existing knowledge of receptors in order to sort the particular receptor from large numbers of candidate genes within the mapping range. Benefiting from the accumulated knowledge of plant PRRs over the last twenty years, we now have a good understanding of the different types of plant PRRs and their elicitors. In our study, the receptor to perceive RsE2 in Arabidopsis is RLP32, an LRR-RLP-type receptor.

LRR-RLP-type PRRs represent a unique class of PRRs attracting more and more attention not only because of the lack of a cytoplasmic kinase domain in their structure but also because of the large number of diversifying homologues

in this protein family and a broad spectrum of microbial ligands they can recognize. The genome-wide characterization of LRR-RLP gene families has been accomplished in many plant species. In Arabidopsis, 57 LRR-RLPs were identified based on their structural compositions and assembled into ~33 loci, implicating that duplicated genes are most likely a consequence of diversifying selection for pathogen recognition (Wang et al., 2008). Interestingly, sequences of LRR-RLPs in Arabidopsis generally do not show high similarity even between two homologues sitting in neighbor position (Wang et al., 2008). In contrast, in the rice (*Oryza sativa*) genome, a total of 90 LRR-RLPs are distributed into ~38 loci along chromosomes (Fritz-Laylin et al., 2005). Except the orthologs of LRR-RLPs implicated in development, most of orthologs of LRR-RLPs between the two different species share low similarity with mean values of about 27% only (Fritz-Laylin et al., 2005). Genome synteny studies between Arabidopsis and rice suggested that most loci containing LRR-RLPs exist in parallel in both genomes, which means significant expansion of LRR-RLP gene clusters from an average of 2.6 homologues per loci in Arabidopsis to an average of 6 homologues of LRR-RLPs in the rice genome (Fritz-Laylin et al., 2005). Phylogenetic studies based on the alignment of the C3-F region (defined by domain organization) of Arabidopsis, rice and other characterized LRR-RLPs/RLKs grouped 83% of the Arabidopsis LRR-RLPs and 92% of the rice LRR-RLPs into four functional superclades, the Cf-9 superclade, the RPP27 superclade, the LeEix superclade and the PSKR superclade (Fritz-Laylin et al., 2005). Recently identified AtSOBIR1-associated AtRLPs (AtRLP23/At2g32680, AtRLP30/At3g05360, AtRLP32/At3g05650 and AtRLP42/At3g25020) fall into the different sub-clades of the Cf-9 superclade while AtRLP1/At1g07390 belongs to the RPP27 superclade (Fritz-Laylin et al., 2005; Gust and Felix, 2014). AtRLP23, AtRLP30, AtRLP32 and AtRLP42 all belong to gene clusters and without any detected methylation on those cluster regions, which implied regions of frequent recombination and fast generation of novel pathogen recognition specificities under infection pressure (<http://www.arabidopsis.org/>). Ever-cheaper sequencing technologies allowed recently to perform a similar LRR-RLP genome-wide spatial arrangement study in two additional species, tomato (*Solanum lycopersicum*) and potato (*Solanum tuberosum*) recently. 176 LRR-RLPs in the tomato genome and 403 LRR-RLPs in the potato genome are

syntenically distributed along chromosomes as cluster patterns even though neither gene order nor content is strictly conserved between the two *Solanum* species (Andolfo et al., 2013). Similar to the previous study on LRR-RLPs in Arabidopsis and rice, phylogenetic studies of 169 tomato LRR-RLPs proteins and 15 characterized RLPs grouped them into seven superclades (Andolfo et al., 2013; Fritz-Laylin et al., 2005). The cluster patterns as well as the distributions of LRR-RLPs in genomes of four plant species Arabidopsis, rice, tomato and potato sheds light on how novel pathogen recognition systems evolved rapidly along lineage speciation, by polyploidization, chromosome rearrangement, ectopic recombination, unequal crossing-over and pathogen-directed selection. Early genetic studies on Cf proteins (Cf-2, Cf-4, Cf-5 and Cf-9), which are LRR-RLPs in tomato, also illustrated how LRR-RLP evolved in single loci. Cf-4 and Cf-9 are contained in two haplotypes in the same genomic locus originating from different *Lycopersicon* species that confer resistance to the fungus *Cladosporium fulvum* races 4 and 9, respectively (Thomas et al., 1998). The Cf-4/Cf-9 locus contains five tandemly duplicated homologous genes *Hcr4s/Hcr9s* (Thomas et al., 1998). Cf-4 protein and Cf-9 protein share 91% identity (Thomas et al., 1998). They are distinguished by a 10 amino-acid deletion in signal peptide of Cf-9 and two complete LRR losses in Cf-9, as well as a 33 amino-acid substitution in the LRR motif of Cf-9, which may account for specific recognition of *Cladosporium fulvum* races 4 and 9 (Thomas et al., 1998). This study also suggested that novel Cf gene variants could be generated through outbreeding the distinct haplotypes of *Hcr* (Thomas et al., 1998). The genome organization of LRR-RLPs implicates rapidly evolved microbial recognition specificities. So far, no study has shown that orthologs of one LRR-RLP perform the same function (such as perceiving the same ligands) in other model plant species, whereas orthologs of some LRR-RLK-type PRRs and LysM domain-type PRRs were shown to recognize the same ligands. For example, FLS2 orthologs, the pattern-recognition receptors of bacterial flagellin, have been confirmed in tomato, *N. benthamiana*, brassica and rice (Robatzek et al., 2007; Hann and Rathjen, 2007; Dunning et al., 2007; Takai et al., 2008). Likewise, orthologs of AtLYM1/LYM3 and OsLYP4/LYP6, the pattern-recognition receptors of bacterial PGN were found in Arabidopsis and rice (Willmann et al., 2011; Liu et al., 2012a). Interestingly, another investigation of the evolution of

pathogen recognition genes in tomato/potato unveiled a closer relationship between CNL (coiled coil nucleotide-binding LRR) and LRR-RLP since proteins of both classes tended to cluster more than other proteins belonging to the TNL (Toll/Interleukin-1 nucleotide-binding LRR) and LRR-RLK receptor classes (Andolfo et al., 2013).

The rapid evolution of LRR-RLP genes in different plant species suggested a possible mechanism for plants to acquire novel recognition specificities for microbial pathogens/races in the battle against pathogen. To check the origin of microbial patterns/elicitors recognized by different LRR-RLPs may contribute to the characterization of the specific elicitor recognized by RLP32. Among plant immunity-related LRR-RLPs, only a few have been assigned molecularly defined ligands. *Cladosporium fulvum* secretes avirulence peptides *Avr4* and *Avr9*, which are recognized by tomato LRR-RLPs Cf-4 and Cf-9 respectively (Thomas et al., 1998). *Avr9* is a 28-residues peptide, and present as a three-stranded anti-parallel  $\beta$  sheet (Vervoort et al., 1997). Three disulfide bridges form a conserved cysteine knot structure, which is indispensable for *Avr9/Cf-9* mediated hypersensitive response (Kooman-Gersmann et al., 1997; van den Hooven et al., 1999). *Avr4* is a chitin-binding lectin containing an invertebrate chitin-binding domain (van den Burg et al., 2006). *Avr4* is constituted of 105 amino acids and four disulfide bridges, which form cysteine knot structures as well (Joosten et al., 1994). *Avr4* binds to chitin on the cell wall of fungi to prevent the hydrolysis by plant chitinases (van den Burg et al., 2006). To avoid *Avr4/Cf-4* mediated resistance in plants, *C. fulvum* evolved diverse *Avr4* isoforms by single amino acid substitution (Joosten et al., 1997). Another defined elicitor is the 22-kD ethylene-inducing xylanase (EIX), which is secreted by the fungus *Trichoderma viride* and which is recognized by tomato LRR-RLP LeEix2 (Dean et al., 2005; Ron and Avni, 2004; Sharfman et al., 2011). EIX protein also serves two roles in plant-microbe interactions: on the one hand, it has endo- $\beta$ -1,4-xylanase activity to cleave the  $\beta$ -1,4 linkage of the xylosyl backbone during pathogenicity; on the other hand, it can cause immunity upon leaf injection in tobacco plants, which is mediated by the EIX2 receptor residing in the on plant plasma membrane (Furman-Matarasso et al., 1999). The third elicitor is Ave1, a virulence factor of several phytopathogenic fungi (Kawchuk et

al., 2001). Ave1 is recognized by tomato LRR-RLP protein Ve1 and activates pathogen resistance in tomato (Kawchuk et al., 2001; de Jonge et al., 2012). The Ave1 gene containing region (~50kb) was identified by genome comparison between two races of the fungus *V. dahliae* (de Jonge et al., 2012). Ave1 encodes a 135aa-secreted protein and belongs to a plant natriuretic peptide family, which has large numbers of homologs in fungi, bacteria and plants. The protein has four conserved cysteine residues which are thought to stabilize the protein structure by disulfide bridges after secretion (de Jonge et al., 2012). The fourth elicitor is a fungal endopolygalacturonase (PG), which is recognized by the Arabidopsis RLP42 receptor (Zhang et al., 2014). In addition to the elicitation of a hypersensitive response mediated by PG/RLP42, PGs are also virulence factors and degrade plant cell walls by hydrolyzing the homogalacturonan backbone as pectinases (Zhang et al., 2014). The PG/RLP42-mediated hypersensitive response is independent of catalytic activity, although catalytic breakdown products, oligo-galacturonides (OGAs), serve as DAMP signals (Zhang et al., 2014). The fifth elicitor nlp20, a highly conserved peptide motif universally found across three microorganism kingdoms, is harbored in effector NLPs (necrosis and ethylene-inducing peptide 1 (Nep1)-like proteins) (Böhm et al., 2014). The immunity triggered by pattern nlp20 is also independent of toxin actions of NLPs (Böhm et al., 2014). A recent study unveiled that in Arabidopsis, RLP23 recognized nlp20 and triggered immunity by forming a tripartite complex with co-receptors, SOBIR1 and BAK1 (Albert and Böhm et al. 2015). Other LRR-RLPs in Arabidopsis, such as RLP1 and RLP30, were determined to recognize microbial-associated molecular patterns, but the molecular identity of these elicitors are not clear yet (Zhang, 2013; Jehle et al., 2013). The five well-studied elicitors shared some characteristics. Firstly, most of them displayed high diversity, such as the natural existence of isoforms of Avr4, many homologous of Ave1 among fungi and multiple alleles of PGs in single species (Joosten et al., 1997; Sharfman et al., 2011; Zhang et al., 2014). Secondly, they are highly expressed during host colonization, for example, the gene transcripts of Ave1 and EIX were detected in infected plants and the transcript levels of PGs ranked top among secreted *Botrytis* proteins in *Botrytis*-infected lettuce leaves, grape berries, and tomato fruits (de Jonge et al., 2012; Cantu, 2014; Sharfman et al., 2011). Finally, they

elicit a hypersensitive response in receptor-containing plants and the elicitation was independent of their enzyme activities (Joosten et al., 1997; Sharfman et al., 2011; Zhang et al., 2014; de Jonge et al., 2012). It is not clear whether all PAMP elicitors perceived by LRR-RLPs share the same characteristics such as those mentioned above. The identification of epitope nlp20 from NLPs recently also buttressed the idea of continuums of PTI and ETI (Böhm et al., 2014; Thomma et al., 2011). Together with the fact that LRR-RLP-type PRRs tend to cluster more than LRR-RLK-type PRRs so as to fast generate novel recognition specificities (Andolfo et al., 2013), It is most likely that LRR-RLP-type PRRs play an important role on recognizing effector-derived patterns that might be more similar to immune receptors of the NLR class, which mediate effector-triggered immunity (ETI).

### **5.3. RLP32-mediated signalling.**

RLP32 contains 23 extracellular LRRs and a short cytoplasmic tail domain. How do RLPs, lacking the cytoplasmic kinase domain, trigger the intracellular immunity in plants is unveiled gradually. Recent studies suggested that a few LRR-RLKs were involved in forming receptor complexes with RLPs. The first co-receptor BAK1 is an inter-connector to mediate the BR signal transduction and plant defense responses (Gruszka, 2013). BAK1 and FLS2 form heterodimers with the flg22 ligand sandwiched in between (Sun et al., 2013). FLS2/BAK1 studies have implied that upon ligand exposure, the heterodimerization of non-RD RLK PRR (FLS2) with the strong RD kinase (BAK1) could boost the intracellular immunity signal (Dardick et al., 2012; Macho and Zipfel, 2014). Phenotype studies of the bak1 mutant, such as disease resistance, ethylene biosynthesis, MAPK activity and immunity marker gene expression suggested that BAK1 was required for some RLP-PRR system (Zhang et al., 2013; Fradin et al., 2011). BAK1 is required to activate LRR-RLP *Ve1* in tomato (Fradin et al., 2009; Fradin et al., 2011). Another LRR-RLP *LeEix1* could compete the ligand binding of *LeEix2* with the help of BAK1 (Bar et al., 2011). In *Arabidopsis*, BAK1 was shown to be involved in RLP30-mediated perception of the necrotrophic fungal pathogen *Sclerotinia sclerotiorum* (Zhang et al., 2013). In addition, the other members of the SERK family (to which BAK1 belongs, BAK1=SERK3) are also involved in the ligand



perception by RLP-PRRs. *Ve1*-mediated resistance to *V. dahliae* race 1 was compromised in the *serk1* and *serk4* mutants in *Arabidopsis* while only *SISERK1* was required for *Ve1*-mediated *Verticillium* resistance in tomato (Fradin et al., 2011). *SISERK1* was required for *Cf-4*-mediated *Cladosporium* resistance (Fradin et al., 2011). *SERK4* was required for RLP23 mediated immunity (Albert and Böhm et al. 2015). All evidences suggested that other SERK proteins seem to functionally redundant to BAK1 in PAMP perception. In our study, RLP32 behaves like most other RLPs implicated in plant immunity as it requires BAK1 for ligand-induced immunity.

Unlike BAK1, the second co-receptor SOBIR1 is believed to serve only in RLP-PRR perception systems (Liebrand et al., 2013). SOBIR1 is required for most of the known LRR-RLP-type PRRs, including *Arabidopsis* RLP1, RLP30, RLP42, RLP23 and tomato *Cf-4*, *Cf-2*, *Cf-9*, *Ve-1* and *EIX2/EIX1* (Gust and Felix, 2014). Either RLP30 or RLP42 was constitutively and physically associated to SOBIR1 (Zhang, 2013; Zhang et al., 2014). A previous study reported that that phosphorylation of SOBIR1 after effector *Avr4* binding to *Cf-4* made it accessible for SERKs to enter the receptor complex (Zhang et al., 2013). Solid evidence showed that RLP23 interacted with SOBIR1 in a *nlp20* (ligand)-independent way and RLP23 SOBIR1 complex further recruits BAK1 to initiate intracellular signal transduction in a *nlp20* dependent way (Albert and Böhm et al. 2015). This new finding strongly supported current notions that RLP SOBIR1 bimolecular module equals RLK function (Gust and Felix, 2014). The evidence also revealed that the transmembrane helix motif of RLP23 is critical for RLP23 to form complex structure with SOBIR1 (correspondence with Dr. Albert). Similarly, we showed that RLP32-mediated *RsE2* perception was compromised in the *bak1/bkk1* double mutant or in the *sobir1* mutant, although the physical interaction of the three proteins in a tripartite complex remains to be shown.

How the immune signal initiated by RLP32/BAK1/SOBIR1 tripartite receptors is transduced is unclear. It might mimic LRR-RLK-type receptors and involve several receptor-like cytoplasmic kinases, such as BIK1, PBL1 (PBS1-like protein 1), PBL2 (PBS1-like protein 2) and PBL5 (PBS1-like protein 5) (Liebrand et al., 2013; Zhang et al., 2010; Ronald, 2012; Liu et al., 2013). *Botrytis*-induced kinase 1 (BIK1) was constitutively associated with FLS2, EFR and CERK1

(Zhang et al., 2010). The ligand binding of FLS2 initiated the release of BIK1 from the FLS2/Bak1 complex (Lu et al., 2010). Another receptor PEPR1 (DAMP Pep1 receptor) could phosphorylate BIK1 directly and consequently elicit the expression of defense genes (Liu et al., 2013). Moreover, NADPH oxidase RBOHD was found to be the substrate of BIK1 and could mediate the elicitor-induced ROS burst and stomata defense (Kadota et al., 2014; Li et al., 2014). Therefore, searching for evidence to associate RLP32/BAK1/SOBIR1 tripartite receptors with RLCKs is an interesting study in the future. Using systematic approaches such as PAMP/receptor stimulated RNAseq analysis and phosphoproteomic methodology might accelerate such an approach (Jones et al., 2006; Nühse et al., 2007; Macho and Zipfel, 2014; Navarro et al., 2004; Tao et al., 2003).

#### 5.4. Biotechnological application of novel PRRs

Although PAMPs represent very conserved molecular structures among microbes, the corresponding recognition systems for most PAMPs are often only contained in limited plant families or species. The elicitor flagellin triggered an alkalization response in cell cultures from many species such as *Arabidopsis*, tomato, *N. benthamiana* and potato (Felix et al., 1999). The perception system of flagellin exists in both monocotyledonous and dicotyledonous species (Lacombe et al., 2010). In contrast, the elicitor EF-Tu triggered immune responses within *Brassicaceae*, such as *Arabidopsis*, *Brassica alboglabra*, *B. oleracea* and *Sinapis alba*, but not in *N. benthamiana*, potato, cucumber, sunflower, soybean and *Yucca alifoli* (Kunze, 2004). Another bacterial elicitor eMax also induced ethylene biosynthesis mainly in the *Brassicaceae* family but not in tomato, *N. benthamiana* and *Pisum sativum* (Jehle et al., 2013). In our study, RsE2 is a partially purified elicitor from *Ralstonia solanacearum* and the preliminary assays of ethylene biosynthesis in multiple garden-grown plants suggested that several species from six families, *Apiaceae*, *Asteraceae*, *Brassicaceae*, *Fabaceae*, *Moraceae* and *Solanaceae* could elicit ethylene biosynthesis upon the RsE2 treatment (Figure 7.2). However, it remains to be verified that such broad elicitation is not due to impurities within the RsE2 preparation.

A long-term goal to study the RsE2 perception system is to confer the pathogen resistance through an interfamily transfer of PAMP perception systems. *Ralstonia solanacearum* is a soil-borne Gram-negative plant pathogen, causing wilt in broad plant host species, such as tomato, pepper, eggplant, potato, banana, ginger, olive and tobacco ([http://en.wikipedia.org/wiki/Ralstonia\\_solanacearum](http://en.wikipedia.org/wiki/Ralstonia_solanacearum)). Our study suggested that transient expression of RLP32 from the *Brassicaceae* plant family in *N. benthamiana* seedlings could confer the capability of elicitor perception in the *Solanaceae* plant family, although we still need to confirm *in vivo* the improved disease resistance to *Ralstonia solanacearum*. Recent evidences showed that rlp32 mutants, Mr-0 and ICE73 (insensitive ecotypes), and sobir1 mutants were more susceptible to *Ralstonia solanacearum* than Col-0 (correspondence with Katja Fröhlich). A few recent studies have suggested that transferring a plant PRR system could confer broad-spectrum pathogen resistance to crops (Lacombe et al., 2010). When the *Brassicaceae*-specific PRR EFR was transferred into two Solanaceous species, *N. benthamiana* and *S. lycopersicum*, homozygous transgenic plants not only gained full responsiveness to the elicitor elf18, but also conferred disease resistance with significant reduced symptoms caused by multiple pathogens, such as *P.syringae* pv. *syringae* (*Pss*), *P.syringae* pv. *tabaci* (*Pta*), *A. tumefaciens* and *Ralstonia solanacearum* (Lacombe et al., 2010). EFR over-expressing transgenic plants, which do not show constitutively activated defense responses, were not found to improve resistance to the fungal pathogen *Verticillium dahliae* (Lacombe et al., 2010). The rlp30 mutant showed susceptibility to the bacterial pathogen *Pseudomonas syringae* pv. *phaseolicola* (*Psp*) as well as to the fungal pathogen, *Sclerotinia sclerotiorum* (Wang et al., 2008, Zhang et al., 2013). This suggested the potential to confer constitutive resistance to crops by expressing RLP30 ectopically. The recent ectopic expression of RLP23 was another successful utilization of inter-family transgenic PRR transfer to enhance immunity. RLP23, specifically found in members of the *Brassicaceae* family, was stably expressed in *Solanaceae* species lacking a nlp20 perception system. Transgenic plants showed less susceptibility to nlp20-producing pathogens *Phytophthora infestans* (Albert and Böhm et al. 2015). In our study, stable RLP32-transgenic-*N. benthamiana* or

tomato plants will be required in the future to illustrate the value to use the RsE2 perception system to improve disease resistance in solanaceous plants, which is the plant family that is most susceptible to the *Ralstonia solanacearum* pathogen. Furthermore, over-expression of RLP32 in transgenic Arabidopsis, which were generated in this study (Table 7.5), will also prove valuable to assess broad-spectrum disease resistance mediated by this receptor.

Our study suggests a potential application of breeding technology to accumulate suitable PAMP receptor alleles within one crop such as tomato, in order to gain broad disease resistance by non-overlapping microbial perception systems. One example would be to express RLP23 and RLP32 together to cope with *P. infestans* (RLP23) and *Ralstonia solanacearum* (RLP32) by the same time. This finding also supports current ideas about the application of stacked PRRs or R genes in transgenic plants to gain broad-spectrum durable disease resistance (Lacombe et al., 2010; Gust et al., 2010). Using ever-cheaper DNA sequencing technology to sequence more pathovars for particular types of pathogens disclosed the concept of core effectors, which allows scientists to engineer stacks of core effector-activated R genes to acquire broad and sustainable disease resistance (Mukhtar et al., 2011; Weßling et al., 2014). The combined application of stacked PRRs and NLRs to activate the two layers of plant immunity (PTI, ETI) extracellularly and intracellularly, together with other strategies such as inhibiting the proliferation of pathogens and coating the seeds with antipathogenic probiotics, are believed to replace the traditional chemical control in future agriculture (Dangl et al., 2013).

## 6. References

- Albert, M., Jehle, A.K., Mueller, K., Eisele, C., Lipschis, M., and Felix, G.** (2010). Arabidopsis thaliana Pattern Recognition Receptors for Bacterial Elongation Factor Tu and Flagellin Can Be Combined to Form Functional Chimeric Receptors. *J. Biol. Chem.* **285**, 19035–19042.
- Albert, I., Böhm, H., Albert, M., Feiler, C.E., Imkampe, J., Wallmeroth, N., Brancato, C., Raaymakers, T.M., Oome, S., Zhang, H., Krol, E., Grefen, C., Gust, A.A., Chai, J., Hedrich, R., van den Ackerveken, G., and Nürnberger, T.** (2015). An RLP23-SOBIR1-BAK1 complex mediates NLP-triggered immunity. *Nat. Plants* **1**, 15140.
- Andolfo, G., Sanseverino, W., Rombauts, S., Peer, Y., Bradeen, J.M., Carputo, D., Frusciante, L., and Ercolano, M.R.** (2013). Overview of tomato (*Solanum lycopersicum*) candidate pathogen recognition genes reveals important *Solanum* R locus dynamics. *New Phytol.* **197**, 223–237.
- Aranzana, M.J., Kim, S., Zhao, K., Bakker, E., Horton, M., Jakob, K., Lister, C., Molitor, J., Shindo, C., Tang, C., Toomajian, C., Traw, B., Zheng, H., Bergelson, J., Dean, C., Marjoram, P., and Nordborg, M.** (2005). Genome-Wide Association Mapping in Arabidopsis Identifies Previously Known Flowering Time and Pathogen Resistance Genes. *PLoS Genet.* **1**, e60.
- Asai, T., Tena, G., Plotnikova, J., Willmann, M.R., Chiu, W.-L., Gómez Gómez, L., Boller, T., Ausubel, F.M., and Sheen, J.** (2002). MAP kinase signalling cascade in Arabidopsis innate immunity. *Nature* **415**, 977–983.
- Atwell, S. et al.** (2010). Genome-wide association study of 107 phenotypes in Arabidopsis thaliana inbred lines. *Nature* **465**, 627–631.
- Baird, N.A., Etter, P.D., Atwood, T.S., Currey, M.C., Shiver, A.L., Lewis, Z.A., Selker, E.U., Cresko, W.A., and Johnson, E.A.** (2008). Rapid SNP Discovery and Genetic Mapping Using Sequenced RAD Markers. *PLoS ONE* **3**, e3376.
- Bar, M., Sharfman, M., and Avni, A.** (2011). LeEix1 functions as a decoy receptor to attenuate LeEix2 signaling. *Plant Signal Behav.* **6**:3, 455-457
- Bar, M., Sharfman, M., Ron, M., and Avni, A.** (2010). BAK1 is required for the attenuation of ethylene-inducing xylanase (Eix)-induced defense responses by the decoy receptor LeEix1. *Plant J.* **63**, 791–800.
- Bauer, Z., Gomez-Gomez, L., Boller, T., and Felix, G.** (2001). Sensitivity of different ecotypes and mutants of Arabidopsis thaliana toward the bacterial elicitor flagellin correlates with the presence of receptor-binding sites. *J. Biol. Chem.* **276**, 45669–45676.
- Blanco-Ulate, B., Morales-Cruz, A., Amrine, K.C.H., Labavitch, J.M., Powell, A.L.T., and Cantu, D.** (2014). Genome-wide transcriptional profiling of Botrytis cinerea genes targeting plant cell walls during infections of different hosts.

Front. Plant Sci. **5**, 435. **Böhm, H., Albert, I., Fan, L., Reinhard, A., and Nürnberger, T.** (2014). Immune receptor complexes at Plant Cell surface. *Curr. Opin. Plant Biol.* **20**, 47-54.

**Böhm, H., Albert, I., Oome, S., Raaymakers, T.M., van den Ackerveken, G., and Nürnberger, T.** (2014). A Conserved Peptide Pattern from a Widespread Microbial Virulence Factor Triggers Pattern-Induced Immunity in Arabidopsis. *PLoS Pathog.* **10**, e1004491.

**Bouwmeester, K., and Govers, F.** (2009). Arabidopsis L-type lectin receptor kinase: phylogeny, classification, and expression profiles. *J. Exp. Bot.* **60**, 4383-4396.

**Bouwmeester, K., Han, M., Blanco-Portales, R., Song, W., Weide, R., Guo, L.-Y., van der Vossen, E.A.G., and Govers, F.** (2014). The Arabidopsis lectin receptor kinase LecRK-I.9 enhances resistance to *Phytophthora infestans* in Solanaceous plants. *Plant Biotechnol. J.* **12**, 10-16.

**Brunner, F., Rosahl, S., Lee, J., Rudd, J.J., Rasmussen, G., Scheel, D., and Nürnberger, T.** (2002). Pep-13, a plant defense-inducing pathogen-associated pattern from *Phytophthora* transglutaminases. *EMBO J.* **21**, 6681-6688.

**Brutus, A., Sicilia, F., Macone, A., Cervone, F., and De Lorenzo, G.** (2010). A domain swap approach reveals a role of the plant wall-associated kinase 1 (WAK1) as a receptor of oligogalacturonides. *Proc. Natl. Acad. Sci. USA* **107**, 9452–9457.

**Buell, C.R., Joardar, V., Lindeberg, M., Selengut, J., Paulsen, I.T., Gwinn, M.L., Dodson, R.J., Deboy, R.T., Durkin, A.S., Kolonay, J.F., Madupu, R., Daugherty, S., Brinkac, L., Beanan, M.J., Haft, D.H., Nelson, W.C., Davidsen, T., Zafar, N., Zhou, L., Liu, J., Yuan, Q., Khouri, H., Feldblyum, T.V., D'Ascenzo, M., Deng, W.L., Ramos, A.R., Alfano, J.R., Cartinhour, S., Chatterjee, A.K., Delaney, T.P., Lazarowitz, S.G., Martin, G.B., Schneider, D.J., Tang, X., Bender, C.L., White, O., Fraser, C.M., and Collmer, A.** (1996). The complete genome sequence of the Arabidopsis and tomato pathogen *Pseudomonas syringae* pv. tomato DC3000. *Proc. Natl. Acad. Sci. USA* **100**, 10181-10186.

**Cao, J., Schneeberger, K., Ossowski, S., Günther, T., Bender, S., Fitz, J., Koenig, D., Lanz, C., Stegle, O., Lippert, C., Wang, X., Ott, F., Müller, J., Alonso-Blanco, C., Borgwardt, K., Schmid, K.J., and Weigel, D.** (2011). Whole-genome sequencing of multiple Arabidopsis thaliana populations. *Nat. Genet.* **43**, 956–963.

**Chae, E., Bomblies, K., Kim, S-T., Karelina, D., Zaidem, M., Ossowski, S., Martin-Pizarro, C., Laitinen, R.A.E., Rowan, B.A., Tenenboim, H., Lechner, S., Demar, M., Habring-Müller, A., Lanz, C., Rättsch, G., and Weigel, D.** (2014). Species-wide genetic incompatibility analysis identifies immune genes as hot spots of deleterious epistasis. *Cell* **159**, 1341–1351.

**Chen, X.W., Shang, J., Chen, D., Lei, C., Zou, Y., Zhai, W., Liu, G., Xu, J., Ling, Z., Cao, G., Ma, B., Wang, Y., Zhao, X., Li, S., and Zhu, L.** (2006). A B-

lectin receptor kinase gene conferring rice blast resistance. *Plant J.* **46**, 794–804.

**Chen, X., Zuo, S., Schwessinger, B., Chern, M., Canlas, P.E., Ruan, D., Zhou, X., Wang, J., Daudi, A., Petzold, C.J., Heazlewood, J.L., and Ronald, P.C.** (2014). An XA21-Associated Kinase (OsSERK2) Regulates Immunity Mediated by the XA21 and XA3 Immune Receptors. *Mol. Plant* **7**, 874–892.

**Chinchilla, D., Bauer, Z., Regenass, M., Boller, T., and Felix, G.** (2006). The Arabidopsis receptor kinase FLS2 binds flg22 and determines the specificity of flagellin perception. *Plant Cell* **18**, 465–476.

**Chinchilla, D., Zipfel, C., Robatzek, S., Kemmerling, B., Nürnberger, T., Jones, J.D.G., Felix, G., and Boller, T.** (2007). A flagellin-induced complex of the receptor FLS2 and BAK1 initiates plant defence. *Nature* **448**, 497–500.

**Choi, J., Tanaka, K., Cao, Y., Qi, Y., Qiu, J., Liang, Y., Lee, S.Y., and Stacey, G.** (2014). Identification of a plant receptor for extracellular ATP. *Science* **343**, 290–294.

**Christiaan Greeff, M.R.J.M.M.P.** (2012). Receptor-like kinase complexes in plant innate immunity. *Front. Plant Sci.* **3**, 209.

**Clark, R.M.** (2010). Genome-wide association studies coming of age in rice. *Nat Genet* **42**: 926–927.

**Coventry, H., and Dubery, I.A.** (2001). Lipopolysaccharides from *Burkholderia cepacia* contribute to an enhanced defensive capacity and the induction of pathogenesis-related proteins in *Nicotiana tabacum*. *Physiol. Mol. Plant Path.* **58**: 149–158.

**Dangl, J.L., Horvath, D.M., and Staskawicz, B.J.** (2013). Pivoting the plant immune system from dissection to deployment. *Science* **341**, 746–751.

**Dardick, C., Schwessinger, B., and RONALD, P.** (2012). Non-arginine-aspartate (non-RD) kinases are associated with innate immune receptors that recognize conserved microbial signatures. *Curr. Opin. Plant Biol.* **15**, 358–366.

**Davey, J.W., Hohenlohe, P.A., Etter, P.D., Boone, J.Q., Catchen, J.M., and Blaxter, M.L.** (2011). Genome-wide genetic marker discovery and genotyping using next-generation sequencing. *Nat. Rev. Genet.* **12**, 499–510.

**de Jonge, R., van Esse, H.P., Maruthachalam, K., Bolton, M.D., Santhanam, P., Saber, M.K., Zhang, Z., Usami, T., Lievens, B., Subbarao, K.V., and Thomma, B.P.H.J.** (2012). Tomato immune receptor Ve1 recognizes effector of multiple fungal pathogens uncovered by genome and RNA sequencing. *Proc. Natl. Acad. Sci. USA* **109**, 5110–5115.

**Decreux, A., Thomas, A., Spies, B., Brasseur, R., Cutsem, P., and Messiaen, J.** (2006). In vitro characterization of the homogalacturonan-binding domain of the wall-associated kinase WAK1 using site-directed mutagenesis. *Phytochemistry* **67**, 1068–1079.

- Du, J., Verzaux, E., Chaparro-Garcia, A., Bijsterbosch, G., Paul Keizer, L.C., Zhou, J., Liebrand, T.W.H., Xie, C., Govers, F., Robatzek, S., van der Vossen, E.A.G., Jacobsen, E., Visser, R.G.F., Kamoun, S. and Vleeshouwers, V.G.A.A. (2015). Elicitin recognition confers enhanced resistance to *Phytophthora infestans* in potato. *Nat. Plants* **1** SP - EP .
- Dunning, F.M., Sun, W., Jansen, K.L., Helft, L., and Bent, A.F. (2007). Identification and Mutational Analysis of Arabidopsis FLS2 Leucine-Rich Repeat Domain Residues That Contribute to Flagellin Perception. *Plant Cell* **19**, 3297–3313.
- Dean, J.F.D., Gross, K.C., and Anderson, J.D. (1991). Ethylene Biosynthesis-Inducing Xylanase. *Plant Physiol.* **96**, 571-576.
- Elshire, R.J., Glaubitz, J.C., Sun, Q., Poland, J.A., Kawamoto, K., Buckler, E.S., and Mitchell, S.E. (2011). A robust, simple genotyping-by-sequencing (GBS) approach for high diversity species. *PLoS ONE* **6**, e19379.
- Felix, G., Duran, J.D., Volko, S., and Boller, T. (1999). Plants have a sensitive perception system for the most conserved domain of bacterial flagellin. *Plant J.* **18**, 265–276.
- Felix, G., Regenass, M., and Boller, T. (1993). Specific perception of subnanomolar concentrations of chitin fragments by tomato cells: induction of extracellular alkalization, changes in protein phosphorylation, and establishment of a refractory state. *Plant J.* **4**, 307-316.
- Fradin, E.F., Abd-El-Hallem, A., Masini, L., van den Berg, G.C.M., Joosten, M.H.A.J., and Thomma, B.P.H.J. (2011). Interfamily transfer of tomato Ve1 mediates *Verticillium* resistance in Arabidopsis. *Plant Physiol.* **156**, 2255–2265.
- Fradin, E.F., Zhang, Z., Juarez Ayala, J.C., Castroverde, C.D.M., Nazar, R.N., Robb, J., Liu, C., and Thomma, B.P.H.J. (2009). Genetic dissection of *Verticillium* wilt resistance mediated by tomato Ve1. *Plant Physiol.* **150**, 320–332.
- Fritz-Laylin, L.K., Krishnamurthy, N., Tör, M., Sjölander, K.V., and Jones, J.D.G. (2005). Phylogenomic analysis of the receptor-like proteins of rice and Arabidopsis. *Plant Physiol.* **138**, 611–623.
- Furman-Matarasso, N., Cohen, E., Du, Q., Chejanovsky, N., Hannania, U., and Avni, A. (1999). A Point Mutation in the Ethylene-Inducing Xylanase Elicitor Inhibits the  $\beta$ -1-4-endoxylanase activity but not the elicitation activity. *Plant Physiol.* **121**, 345-351.
- Gómez Gómez, L., and Boller, T. (2000). FLS2: An LRR Receptor-like Kinase Involved in the Perception of the Bacterial Elicitor Flagellin in Arabidopsis. *Mol. Cell* **5**, 1003-1011.
- Gómez Gómez, L., Felix, G., and Boller, T. (1999). A single locus determines sensitivity to bacterial flagellin in Arabidopsis thaliana. *Plant J.* **18**, 277–284.



- Gruszka, D.** (2013). The Brassinosteroid Signaling Pathway—New Key Players and Interconnections with Other Signaling Networks Crucial for Plant Development and Stress Tolerance. *Int. J. Mol. Sci.* **14**, 8740–8774.
- Gust, A.A. and Felix, G.** (2014). ScienceDirect Receptor like proteins associate with SOBIR1-type of adaptors to form bimolecular receptor kinases. *Curr. Opin. Plant Biol.* **21**, 104–111.
- Gust, A.A., Biswas, R., Lenz, H.D., Rauhut, T., Ranf, S., Kemmerling, B., Gotz, F., Glawischnig, E., Lee, J., Felix, G., and Nürnberger, T.** (2007). Bacteria-derived Peptidoglycans Constitute Pathogen-associated Molecular Patterns Triggering Innate Immunity in Arabidopsis. *J. Biol. Chem.* **282**, 32338–32348.
- Gust, A.A., Brunner, F.D.R., and Nürnberger, T.** (2010). Biotechnological concepts for improving plant innate immunity. *Curr. Opin. Biotechnol.* **21**, 204–210.
- Gust, A.A., Willmann, R., Desaki, Y., Grabherr, H.M., and Nürnberger, T.** (2012). Plant LysM proteins: modules mediating symbiosis and immunity. *Trends Plant Sci.* **17**, 495–502.
- Hann, D.R. and Rathjen, J.P.** (2007). Early events in the pathogenicity of *Pseudomonas syringae* on *Nicotiana benthamiana*. *Plant J.* **49**, 607–618.
- Hao, G., Pitino, M., Ding, F., Lin, H., Stover, E., and Duan, Y.** (2014). Induction of innate immune responses by flagellin from the intracellular bacterium, '*Candidatus Liberibacter solanacearum*'. *BMC Plant Biol.* **14**, 211.
- Heese, A., Hann, D.R., Gimenez-Ibanez, S., Jones, A.M.E., He, K., Li, J., Schroeder, J.I., Peck, S.C., and Rathjen, J.P.** (2007). The receptor-like kinase SERK3/BAK1 is a central regulator of innate immunity in plants. *Proc. Natl. Acad. Sci. USA* **104**, 12217–12222.
- Holton, N., Nekrasov, V., Ronald, P.C., and Zipfel, C.** (2015). The phylogenetically-related pattern recognition receptors EFR and XA21 recruit similar immune signaling components in monocots and dicots. *PLoS Pathog.* **11**, e1004602.
- Hosford, R.M., Jr** (1975). *Platyspora pentamera*, a Pathogen of Wheat. *Phytopathology* **65**, 499.
- Jehle, A.K., Fürst, U., Lipschis, M., Albert, M., and Felix, G.** (2013). Perception of the novel MAMP eMax from different *Xanthomonas* species requires the Arabidopsis receptor-like protein ReMAX and the receptor kinase SOBIR. *Plant Signal Behav.* **8**, e27408.
- Jehle, A.K., Lipschis, M., Albert, M., Fallahzadeh-Mamaghani, V., Fürst, U., Mueller, K., and Felix, G.** (2013). The receptor-like protein ReMAX of Arabidopsis detects the microbe-associated molecular pattern eMax from *Xanthomonas*. *Plant Cell* **25**, 2330–2340.

- Jeong, S., Trotochaud, A.E., and Clark, S.E.** (1999). The Arabidopsis CLAVATA2 gene encodes a receptor-like protein required for the stability of the CLAVATA1 receptor-like kinase. *Plant Cell* **11**, 1925-1933.
- Jones, A.M.E., Bennett, M.H., Mansfield, J.W., and Grant, M.** (2006). Analysis of the defence phosphoproteome of Arabidopsis thaliana using differential mass tagging. *Proteomics* **6**, 4155–4165.
- Jones, D.A., Thomas, C.M., Hammond-Kosack, K.E., Balint-Kurti, P.J., and Jones, J.D.** (1994). Isolation of the tomato Cf-9 gene for resistance to Cladosporium fulvum by transposon tagging. *Science* **266**, 789–793.
- Jones, J.D.G., Witek, K., Verweij, W., Jupe, F., Cooke, D., Dorling, S., Tomlinson, L., Smoker, M., Perkins, S., and Foster, S.** (2014). Elevating crop disease resistance with cloned genes. *Philos. Trans. R. Soc. Lond. B. Biol. Sci.* **369**, 20130087–20130087.
- Joosten, M.H., Cozijnsen, T.J., and De Wit, P.J.** (1994). Host resistance to a fungal tomato pathogen lost by a single base-pair change in an avirulence gene. *Nature* **367**, 384–386.
- Joosten, M.H., Vogelsang, R., Cozijnsen, T.J., Verberne, M.C., and De Wit, P.J.** (1997). The biotrophic fungus Cladosporium fulvum circumvents Cf-4-mediated resistance by producing unstable AVR4 elicitors. *Plant Cell* **9**, 367–379.
- Kadota, Y., Sklenar, J., Derbyshire, P., Stransfeld, L., Asai, S., Ntoukakis, V., Jones, J.D., Shirasu, K., Menke, F., Jones, A., and Zipfel, C.** (2014). Direct Regulation of the NADPH Oxidase RBOHD by the PRR-Associated Kinase BIK1 during Plant Immunity. *Mol. Cell* **54**, 43–55.
- Kaku, H., Nishizawa, Y., Ishii-Minami, N., Akimoto-Tomiyama, C., Dohmae, N., Takio, K., Minami, E., and Shibuya, N.** (2006). Plant cells recognize chitin fragments for defense signaling through a plasma membrane receptor. *Proc. Natl. Acad. Sci. USA* **103**, 11086-11091.
- Karimi, M., Depicker, A., and Hilson, P.** (2007). Recombinational Cloning with Plant Gateway Vectors. *Plant Physiol.* **145**, 1144–1154.
- Karimi, M., Inzé, D., and Depicker, A.** (2002). GATEWAY™ vectors for Agrobacterium-mediated plant transformation. *Trends Plant Sci.* **7**, 193–195.
- Kawchuk, L.M., Hachey, J., Lynch, D.R., Kulcsar, F., van Rooijen, G., Waterer, D.R., Robertson, A., Kokko, E., Byers, R., Howard, R.J., Fischer, R., and Pruffer, D.** (2001). Tomato Ve disease resistance genes encode cell surface-like receptors. *Proc. Natl. Acad. Sci. USA* **98**, 6511–6515.
- Khakh, B.S. and Burnstock, G.** (2009). The double life of ATP. *Sci. Am.* **301**, 84-92.
- Klein, R.J. et al.** (2005). Complement factor H polymorphism in age-related macular degeneration. *Science* **308**, 385–389.

- Konieczny, A. and Ausubel, F.M.** (1993). A procedure for mapping Arabidopsis mutations using co-dominant ecotype-specific PCR-based markers. *Plant J.* **4**, 403–410.
- Kooman-Gersmann, M., Vogelsang, R., Hoogendijk, E.C.M., and de Wit, P.J.G.M.** (1997). Assignment of Amino Acid Residues of the AVR9 Peptide of *Cladosporium fulvum* That Determine Elicitor Activity. *Mol. Plant Microbe Interact.* **10**, 821–829.
- Kovtun, Y., Chiu, W.L., Tena, G., and Sheen, J.** (2000). Functional analysis of oxidative stress-activated mitogen-activated protein kinase cascade in plants. *Proc. Natl. Acad. Sci. USA* **97**, 2940–2945.
- KRUIJT, M., DE KOCK, M.J.D., and de Wit, P.J.G.M.** (2005). Receptor-like proteins involved in plant disease resistance. *Mol. Plant Path.* **6**, 85–97.
- Kunze, G.** (2004). The N Terminus of Bacterial Elongation Factor Tu Elicits Innate Immunity in Arabidopsis Plants. *Plant Cell* **16**, 3496–3507.
- Lacombe, S., Rougon-Cardoso, A., Sherwood, E., Peeters, N., Dahlbeck, D., van Esse, H.P., Smoker, M., Rallapalli, G., Thomma, B.P.H.J., Staskawicz, B., Jones, J.D.G., and Zipfel, C.** (2010). Interfamily transfer of a plant pattern-recognition receptor confers broad-spectrum bacterial resistance. *Nat. Biotechnol.* **28**, 365–369.
- Li, L., Li, M., Yu, L., Zhou, Z., Liang, X., Liu, Z., Cai, G., Gao, L., Zhang, X., Wang, Y., Chen, S., and Zhou, J.-M.** (2014). The FLS2-Associated Kinase BIK1 Directly Phosphorylates the NADPH Oxidase RbohD to Control Plant Immunity. *Cell Host Microbe* **15**, 329–338.
- Liebrand, T.W.H., van den Burg, H.A., and Joosten, M.H.A.J.** (2013). Two for all: receptor-associated kinases SOBIR1 and BAK1. *Trends Plant Sci.* **19**, 123–132.
- Liebrand, T.W.H., van den Berg, G.C.M., Zhang, Z., Smit, P., Cordewener, J.H.G., America, A.H.P., Sklenar, J., Jones, A.M.E., Tameling, W.I.L., Robatzek, S., Thomma, B.P.H.J., and Joosten, M.H.A.J.** (2013). Receptor-like kinase SOBIR1/EVR interacts with receptor-like proteins in plant immunity against fungal infection. *Proc. Natl. Acad. Sci. USA* **110**, 10010–10015.
- Lindeberg, M., Stavrinides, J., Chang, J.H., Alfano, J.R., Collmer, A., Dangl, J.L., Greenberg, J.T., Mansfield, J.W., and Guttman, D.S.** (2005). Unified nomenclature and phylogenetic analysis of extracellular proteins delivered by the type III secretion system of the plant pathogenic bacterium *Pseudomonas syringae*. *Mol. Plant Microbe Interact.* **18**, 275–282.
- Liu, B., Li, J-F., Ao, Y., Qu, J., Li, Z., Su, J., Zhang, Y., Liu, J., Feng, D., Qi, K., He, Y., Wang, J., and Wang, H-B.** (2012a). Lysin motif-containing proteins LYP4 and LYP6 play dual roles in peptidoglycan and chitin perception in rice innate immunity. *Plant Cell* **24**, 3406–3419.
- Liu, T., Liu, Z., Song, C., Hu, Y., Han, Z., She, J., Fan, F., Wang, J., Jin, C.,**

- Chang, J., Zhou, J.M., and Chai, J.** (2012b). Chitin-Induced Dimerization Activates a Plant Immune Receptor. *Science* **336**, 1160–1164.
- Liu, Z., Wu, Y., Yang, F., Zhang, Y., Chen, S., Xie, Q., Tian, X., and Zhou, J.** (2013). BIK1 interacts with PEPRs to mediate ethylene-induced immunity. *Proc. Natl. Acad. Sci. USA* **110**, 6205-6210.
- Lu, D., Wu, S., Gao, X., Zhang, Y., Shan, L., and He, P.** (2010). A receptor-like cytoplasmic kinase, BIK1, associates with a flagellin receptor complex to initiate plant innate immunity. *Proc. Natl. Acad. Sci. USA* **107**, 496–501.
- Luna, E., Pastor, V., Robert, J., Flors, V., Mauch-Mani, B., and Ton, J.** (2011). Callose deposition: a multifaceted plant defense response. *Mol. Plant Microbe Interact.* **24**, 183–193.
- Macho, A.P. and Zipfel, C.** (2014). Plant PRRs and the Activation of Innate Immune Signaling. *Mol. Cell* **54**, 263–272.
- Malinovsky, F.G., Fangel, J.U., and Willats, W.G.T.** (2014). The role of the cell wall in plant immunity. *Front. Plant Sci.* **5**, 178.
- Manolio, T.A., Collins, F.S., Cox, N.J., Goldstein, D.B., Hindorff, L.A., Hunter, D.J., McCarthy, M.I., Ramos, E.M., Cardon, L.R., Chakravarti, A., Cho, J.H., Guttmacher, A.E., Kong, A., Kruglyak, L., Mardis, E., Rotimi, C.N., Slatkin, M., Valle, D., Whittemore, A.S., Boehnke, M., Clark, A.G., Eichler, E.E., Gibson, G., Haines, J.L., Mackay, T.F.C., McCarroll, S.A., and Visscher, P.M.** (2009). Finding the missing heritability of complex diseases. *Nature* **461**, 747–753.
- Melzer, E.** (2013). Charakterisierung eines neuen bakteriellen Elicitors von *Ralstonia solanacearum* in *Arabidopsis thaliana*. Dissertation 1–139.
- Meyer, A., Pühler, A., and Niehaus, K.** (2001). The lipopolysaccharides of the phytopathogen *Xanthomonas campestris* pv. *campestris* induce an oxidative burst reaction in cell cultures of *Nicotiana tabacum*. *Planta* **213**, 214-222.
- Miya, A., Albert, P., Shinya, T., Desaki, Y., Ichimura, K., Shirasu, K., Narusaka, Y., Kawakami, N., Kaku, H., and Shibuya, N.** (2007). CERK1, a LysM receptor kinase, is essential for chitin elicitor signaling in Arabidopsis. *Proc. Natl. Acad. Sci. USA* **104**, 19613-19618.
- Monaghan, J. and Zipfel, C.** (2012). Plant pattern recognition receptor complexes at the plasma membrane. *Curr. Opin. Plant Biol.* **15**, 349–357.
- Mukhtar, M.S., Carvunis, A-R., Dreze, M., Epple, P., Steinbrenner, J., Moore, J., Tasan, M., Galli, M., Hao, T., Nishimura, M.T., Pevzner, S.J., Donovan, S.E., Ghamsari, L., Santhanam, B., Romero, V., Poulin, M.M., Gebreab, F., Gutierrez, B.J., Tam, S., Monachello, D., Boxem, M., Harbort, C.J., McDonald, N., Gai, L., Chen, H., He, Y., EU Effectoromics Consortium, Vandenhoute, J., Roth, F.P., Hill, D.E., Ecker, J.R., Vidal, M., Beynon, J., Braun, P., and Dangl, J.L.** (2011). Independently Evolved Virulence Effectors Converge onto Hubs in a Plant Immune System Network. *Science* **333**, 596–

601.

**Nadeau, J.A.** (2002). Control of Stomatal Distribution on the Arabidopsis Leaf Surface. *Science* **296**, 1697–1700.

**Nakagawa, T., Kurose, T., Hino, T., Tanaka, K., Kawamukai, M., Niwa, Y., Toyooka, K., Matsuoka, K., Jinbo, T., and Kimura, T.** Development of series of gateway binary vectors, pGWBs, for realizing efficient cloning of fusion genes for plant transformation. *J. Biosci. Bioeng.* **104**, 34–41.

**Nam, K.H., and Li, J.** (2002). BRI1/BAK1, a receptor kinase pair mediating brassinosteroid signaling. *Cell* **110**, 203–212.

**Navarro, L., Zipfel, C., Rowland, O., Keller, I., Robatzek, S., Boller, T., and Jones, J.D.G.** (2004). The transcriptional innate immune response to flg22. Interplay and overlap with Avr gene-dependent defense responses and bacterial pathogenesis. *Plant Physiol.* **135**, 1113–1128.

**Nieves, W., Heang, J., Asakrah, S., Höner zu Bentrup, K., Roy, C.J., and Morici, L.A.** (2010). Immunospecific Responses to Bacterial Elongation Factor Tu during Burkholderia Infection and Immunization. *PLoS ONE* **5**, e14361.

**Nishimura, M.T. and Dangl, J.L.** (2010). Arabidopsis and the plant immune system. *Plant J.* **61**, 1053–1066.

**Nishimura, M.T., Stein, M., Hou, B.-H., Vogel, J.P., Edwards, H., and Somerville, S.C.** (2003). Loss of a callose synthase results in salicylic acid-dependent disease resistance. *Science* **301**, 969–972.

**Norman, D.J., Zapata, M., Gabriel, D.W., Duan, Y.P., Yuen, J.M.F., Mangravita-Novo, A., Donahoo, R.S.** (2009). Genetic Diversity and Host Range Variation of *Ralstonia solanacearum* Strains Entering North America. *Phytopathology* **99**, 1070–1077.

**Nühse, T.S., Bottrill, A.R., Jones, A.M.E., and Peck, S.C.** (2007). Quantitative phosphoproteomic analysis of plasma membrane proteins reveals regulatory mechanisms of plant innate immune responses. *Plant J.* **51**, 931–940.

**Nürnberg, T., Nennstiel, D., Jabs, T., Sacks, W.R., Hahlbrock, K., and Scheel, D.** (1994). High affinity binding of a fungal oligopeptide elicitor to parsley plasma membranes triggers multiple defense responses. *Cell* **78**, 449–460.

**Park, C.-J., Caddell, D.F., and Ronald, P.C.** (2012). Protein phosphorylation in plant immunity: insights into the regulation of pattern recognition receptor-mediated signaling. *Front. Plant Sci.* **3**, 177.

**Petnicki-Ocwieja, T., Schneider, D.J., Tam, V.C., Chancey, S.T., Shan, L., Jamir, Y., Schechter, L.M., Janes, M.D., Buell, C.R., Tang, X., Collmer, A., and Alfano, J.R.** (2002). Genomewide identification of proteins secreted by the Hrp type III protein secretion system of *Pseudomonas syringae* pv. tomato DC3000. *Proc. Natl. Acad. Sci. USA* **11**, 7652–7657.

- Poland, J.A., Brown, P.J., Sorrells, M.E., and Jannink, J.-L.** (2012). Development of High-Density Genetic Maps for Barley and Wheat Using a Novel Two-Enzyme Genotyping-by-Sequencing Approach. *PLoS ONE* **7**, e32253.
- Ranf, S., Gisch, N., Schäffer, M., Illig, T., Westphal, L., Knirel, Y.A., Sánchez-Carballo, P.M., Zähringer, U., Hückelhoven, R., Lee, J., and Scheel, D.** (2015). A lectin S-domain receptor kinase mediates lipopolysaccharide sensing in *Arabidopsis thaliana*. *Nat. Immunol.* **16**, 426-436.
- Robatzek, S., Bittel, P., Chinchilla, D., Köchner, P., Felix, G., Shiu, S.-H., and Boller, T.** (2007). Molecular identification and characterization of the tomato flagellin receptor LeFLS2, an orthologue of *Arabidopsis* FLS2 exhibiting characteristically different perception specificities. *Plant Mol. Biol.* **64**, 539–547.
- Ron, M. and Avni, A.** (2004). The receptor for the fungal elicitor ethylene-inducing xylanase is a member of a resistance-like gene family in tomato. *Plant Cell* **16**, 1604–1615.
- Roukos, D.H.** (2010). Next-generation sequencing and epigenome technologies: potential medical applications. *Expert Rev. Med. Devices* **7**, 723-726.
- Roux, M., Schwessinger, B., Albrecht, C., Chinchilla, D., Jones, A., Holton, N., Gro Malinovsky, F., Tör, M., de Vries, S., and Zipfel, C.** (2011). The *Arabidopsis* leucine-rich repeat receptor-like kinases BAK1/SERK3 and BKK1/SERK4 are required for innate immunity to hemibiotrophic and biotrophic pathogens. *Plant Cell* **23**, 2440–2455.
- Scheer, J.M., and Ryan, Jr., C.A.** (2002). The systemin receptor SR160 from *Lycopersicon peruvianum* is a member of the LRRreceptor kinase family. *Proc. Natl. Acad. Sci. USA* **99**, 9585-9590.
- Schneeberger, K., Ossowski, S., Lanz, C., Juul, T., Petersen, A.H., Nielsen, K.L., Jørgensen, J.-E., Weigel, D., and Andersen, S.U.** (2009). SHOREmap: simultaneous mapping and mutation identification by deep sequencing. *Nat. Methods.* **6**, 550–551.
- Sharfman, M., Bar, M., Ehrlich, M., Schuster, S., Melech-Bonfil, S., Ezer, R., Sessa, G., and Avni, A.** (2011). Endosomal signaling of the tomato leucine-rich repeat receptor-like protein LeEix2. *Plant J.* **68**, 413–423.
- Shimizu, T., Nakano, T., Takamizawa, D., Desaki, Y., Ishii Minami, N., Nishizawa, Y., Minami, E., Okada, K., Yamane, H., Kaku, H., and Shibuya, N.** (2010). Two LysM receptor molecules, CEBiP and OsCERK1, cooperatively regulate chitin elicitor signaling in rice. *Plant J.* **64**, 204–214.
- Shiu, S.-H. and Bleecker, A.B.** (2003). Expansion of the receptor-like kinase/Pelle gene family and receptor-like proteins in *Arabidopsis*. *Plant Physiol.* **132**, 530–543.
- Shiu, S.-H., and Bleecker, A.B.** (2001). Receptor-like kinases from *Arabidopsis*

form a monophyletic gene family related to animal receptor kinases. *Proc. Natl. Acad. Sci. USA.* **98**, 10763–10768.

**Shiu, S.-H. and Bleecker, A.B.** (2001). Plant Receptor-Like Kinase Gene Family: Diversity, Function, and Signaling. *Sci. Signal.* **113**, re22–re22.

**Sohn, K.H., Lei, R., Nemri, A., and Jones, J.D.G.** (2007). The Downy Mildew Effector Proteins ATR1 and ATR13 Promote Disease Susceptibility in *Arabidopsis thaliana*. *Plant Cell* **19**, 4077–4090.

**Song, W.Y., Wang, G.L., Chen, L.L., Kim, H.S., Pi, L.Y., Holsten, T., Gardner, J., Wang, B., Zhai, W.X., Zhu, L.H., Fauquet, C., and Ronald, P.** (1995). A receptor kinase-like protein encoded by the rice disease resistance gene, Xa21. *Science* **270**, 1804–1806.

**Stolle, E. and Moritz, R.F.A.** (2013). RESTseq – Efficient Benchtop Population Genomics with RESTriction Fragment SEQuencing. *PLoS ONE* **8**, e63960.

**Sun, Y., Li, L., Macho, A.P., Han, Z., Hu, Z., Zipfel, C., Zhou, J.M., and Chai, J.** (2013). Structural Basis for flg22-Induced Activation of the Arabidopsis FLS2-BAK1 Immune Complex. *Science* **342**, 624–628.

**Swanson-Wagner, R.A., Jia, Y., DeCook, R., Borsuk, L.A., Nettleton, D., and Schnable, P.S.** (2006). All possible modes of gene action are observed in a global comparison of gene expression in a maize F1 hybrid and its inbred parents. *Proc. Natl. Acad. Sci. USA* **103**, 6805–6810.

**Takai, R., Isogai, A., Takayama, S., and Che, F.-S.** (2008). Analysis of Flagellin Perception Mediated by flg22 Receptor OsFLS2 in Rice. *Mol. Plant Microbe Interact.* **21**, 1635–1642.

**Tanaka, K., Choi, J., Cao, Y., and Stacey, G.** (2014). Extracellular ATP acts as a damage-associated molecular pattern (DAMP) signal in plants. *Front. Plant Sci.* **5**, 446.

**Tang, J., Han, Z., Sun, Y., Zhang, H., Gong, X., and Chai, J.** (2014). Structural basis for recognition of an endogenous peptide by the plant receptor kinase PEPR1. *Cell Res.* **25**, 110–120.

**Tao, Y., Xie, Z., Chen, W., Glazebrook, J., Chang, H.-S., Han, B., Zhu, T., Zou, G., and Katagiri, F.** (2003). Quantitative nature of Arabidopsis responses during compatible and incompatible interactions with the bacterial pathogen *Pseudomonas syringae*. *Plant Cell* **15**, 317–330.

**Thomas, C.M., Dixon, M.S., Parniske, M., Golstein, C., and Jones, J.D.G.** (1998). Genetic and molecular analysis of tomato Cf genes for resistance to *Cladosporium fulvum*. *Phil. Trans. R. Soc. Lond. B* **353**, 1413–1424.

**Thomma, B.P.H.J., Nürnberger, T., and Joosten, M.H.A.J.** (2011). Of PAMPs and effectors: the blurred PTI-ETI dichotomy. *Plant Cell* **23**, 4–15.

**Thuerig, B., Felix, G., Binder, A., Boller, T., and Tamm, L.** (2005). An extract

of *Penicillium chrysogenum* elicits early defense-related responses and induces resistance in *Arabidopsis thaliana* independently of known signalling pathways. *Physiol. Mol. Plant Path.* **67**, 180–193.

**Umemoto, N., Kakitani, M., Iwamatsu, A., Yoshikawa, M., Yamaoka, N., and Ishida, I.** (1997). The structure and function of a soybean  $\beta$ -glucan-elicitor-binding protein. *Proc. Natl. Acad. Sci. USA* **94**, 1029-1034.

**van den Burg, H.A., Harrison, S.J., Joosten, M.H.A.J., Vervoort, J., and de Wit, P.J.G.M.** (2006). *Cladosporium fulvum* Avr4 protects fungal cell walls against hydrolysis by plant chitinases accumulating during infection. *Mol. Plant Microbe Interact.* **19**, 1420-1430.

**van den Hooven, H.W., Appelman, A.W.J., Zey, T., de Wit, P.J.G.M., and Vervoort, J.** (1999). Folding and conformational analysis of AVR9 peptide elicitors of the fungal tomato pathogen *Cladosporium fulvum*. *Eur. J. Biochem.* **264**, 9–18.

**van Orsouw, N.J., Hogers, R.C.J., Janssen, A., Yalcin, F., Snoeijers, S., Verstege, E., Schneiders, H., van der Poel, H., van Oeveren, J., Verstegen, H., and van Eijk, M.J.T.** (2007). Complexity Reduction of Polymorphic Sequences (CRoPS™): A Novel Approach for Large-Scale Polymorphism Discovery in Complex Genomes. *PLoS ONE* **2**, e1172.

**Veit, S., Worle, J.M., Nurnberger, T., Koch, W., and Seitz, H.U.** (2001). A Novel Protein Elicitor (PaNie) from *Pythium aphanidermatum* Induces Multiple Defense Responses in Carrot, *Arabidopsis*, and Tobacco. *Plant Physiol.* **127**, 832–841.

**Vervoort, J., van den Hooven, H.W., Berg, A., Vossen, P., Vogelsang, R., Joosten, M.H.A.J., and de Wit, P.J.G.M.** (1997). The race-specific elicitor AVR9 of the tomato pathogen *Cladosporium fulvum*: a cystine knot protein. *FEBS Lett.* **404**, 153–158.

**Vetter, M.M., Kronholm, I., He, F., Häweker, H., Reymond, M., Bergelson, J., Robatzek, S., and de Meaux, J.** (2012). Flagellin perception varies quantitatively in *Arabidopsis thaliana* and its relatives. *Mol. Biol. Evol.* **29**, 1655–1667.

**Vogel, J., and Somerville, S.** (2000). Isolation and characterization of powdery mildew-resistant *Arabidopsis* mutants. *Proc. Natl. Acad. Sci. USA* **97**, 1897-1902.

**Voinnet, O., Rivas, S., Mestre, P., and Baulcombe, D.** (2003). An enhanced transient expression system in plants based on suppression of gene silencing by the p19 protein of tomato bushy stunt virus. *Plant J.* **33**, 949–956.

**Wang, G., Ellendorff, U., Kemp, B., Mansfield, J.W., Forsyth, Alec., Mitchell, K., Bastas, K., Liu, C., Woods-Tör, A., Zipfel, C., de Wit, P.J.G.M., Jones, J.D.G., Tör, M., and Thomma, B.P.H.J.** (2008). A genome-wide functional investigation into the roles of receptor-like proteins in *Arabidopsis*. *Plant Physiol.* **147**, 503–517.



Weßling, R., Epple, P., Altmann, S., He, Y., Yang, L., Henz, S.R., McDonald, N., Wiley, K., Christian Bader, K., Gläßer, C., Mukhtar, M.S., Haigis, S., Ghamsari, L., Stephens, A.E., Ecker, J.R., Vidal, M., Jones, J.D.G., Mayer, K.F.X., van Themaat, E.V.L., Weigel, D., Schulze-Lefert, P., Dangl, J.L., Panstruga, R., and Braun, P. (2014). Convergent targeting of a common host protein-network by pathogen effectors from three kingdoms of life. *Cell Host Microbe* **16**, 364–375.

Willmann, R., Lajunen, H.M., Erbs, G., Newman, M., Kolb, D., Tsuda, K., Katagiri, F., Fliegmann, J., Bono, J., Cullimore, J.V., Jehle, A.K., Götz, F., Kulik, A., Molinaro, A., Lipka, V., Gust, A.A., and Nürnberger, T. (2011). Arabidopsis lysin-motif proteins LYM1 LYM3 CERK1 mediate bacterial peptidoglycan sensing and immunity to bacterial infection. *Proc. Natl. Acad. Sci. USA* **108**, 19824–19829.

Wilson, K. (1997). Preparation of genomic DNA from bacteria. *Curr. Protoc. Mol. Biol.* **2.4.1-2.2.5**.

Yoo, S.-D., Cho, Y.-H., and Sheen, J. (2007). Arabidopsis mesophyll protoplasts: a versatile cell system for transient gene expression analysis. *Nat Protoc.* **2**, 1565–1572.

Zhang, J., Li, W., Xiang, T., Liu, Z., Laluk, K., Ding, X., Zou, Y., Gao, M., Zhang, X., Chen, S., Mengiste, T., Zhang, Y., and Zhou, J.-M. (2010). Receptor-like Cytoplasmic Kinases Integrate Signaling from Multiple Plant Immune Receptors and Are Targeted by a *Pseudomonas syringae* Effector. *Cell Host Microbe* **7**, 290–301.

Zhang, L., Kars, I., Essenstam, B., Liebrand, T.W.H., Wagemakers, L., Elberse, J., Tagkalaki, P., Tjoitang, D., van den Ackerveken, G., and van Kan, J.A.L. (2014). Fungal endopolygalacturonases are recognized as microbe-associated molecular patterns by the arabidopsis receptor-like protein RESPONSIVENESS TO BOTRYTIS POLYGALACTURONASES1. *Plant Physiol.* **164**, 352–364.

Zhang, W. (2013). Identification and characterization of the novel fungal MAMP SsE1 and its Receptor-like Protein (RLP30)-based perception system in *Arabidopsis*. Dissertation, 1–135.

Zhang, W., Fraiture, M., Kolb, D., Löffelhardt, B., Desaki, Z., Boutrot, F.F.G., Tör, M., Zipfel, C., Gust, A.A., and Brunner, F. (2013). Arabidopsis receptor-like protein30 and receptor-like kinase suppressor of BIR1-1/EVERSHED mediate innate immunity to necrotrophic fungi. *Plant Cell* **25**, 4227–4241.

Zhu, S., Li, Y., Vossen, J.H., Visser, R.G.F., and Jacobsen, E. (2011). Functional stacking of three resistance genes against *Phytophthora infestans* in potato. *Transgenic Res.* **21**, 89–99.

Zipfel, C. (2006). Receptor-like kinases and pathogen-associated molecular patterns perception in *Arabidopsis*. dissertation, 1–163.

**Zipfel, C., Kunze, G., Chinchilla, D., Caniard, A., Jones, J.D.G., Boller, T., and Felix, G.** (2006). Perception of the Bacterial PAMP EF-Tu by the Receptor EFR Restricts Agrobacterium-Mediated Transformation. *Cell* **125**, 749–760.

**Zipfel, C., Robatzek, S., Navarro, L., and Oakeley, E.J.** (2004). Bacterial disease resistance in Arabidopsis through flagellin perception. *Nature* **428**, 764-767.

## 7. Appendix

### 7.1 Supplementary figures and tables

Table 7. 1 Recombination breakpoint was identified based on genotyping between markers Chr3: 1321901 to 1587717 of individual plant P2A03.

individual	Chr	position	ref	call	quality	read support	concordance	genotype
RAD_R146_8_P2A03	3	<b>1321901</b>	G	A	40	66	1	B
RAD_R146_8_P2A03	3	1323879	G	A	4	1	0,5	
RAD_R146_8_P2A03	3	1357672	T	G	19	63	0,777778	
RAD_R146_8_P2A03	3	<b>1399533</b>	T	C	40	7	1	B
RAD_R146_8_P2A03	3	1420448	A	C	12	1	0,333333	
RAD_R146_8_P2A03	3	1432648	T	A	40	19	0,463415	H
RAD_R146_8_P2A03	3	1527157	A	C	30	21	0,272727	H
RAD_R146_8_P2A03	3	1527265	T	C	40	10	0,47619	H
RAD_R146_8_P2A03	3	1528390	C	T	25	2	0,4	
RAD_R146_8_P2A03	3	1528457	T	A	4	1	0,25	
RAD_R146_8_P2A03	3	1529342	T	C	14	1	0,5	
RAD_R146_8_P2A03	3	1546609	A	G	25	2	1	
RAD_R146_8_P2A03	3	1546614	A	G	25	2	1	
RAD_R146_8_P2A03	3	1546639	G	T	25	2	1	
RAD_R146_8_P2A03	3	1546715	T	G	40	5	0,416667	H
RAD_R146_8_P2A03	3	1565389	A	C	40	5	0,833333	B
RAD_R146_8_P2A03	3	1569698	G	A	24	2	1	
RAD_R146_8_P2A03	3	1569864	G	A	14	1	1	
RAD_R146_8_P2A03	3	1569947	C	A	40	40	1	B
RAD_R146_8_P2A03	3	1575596	G	A	40	114	1	B
RAD_R146_8_P2A03	3	1587670	T	A	40	10	1	B
RAD_R146_8_P2A03	3	1587708	T	C	40	11	1	B
RAD_R146_8_P2A03	3	1587717	C	T	24	11	1	B

P2A03 is a RsE2 sensitive plant. A genotype transition from B to H is detected at downstream of Chr3: 1399533.

Genotype B indicates the allele of insensitive ecotype ICE73;

Genotype A indicates the allele of sensitive ecotype ICE153;

Genotype H indicates heterozygosity (the concordance was set between 0.3-0.7);

Genotype blank means the genotype could not be supported by statistic significance.

Table 7. 2 Recombination breakpoint was identified based on genotyping between markers Chr3: 2206537 to 2674522 of individual plant P1H03.

individual	Chr	position	ref	call	quality	read support	concordance	genotype
RAD_R146_8_P1H03	3	2206537	G	T	8	85	1	B
RAD_R146_8_P1H03	3	2224583	A	C	8	1	1	
RAD_R146_8_P1H03	3	2248915	G	-	40	20	1	B
RAD_R146_8_P1H03	3	2248917	T	A	40	20	1	B
RAD_R146_8_P1H03	3	2265386	G	A	40	20	1	B
RAD_R146_8_P1H03	3	2279112	C	A	40	48	1	B
RAD_R146_8_P1H03	3	2282533	T	A	8	69	1	B
RAD_R146_8_P1H03	3	2282553	C	T	40	69	1	
RAD_R146_8_P1H03	3	2293396	T	A	5	1	0,5	
RAD_R146_8_P1H03	3	2325603	G	A	40	133	1	
RAD_R146_8_P1H03	3	2328838	T	C	40	29	1	
RAD_R146_8_P1H03	3	2342682	G	A	40	9	1	B
RAD_R146_8_P1H03	3	2369546	T	G	6	18	0,333333	
RAD_R146_8_P1H03	3	2398064	G	T	5	1	1	
RAD_R146_8_P1H03	3	2405040	C	A	40	25	1	
RAD_R146_8_P1H03	3	2413253	C	A	4	1	1	
RAD_R146_8_P1H03	3	2421258	G	C	8	93	1	B
RAD_R146_8_P1H03	3	2421305	T	C	40	93	1	B
RAD_R146_8_P1H03	3	2421306	G	A	40	93	1	B
RAD_R146_8_P1H03	3	2421321	A	C	40	93	1	B
RAD_R146_8_P1H03	3	2421327	T	A	40	92	1	
RAD_R146_8_P1H03	3	2438261	T	C	21	3	0,5	
RAD_R146_8_P1H03	3	2438269	T	C	23	2	0,25	
RAD_R146_8_P1H03	3	2448107	A	G	10	1	1	
RAD_R146_8_P1H03	3	2480870	C	T	40	155	0,99359	
RAD_R146_8_P1H03	3	<b>2485009</b>	<b>G</b>	<b>T</b>	40	<b>15</b>	<b>0,6</b>	H
RAD_R146_8_P1H03	3	2486578	A	G	4	1	1	
RAD_R146_8_P1H03	3	2486580	G	T	5	1	1	
RAD_R146_8_P1H03	3	2493819	T	G	32	19	0,791667	
RAD_R146_8_P1H03	3	2493839	A	G	6	2	0,333333	
RAD_R146_8_P1H03	3	2493846	A	G	4	1	0,5	
RAD_R146_8_P1H03	3	2500030	T	C	24	<b>7</b>	<b>0,368421</b>	H
RAD_R146_8_P1H03	3	2544078	A	C	7	1	0,25	
RAD_R146_8_P1H03	3	2544080	T	G	7	1	0,25	
RAD_R146_8_P1H03	3	2544088	A	C	2	1	0,25	
RAD_R146_8_P1H03	3	2547735	C	T	24	<b>7</b>	<b>0,538462</b>	H
RAD_R146_8_P1H03	3	2554154	T	C	24	<b>50</b>	<b>0,420168</b>	H
RAD_R146_8_P1H03	3	2623693	G	A	40	<b>9</b>	<b>0,529412</b>	H
RAD_R146_8_P1H03	3	2625445	A	C	40	18	0,545455	
RAD_R146_8_P1H03	3	2625447	T	C	25	7	0,212121	
RAD_R146_8_P1H03	3	2658483	T	G	24	2	1	
RAD_R146_8_P1H03	3	2671730	A	G	40	10	0,5	
RAD_R146_8_P1H03	3	2671791	G	T	38	11	0,44	
RAD_R146_8_P1H03	3	2671792	C	T	32	11	0,44	
RAD_R146_8_P1H03	3	2671852	T	A	40	62	1	
RAD_R146_8_P1H03	3	2674522	C	T	40	<b>7</b>	<b>0,636364</b>	H

P1H03 is a RsE2-insensitive plant. A genotype transition from H to B is detected at upstream of Chr3: 2485009.

Genotype B indicates the allele of insensitive ecotype ICE73;

Genotype A indicates the allele of sensitive ecotype ICE153;

Genotype H indicates heterozygosity (the concordance was set between 0.3-0.7);

Genotype blank means the genotype could not be supported by statistic significance.

Table 7. 3 Phenotype layout for RAD-seq library

	1	2	3	4	5	6	7	8	9	10	11	12
P1A	1,91655	3,47145	1,0143	1,4814	1,4033	1,48605	1,5005	1,54305	1,6083	1,46835	1,4754	2,41755
P1B	1,005	1,33335	3,0303	0,8859	1,0346	1,2024	0,7202	1,3182	1,38135	2,0142	3,8636	4,11075
P1C	1,179	1,5378	1,2258	1,431	1,5875	2,54955	2,6018	1,50435	0,97455	1,3641	1,2882	1,17015
P1D	2,5278	0,9729	1,5749	3,8811	1,6524	1,33425	1,3553	1,14855	3,61185	1,24155	0,993	2,6265
P1E	2,415	1,152	1,5911	1,53915	1,6052	1,49595	4,5407	0,74175	4,60725	2,5299	5,6157	3,98985
P1F	3,37425	3,9063	1,6362	3,01425	2,5523	3,00315	1,2047	2,7084	1,5318	4,6152	1,5587	4,00665
P1G	2,4825	2,9937	0,9063	2,9313	0,9771	1,11225	2,6576	1,2138	2,5104	1,46085	2,4287	4,37625
P1H	2,979	3,4161	1,0847	5,02215	3,4377	1,0002	4,5215	2,92365	2,76405	1,0914	4,0986	2,99715
	1	2	3	4	5	6	7	8	9	10	11	12
P2A	3,6009	3,27945	4,397	1,3029	2,7522	3,58515	0,6138	1,5837	4,8801	5,4066	1,568	1,22955
P2B	4,3638	3,2106	0,945	3,36705	2,8455	1,4175	5,8269	1,2027	3,60945	2,93295	3,54	5,99685
P2C	4,6662	1,6389	2,4101	4,36245	7,8795	4,8021	4,4676	4,8774	2,4612	3,43065	4,508	2,73285
P2D	1,33635	4,47735	1,1472	2,715	5,5752	1,35915	2,4086	3,6921	1,2213	3,6486	8,6733	5,71695
P2E	0,7983	1,3179	4,7465	2,5458	7,9485	6,699	1,4367	2,4567	5,08095	1,46055	8,3552	7,36905
P2F	4,5873	1,55355	7,2086	3,081	4,5159	5,70915	6,3836	1,35075	5,00805	7,4586	5,7563	0,9135
P2G	1,2435	0,7587	1,0992	2,5005	3,791	1,46925	2,6624	5,30625	0,66975	1,4127	1,176	2,57835
P2H	1,4517	3,054	3,8697	1,629	2,67	3,6288	2,4749	3,38445	4,61295	0,77925	0,9993	5,4105

Note: The layout was designed according to 96-well format. Each well is filled with the value of ethylene response of each individual F2 plant by elicitor RsE2. Yellow: insensitive phenotype.

Table 7. 4 Phenotype score upon RsE1 treatment among ecotypes

accession	score	accession	score	accession	score
Agu-1	4	ICE 216	2	NFA-8	2
Bak-2	4	ICE 226	2	Nie1-2	2
Bak-7	2	ICE 228	2	Ped-0	2
Bur-0	3	ICE 29	3	Pra-6	2
cdm-0	2	ICE 33	1	PRS-10	2
Col-0	2	ICE 36	2	Pu2-23	2
Del-10	2	ICE 50	2	Pua-10	3
Dog-4	1	ICE 60	2	Qui-0	2
Edi-0	2	ICE 61	3	Ra-0	2
Ey1.5-2	2	ICE 7	3	Reu-1	1
Fab-2	2	ICE 70	2	RmxA180	2
Fei-0	2	ICE 72	3	Rü3.1+31	2
Got-22	3	ICE 73	1	Sha	2
Gu-0	1	ICE 79	3	sorbo	2
Gy-0	2	ICE 91	4	sq-8	2
HKT2-4	2	ICE 93	4	Star-8	2
ICE 102	3	ICE 97	2	Strand-1	4
ICE 104	3	ICE 98	3	Tn2-1	3
ICE 106	3	ICE-1	4	Tsu-1	2
ICE 111	3	ICE150	2	TüSB30-3	2
ICE 112	4	ICE-152	3	Tü-Scha-9	3
ICE 119	3	ICE-49	3	Tü-v-13	3
ICE 120	4	ICE63	2	Tü-wal-2	2
ICE 127	4	ICE71	3	Ty-0	4
ICE 130	2	ICE75	3	ull-2-3	2
ICE 134	3	Istisu-1	3	Vash-1	4
ICE 138	2	Kastel-1	4	Vie-0	4
ICE 153	4	kin-0	3	vod-1	2
ICE 163	3	Koch-1	2	Wal-HäsB-4	3
ICE 169	3	KZ-9	3	Ws-0	2
ICE 173	3	Lag2-2	2	Ws-2	2
ICE 181	3	Leo-1	4	Wt-5	1
ICE 21	1	Lerik1-3	2	Xan-1	4
ICE 212	2	Mr-0	2	Yeq-1	1
ICE 213	4	Nemrut	3	zu-9	2

Note: the original ethylene production was normalized into score value by using Col-0 (score value is 2), insensitive ecotypes Dog-4, ICE21, ICE33, Wt-5, ICE73 (score value is 1) and sensitive ecotypes Leo-1 and Bak-2 (score value is 4) as control.

Table 7. 5 List of stable transgenic Rlp32 of Arabidopsis

Ecotype	promoter	the source of rlp32	tag	vector	clones	transgenic T0 seeds
Wt-5	CaMV35S promoter	Col-0	GFP	pB7FWG2	eric supplied	ready
ICE73	CaMV35S promoter	Col-0	GFP	pB7FWG2	eric supplied	ready
ICE73	native promoter from ICE153	ICE153	3xHA	pGWB13	ready	ready
ICE73	native promoter from ICE153	ICE153	GFP	pGWB4	ready	ready
ICE73	CaMV35S promoter	ICE153	GFP	pB7FWG2	ready	ready
ICE73	CaMV35S promoter	ICE153	GFP	pGWB5	ready	ready
ICE153	CaMV35S promoter	ICE153	GFP	pGWB5	ready	ready
ICE153	native promoter from ICE153	ICE153	GFP	pGWB4	ready	ready
ICE153	CaMV35S promoter	ICE153	GFP	pB7FWG2	ready	ready
ICE21	native promoter from ICE153	ICE153	GFP	pGWB4	ready	ready
ICE21	CaMV35S promoter	ICE153	GFP	pB7FWG2	ready	ready
Yeg-1	CaMV35S promoter	ICE153	GFP	pGWB5	ready	ready
Dog-4	native promoter from ICE153	ICE153	GFP	pGWB4	ready	ready
Dog-4	CaMV35S promoter	ICE153	GFP	pGWB5	ready	ready

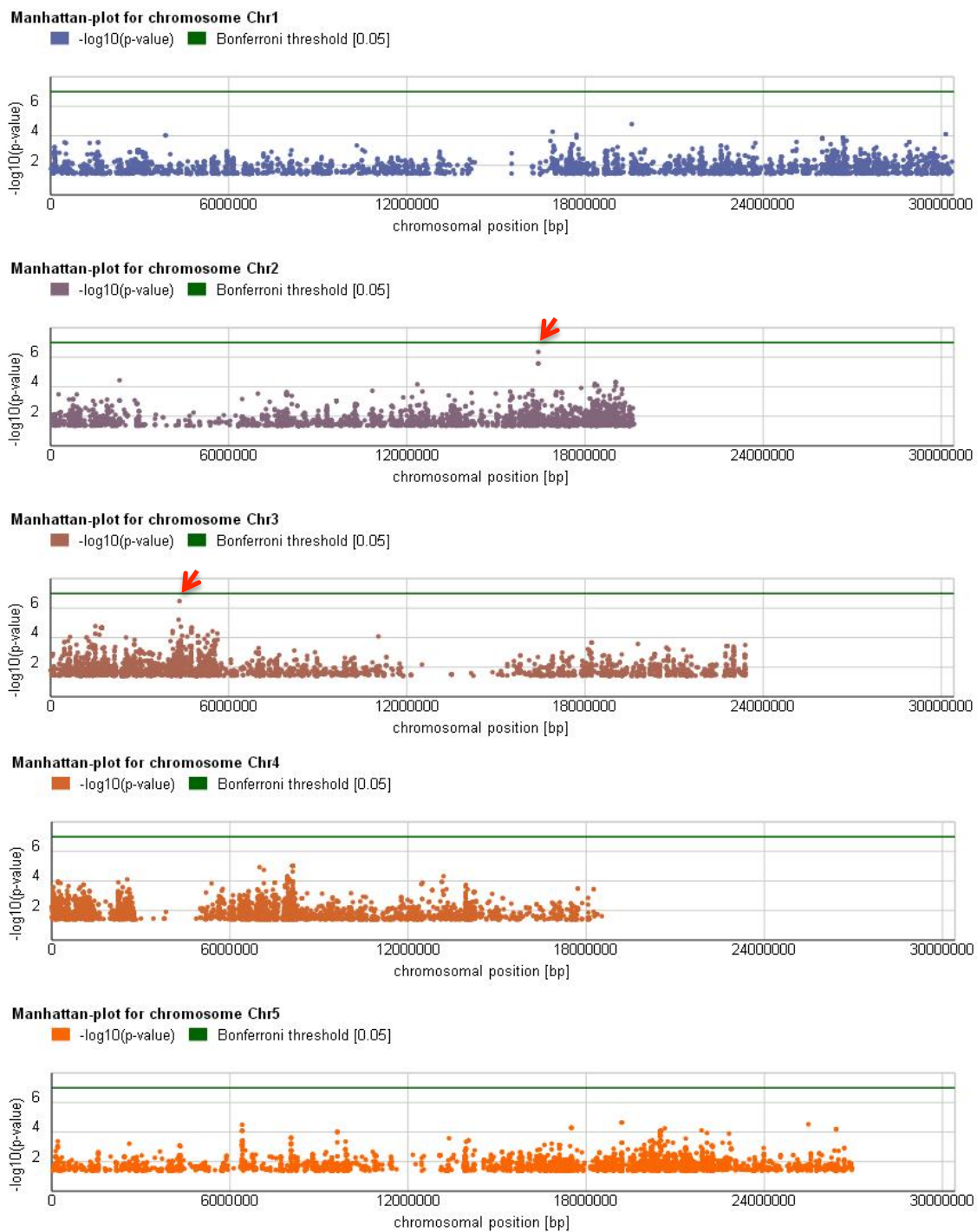


Figure 7. 1 Manhattan plot of the top 10% of all p-value upon Rse1 treatment

The x-axis shows genomic coordinates, and the y-axis shows negative logarithm of the associated P-value for each SNPs. Horizontal green lines represent the thresholds for Bonferroni significance. One significant SNP is located on Chr2; the other significant SNPs are located on Chr3 (red arrows).



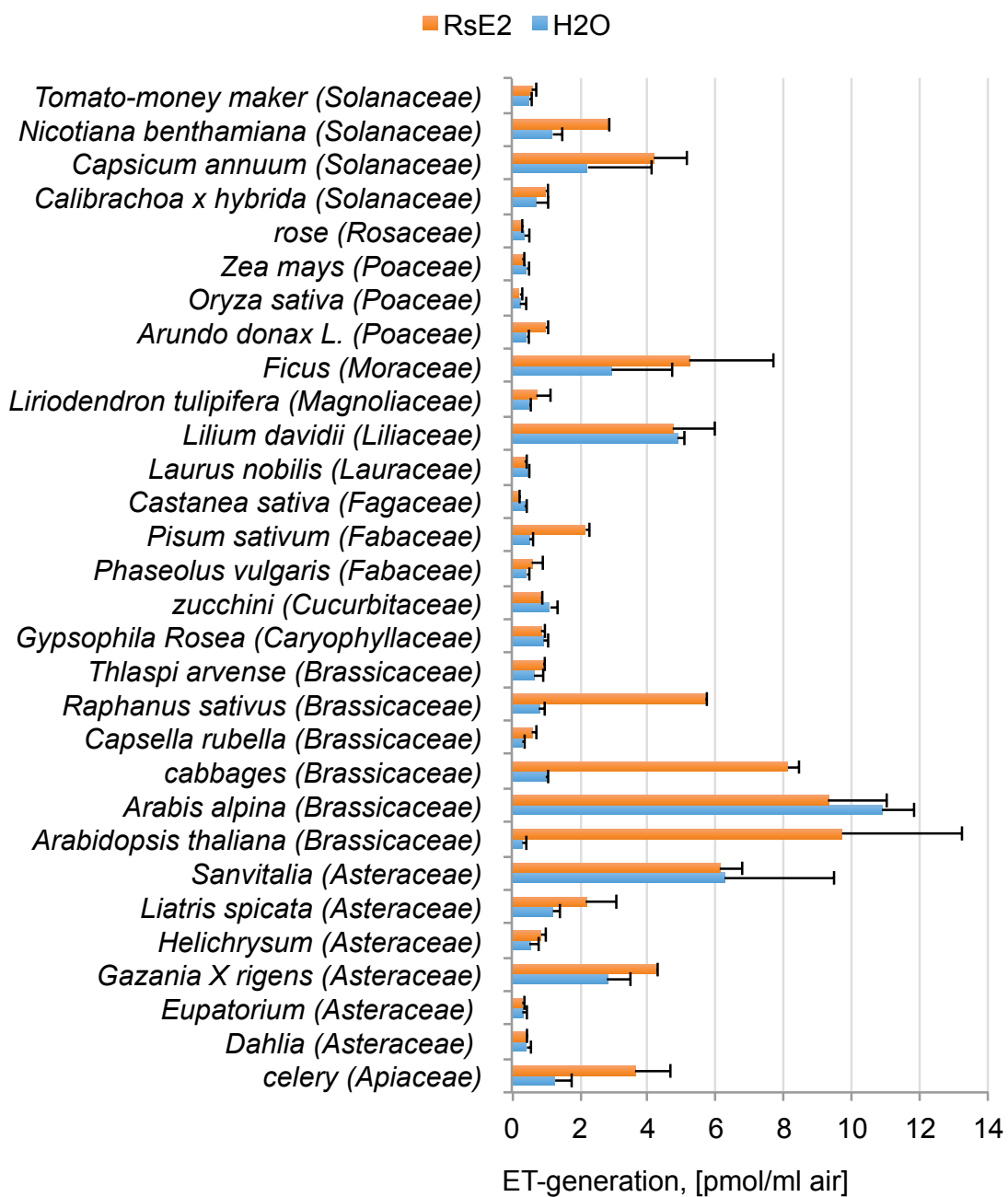


Figure 7. 2 Perception of RsE2 in different plant families

RsE2 elicited ethylene responses were measured in various plant families and species, contrasting to H<sub>2</sub>O control. The error bars indicate standard deviations of two individual plants. Plant families were denoted with brackets. Some of species from the six families, *Apiaceae*, *Asteraceae*, *Brassicaceae*, *Fabaceae*, *Moraceae* and *Solanaceae* most likely contain the RsE2 perception system.

## 7.2 Identification of novel PAMPs from *Pseudomonas syringae* pv tomato strain DC3000

*Pseudomonas syringae* pv tomato strain DC3000 is a gram negative strain, causing bacterial speck in tomato and cruciferous vegetables. Since 1991 *Pseudomonas syringae* pv tomato strain DC3000 was found to be hosted not only in tomato but also in laboratory plant species Arabidopsis, this bacteria strain has been fully studied for the potential type III effectors and triggered ETI in Arabidopsis by employing powerful genomics tools (Lindeberg et al., 2005; Petnicki-Ocwieja et al., 2002; Buell et al., 1996). As a model pathogen, DC3000-triggered PTI in Arabidopsis was deduced from limited PAMP-receptor pairs (such as flagellin/FLS2 and EF-Tu/EFR). Therefore, great interests lay in whether *Pseudomonas syringae* pv tomato strain DC3000 contains other proteinaceous PAMPs, which could also initiate PTI of plants in addition to flagellin and EF-Tu. In this study, we did protein screening and isolated two active fractions that could trigger the ethylene response in fls2/efr double mutant Arabidopsis. Two active proteins and corresponding active peptides were identified to be potential novel PAMPs.

### 7.2.1 Workflow for purification of novel PAMPs from *Pseudomonas syringae* pv tomato strain DC3000

Two Liters of *Pseudomonas syringae* pv tomato strain DC3000 cell cultures were incubated in 28°C shaker for 36-48 hours. The cell cultures were heat to boiling, and then cooled it down on ice or cold water bath. The whole cell cultures were centrifuged at 5000 rpm for 15 minutes and supernatants were kept for next steps. The required amount of Ammonium Sulfate for precipitation is calculated by web-based tool (<http://www.encorbio.com/protocols/AM-SO4.htm>). Usually for 2L supernatants, about 402.19 g solid Ammonium Sulfate is required for making 35% saturated solution at 4°C. The precipitated proteins were removed from supernatants by batch centrifuging at 12000 rpm for 10 minutes. Repeatedly doing precipitations and centrifuges, we collected precipitated protein pellets from 35%-45% saturated Ammonium Sulfate solutions (group PS45) and from 65%-85% saturated Ammonium Sulfate solutions (group PS65) (Figure 7.3).

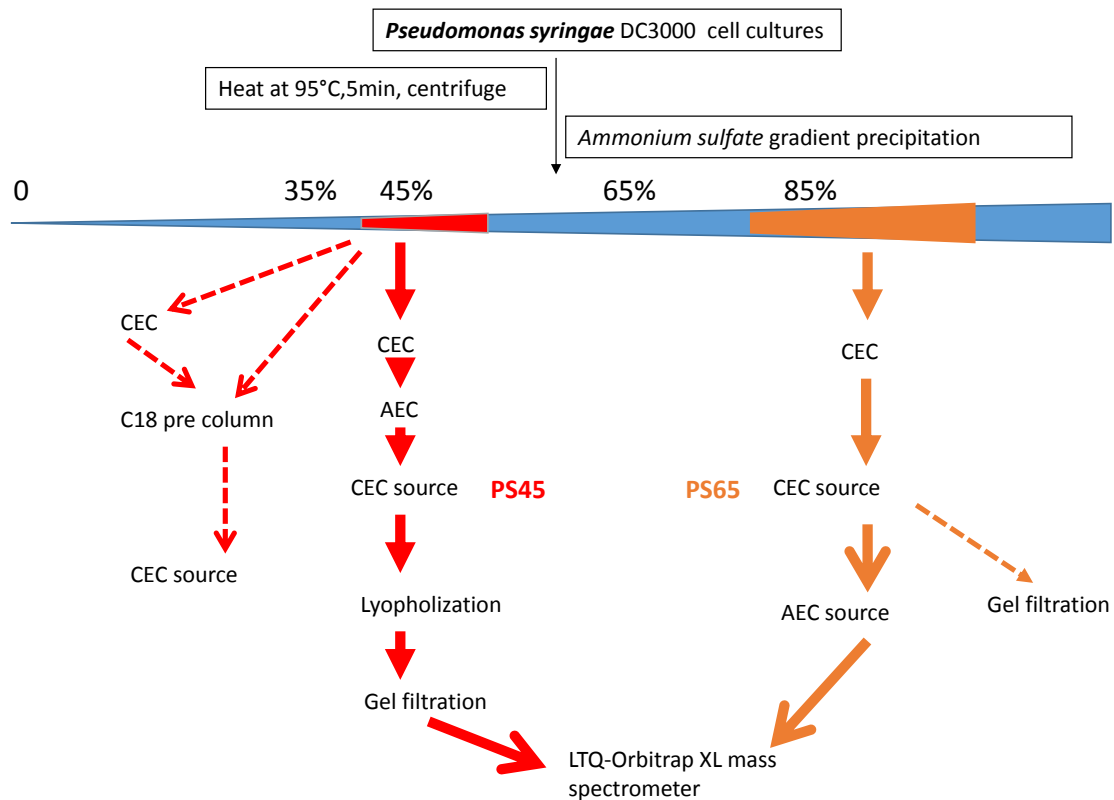


Figure 7. 3 Scheme of PAMPs purification from *Pseudomonas syringae* DC3000

The group PS45 was dissolved in water, dialysed in MES buffer (pH5.2), and then loaded into MES buffer-equilibrated (pH5.2) cation exchange chromatography column. The eluted fractions were measured ethylene response using *fls2/efr* double mutant Arabidopsis leaves. The fractions that can elicit ethylene response were pooled together, dialysed in Tris buffer (pH8.5) and apply to Anion exchange column. 100% buffer B was used to elute bound proteins and the bound proteins (dialysed in buffer MES, pH5.2) were loaded into Äkta explore-controlled Source cation column. Gradient elution (10 column-volumes) was used with an increasing ionic strength up to 0.5 M KCl. All the fractions were examined for the ethylene response. The active fractions after source column were pooled together and named PS45, which is partially purified elicitor.

The group PS65 was going through all above processes as group PS45 except anion exchange chromatograph. The active fractions after Source cation column were pooled together and apply to Source anion column. The active fractions after Source anion were named partial purified elicitor PS65.

PS45 and PS65 are used to measure immunity assay in plants. They are further purified by size preference chromatography, gel filtration. PS45 and PS65 were separately loaded into column HiLoad™ 16/600 Superdex 75 with the MES buffer (pH6.5); the eluted fractions were measured ethylene response in double mutant plants. An active fraction was detected in PS45, but not in PS65.

With regard to the reduction of complexity of fractions of group PS65 after Source cation chromatography, we diluted active fractions in 20 times volume of buffer 1,3-Diaminopropan (pH 11.1) and apply to Source anion chromatography. The fractions were dialysed in MES buffer (5.2) and examined for ethylene response.

An alternative method to purify the PS45 was developed using reverse phase chromatography. The crude extract in 0.1% TFA (pH 2) was loaded into reverse phase chromatography pre-column C18, step-wise eluted with acetonitrile (ACN). The protocol is below:

Pre-rinsing the column with organic solvents 5ml, 100% ACN

Equilibrating the pre C18 with 10ml, 0.1% TFA (pH 2.0)

Loading crude extract with 1% TFA (pH 2.0)

Washing the column with 5ml, 0.1% TFA (pH 2.0)

Step-wise eluting with 5ml, 25% ACN, 0.1% TFA; 5ml, 50% ACN, 0.1% TFA; 5ml, 75% ACN, 0.1% TFA; 5ml, 100% ACN, 0.1% TFA.

Using speedvac to evaporate the organic solvents and dissolving sample in MES buffer (pH5.2)

Measuring the ethylene response in double mutant Arabidopsis plants.

The active fractions from a few of rounds of pre-column were pooled up to 3ml and diluted in 25ml MES buffer (pH5.2). This sample was loaded onto Source 15 cation column for further purification. In parallel, the pooled active fraction from pre-column was concentrated and dissolved in 100µl, 0.1% TFA (pH2) in order to running C18 column.

After the series of purification process, the elicitor-contained fractions were shown in Tricine-SDS gel by silver staining. Those candidate bands were sliced from the gel and were analyzed by Mass spectrometry, the service supplied by

Protein Center Tuebingen (<http://www.pct.uni-tuebingen.de/>). The main processes and results were shown in each following sections.

### 7.2.2 Two active fractions were separated by step-wise ammonium sulfate precipitation

To reduce the complexity precipitated along with major elicitors, step-wise ammonium sulfate precipitation was conducted. The crude proteins were divided by different ammonium sulfate-saturated solutions,  $\leq 35\%$ , 35-45%, 45-55%, 55-65%, 65-75%, 75-85%, and 85-95%. Protein complexes from two saturation groups, 35-45% and 65-85% could elicit higher ethylene products in fls2/efr double mutant Arabidopsis plant (Figure 7.4).

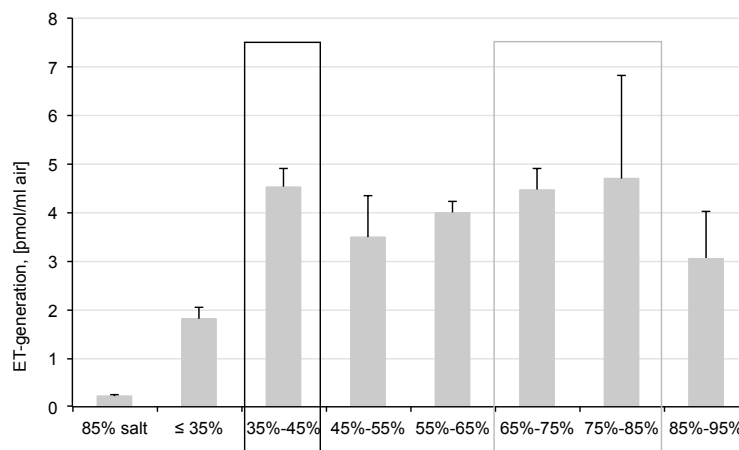


Figure 7. 4 Ethylene responses in fls2/efr Arabidopsis elicited by protein fractions through step-wise precipitating from crude extract of *Pseudomonas syringae* DC3000

Precipitated proteins from 35-45% saturated solution elicit strong ethylene response (dark box) as well as those from 65-85% saturated solution (grey box).

### 7.2.3 Identification of a series of candidate PAMPs by further purification of PS45

Crude extract group 35-45% was purified by a series of chromatography: cation exchange chromatography, anion exchange chromatography and higher resolution cation exchange chromatography. During each step, the activities of fractions were determined by ethylene assay. The active fractions were examined for the complexity by Tricine-SDS-PA electrophoresis before pooled together and purified further. One of active fractions showed an isolated

ethylene eliciting capability after size-exclusion chromatography. To identify the active material, the isolated ethylene eliciting fraction was displayed on Tricine-SDS PA gel by silver staining and the silver stained protein bands were sliced out for Mass Spectrometry analysis (Figure 7.5).

Mass Spectrometry detected a total of 38 potential proteins. Among them, 15 proteins are significantly blast-supported, and with expected molecular size and isoelectric point. These 15 proteins are good PAMP candidates (Table 7.6).

Table 7. 6 PS45 candidates from Mass Spectrometry

Protein IDs	Protein Descriptions	Sequence Coverage [%]	MW[kDa]	Sequence Length	cut1	cut2	cut3	cut4	PEP
Q883T2	Acyl-CoA thioesterase, PSPTO_2268	35,3	21,156	201	5	1			1,58E-49
Q882V8	Putative uncharacterized protein, PSPTO_2514	40,1	19,331	172		7			1,55E-38
Q88B16	Nitrogen regulatory protein P-II, glnK, PSPTO_0217	64,3	12,33	112			7		1,78E-23
O52376	Thiol:disulfide interchange protein DsbA, dsbA	38,8	23,34	214	7	6			1,06E-19
Q887V3	Putative uncharacterized protein, PSPTO_1180	52	11,368	98			6		1,63E-14
Q87VA6	Type IV pilus response regulator PilH, pilH	23,1	13,325	121			2		5,84E-13
Q887A0	Iron-binding protein IscU, iscU, PSPTO_1424	33,6	13,865	128	1	6	3		1,77E-12
Q87V70	UPF0312 protein, PSPTO_5071	41,7	20,633	192	5	4			3,40E-09
Q880P9	Putative uncharacterized protein, PSPTO_3105	17,6	26,125	238		7			4,07E-09
Q887L1	Putative uncharacterized protein, PSPTO_1281	15,3	13,609	118			2		2,12E-08
Q880X2	Peptidyl-prolyl cis-trans isomerase C, ppiC-1	31,2	9,945	93				2	1,33E-07
Q87XT6	Peptidyl-prolyl cis-trans isomerase, ppiA	18,2	20,227	187	3	1			1,59E-07
Q881N8	Putative uncharacterized protein, PSPTO_2850	12,3	17,657	162			2		1,74E-07
Q885W2	Glutathione peroxidase, PSPTO_1719	14,8	20,134	183		3			5,18E-06
Q886S1	OmpA family protein, PSPTO_1506	9,2	28,401	260	1	1	2		6,71E-05

#### 7.2.4 Mass spectrometer detects a single candidate from purified PS65

Crude extract group 65%-85% was purified with cation exchange chromatography and cation Source column. Unlike fractions eluted from source column for the group 35-45%, the active fractions from group 65-85% showed reduced complexity on silver stained Tricine SDS page gel. To further identify this active protein, instead of size exclusion chromatography, a higher resolution anion exchange chromatography was used to isolate the active protein (Source 15Q 4.6/100 PE). The ethylene inducible fraction was spread on silver stained Tricine SDS page gel (Figure 7.5). The protein band was sliced out from the gel and was analyzed by MS. An uncharacterized *Pseudomonas syringae* pv. tomato protein (PSPTO\_3270) was identified.

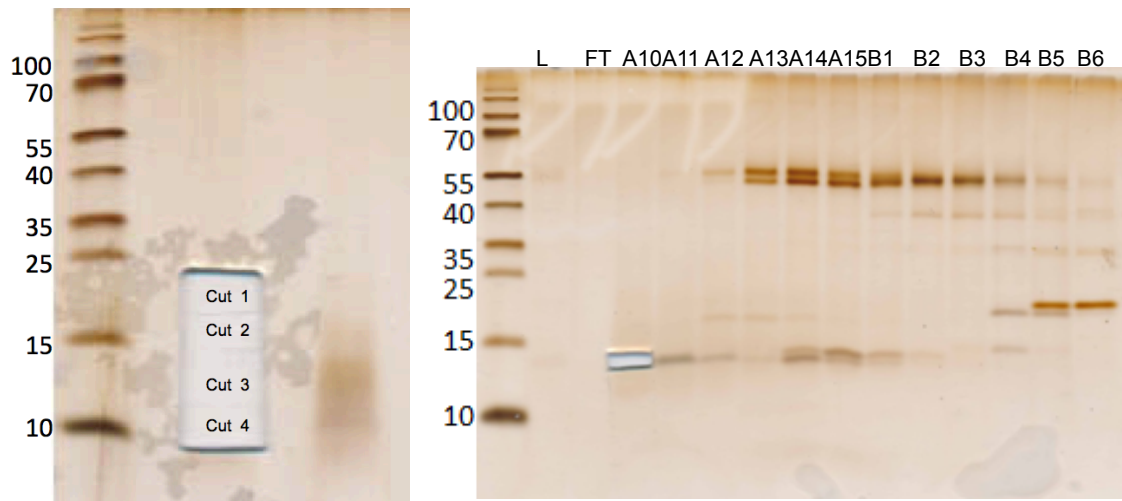


Figure 7. 5 PS45 candidates (left) and PS65 candidates (right) were spread on silver stained Tricine SDS page gels

PS45 active fraction was spread on silver stained Tricine SDS page gel (left). Two lanes are duplicates. Cut1, Cut2, Cut3 and Cut4 are four sliced gels for Mass Spectrometry analysis. Fractions after Source 15Q 4.6/100 PE was spread on silver stained Tricine SDS page gel (right). Lanes from left to right are: L (loading sample), FT (flow through) and fractions A10 to B6. Fraction A10 contained PS65 activity. Single sliced gel from A10 was used for Mass Spectrometry analysis.

#### 7.2.5 PAMP candidates were validated by over-expression in *E. coli*.

The genomic DNA was isolated from *Pseudomonas syringae* pv tomato strain DC3000 using mini-prep protocol (Wilson, 1997). The cell culture was re-suspended in 567µl TE buffer. Proteinase K treated the sample for 1 hr at 37°C. 100µl 5M NaCl and 80µl CTAB/NaCl solution (10% CTAB in 0.7 M NaCl) were added into solution, mixed gently and incubated in 65°C oven for half hour. DNA was extracted by chloroform/isoamyl alcohol (24:1) and phenol/chloroform/isoamyl alcohol (25:24:1) respectively. The aqueous phase was transferred into a fresh tube and extracted DNA was precipitated by isopropanol. The pellet was washed in 70% ethanol and dried out.

The primers to amplify the candidate genes PSPTO\_3270, PSPTO\_0217 and PSPTO\_1424 are following:

```

3270f  CACCATCAAGACCAAAGTACTGACT
3270r  CTAAGTACTGAGTCTTGGTTTTCTCGGTA
0217f  CACCAAGCTAGTCACTGCCATC
0217r  CTAAATTGCGTCTGTATCGGTCT

```

1424f CACCGCTTACAGCGAAAAG

1424r CTACAGCAGGCCCTTCTTCTG

Phusion enzyme was used to amplify the blunt end products PSPTO\_3270 (286bp), PSPTO\_0217 (340bp) and PSPTO\_1424 (388bp). The amplified products were cloned into vector Champion™ pET100 Directional TOPO® (Invitrogen), which contains N-terminal 6xHis tag. The cloning, transformation and expression were carried out according to the manual supplied.

To purify the expressed proteins, HisTrap FF (1ml) column was used (Table 3.1). In case some of proteins were in inclusion body, the cell culture was sonicated in 1%-5% N-Laurylsarcosine, 20mM Tris buffer (pH8.1).

Three proteins that predicted to harbor PAMPs originated from *Pseudomonas syringae* pv tomato strain DC3000 were purified by HisTrap columns from crude extracts of over-expressed *E.coli*. The main fractions affinity to his-tag column from over expressed iron-binding protein (PSPTO\_1424) and hypothetical protein (PSPTO\_3270) exhibited the ability to elicit ethylene response in fls/efr double mutant Arabidopsis (Figure 7.6), although nitrogen regulation protein II (PSPTO\_0217) didn't exhibit strong ability to elicit ethylene response. The purified proteins were illustrated on SDS-PAGE gel and quantified (not shown in thesis).

In this study, a fast and efficient cloning and expression system for over-expressing candidate PAMPs was established, which accelerated our process to validate large amount of candidate PAMPs from implication of Mass-Spec analysis. However, the ambiguity of the his-tag column affinity deserve cautions, certain unknown non-specific Ni<sup>2+</sup> affinitive molecular display the ethylene inducing capability, which might produce high background in ethylene assay. Therefore, additional independent expression systems are required before reaching conclusion.



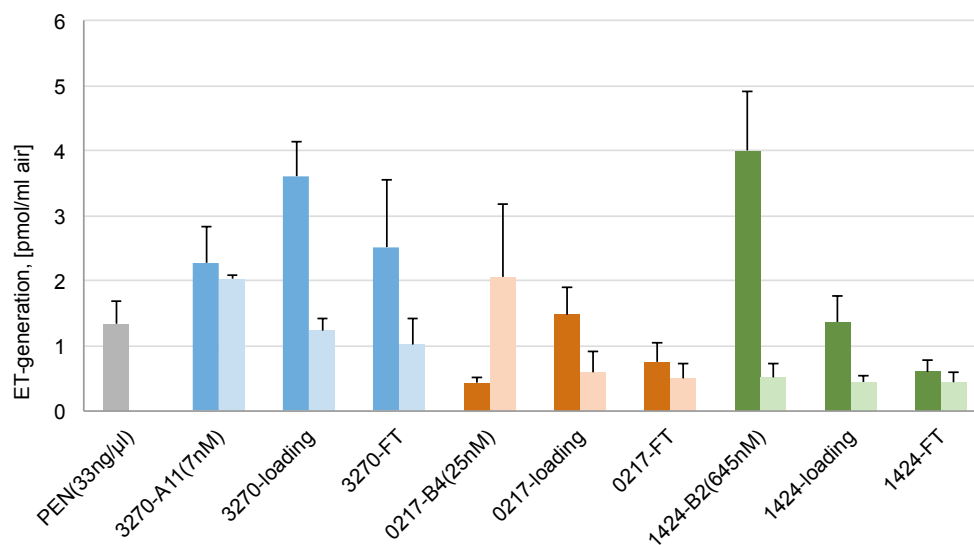


Figure 7. 6 Ethylene responses in *fls2/efr* double mutants elicited by candidate PAMPs from *DC3000*

Multiple colors represented different elicitors. Grey: PEN as control; blue: PSPTO\_3270; orange: PSPTO\_0217; green: PSPTO\_1424. Dark color series: purified proteins in MES buffer (pH 5.2); light color series: purified proteins in MES buffer (pH 5.2, contained 0.1%SDS) were heated 95°C for 5min.

### 7.2.6 Peptides derived of PSPTO\_3270 and PSPTO\_1424 elicit ethylene responses in *fls2/efr* Arabidopsis

A series of nested peptides with 30 amino acids length from the three candidate proteins were synthesized (by Genescript) (Figure 7.9; Figure 7.10; Figure 7.11). They were examined for the activities of ethylene eliciting in *fls2/efr* double mutant Arabidopsis. Two peptides from PSPTO\_1424 could independently induce ethylene responses in MES buffer (50mM, pH 5.2) with concentration of 5μM (Figure 7.7). To optimize the ethylene assay, 1μM iron ions was included in the mixture of peptide1424-51 and peptide1424-97. The threshold of 1μM was obtained to elicit ethylene in *fls2/efr* double mutants. Meanwhile, the mixture of peptides 3270-61 and 3270-71 from the other candidate PAMP protein PSPTO\_3270 had capability to elicit ethylene while reaching to 5μM (Figure 7.8). No ethylene responses were detected from double mutant plants upon treatment of peptides of nitrogen regulate protein II (Figure 7.12).

Currently the minimal eliciting concentration is at about  $\mu\text{M}$  level, which is higher than most of the known elicitors. It is needed to determine whether those PAMP candidates from purification of proteins are representing the genuine properties as PAMPs in nature, one way is to investigate their capabilities to elicit other immunity responses, such as ROS, callose deposition and MAPK; the other way is to check the natural variations of ethylene responses in our ecotypes collection, and therefore to map those peptides recognition system. If the specific recognition by receptors was validated, the conclusion also could be drawn that the candidate is the authentic PAMP.

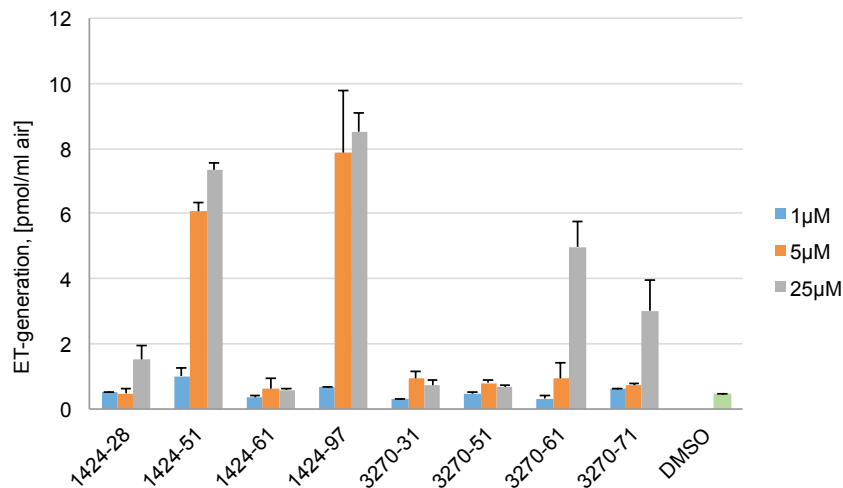


Figure 7. 7 Peptides-induced ethylene responses in *fls2/efr* double mutant plants

The different concentration of peptides that are derived of protein PSPTO\_1424 and PSPTO\_3270 were used to elicit ethylene responses in *fls2/efr* double mutant plants. 5μM peptide 1424-51 or 1424-97 could induce ethylene responses in *fls2/efr* double mutant plants independently. 25μM peptide 3270-61 or 3270-71, which is derived of protein PSPTO\_3270, could induce ethylene responses in *fls2/efr* double mutant plants independently (DMSO as control).

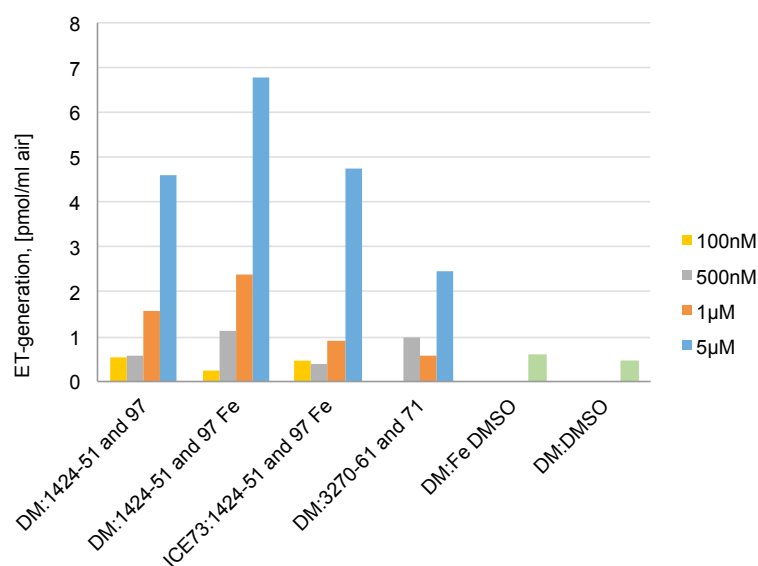
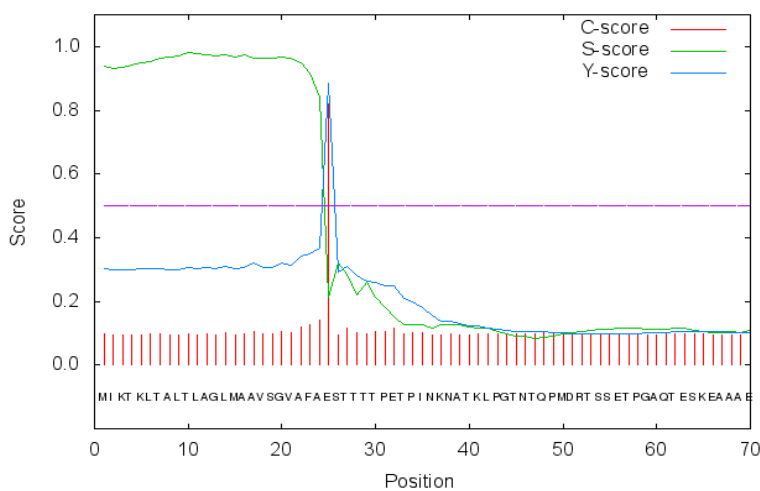


Figure 7. 8 Peptides-induced ethylene responses in *fls2/efr* double mutant plants or ecotype ICE73 with optimized conditions

Two active peptides, 1424-51 and 1424-97, were mixed with different concentrations and they could elicit ethylene responses in *fls2/efr* double mutant plants (DM) or ecotype ICE73. With additional 1μM  $Fe^{2+}/Fe^{3+}$ , 1μM 1424-51 and 1424-97 could induce ethylene responses both in *fls2/efr* double mutant plants and ecotype ICE73. The other two active peptides, 3270-61 and 3270-71, were mixed together. 5μM both peptides could induce ethylene responses in *fls2/efr* double mutant plants. In this assay, DMSO and 1μM  $Fe^{2+}/Fe^{3+}$ -contained DMSO are controls.

SignalP-4.1 prediction (gram- networks): gi\_81730628\_sp\_Q880A2\_Q880A2\_PSES



CLUSTAL W (1.83) multiple sequence alignment

```

Pseudomonas_syringae_DC3000      MIKTKLTALTLAGLMAAVSGVAFVFAESTTTT PETPINKNATKLPGTNTQPM
Pseudomonas_syringae             MIKTKLTALTLAGLMAVASGAFAES-TTTPETPINKNATKLPGTNTQPM
Pseudomonas_syringae_syringae    MIKTKLTALTLAGLMAVASGAFAES-TTTPETPINKNATKLPGTNTQPM
Pseudomonas_syringae_phaseolic   MIKTKLTALTLAGLMAVASGAFAES-TTSSETPINKNATKLPGTNTQPM
Pseudomonas_amygdali             MIKTKLTALTLAGLMAVASGAFAES-TTSSETPINKNATKLPGTNTQPM
Pseudomonas_savastanoi           MIKTKLTALTLAGLMAVASGAFAES-TTSSETPINKNATKLPGTNTQPM
Pseudomonas_coronafaciens        MIKTKLTALTLAGLMAVASGAVFAES-TTGNETPINKNATKLPGTNTQPM
Pseudomonas_syringae_g3          MIKTKLTALTLAGLMAVASGAVFAES---TPANPVNPNATKLPGNTEPM
***** **..**.*
Pseudomonas_syringae_DC3000      DRTSSETPGAQTESKEAAAERSMKHKDT-HGKHKDSNVTEKTKTQ
Pseudomonas_syringae             DRTSSETPGVQTESKEAAAERSMKHKDKATHGTHDKSTVTEKTKTQ
Pseudomonas_syringae_syringae    DRTSSETPGVQTESKEAAAERSMKHKDKTHGTHDKSTPTEKTKTQ
Pseudomonas_syringae_phaseolic   DRTSSETPGAQDTSKAAAEEKSMNHDKGAGHGHDKSNVTEKTKTQ
Pseudomonas_amygdali             DRTSSETPGAQDTSKAAAEEKSMNHDKGAGHGHDKSNVTEKTKTQ
Pseudomonas_savastanoi           DRTSSETPGAQDTSKAAAEEKSMNHDKGAGHGHDKSNVTEKTKTQ
Pseudomonas_coronafaciens        DRTSSETPGAQNESKEAAAERSMKHKDKGAGHGHDKSKVTEKTKTN
Pseudomonas_syringae_g3          DRTSSETPGAQKESREAAAERAKKHDNAAHGTHDKTGVTETKTKTQ
*****.:.:.:*:*:*:*.:.:*.:*.:*.:*.:*.:*.:*.:*.:*.:*.:*.:*.:*.:*.:
    
```

```

MIKTKLTALT LAGLMAAVSG VAFVFAESTTTT PETPINKNAT KLPGTNTQPM
          TTTT PETPINKNAT KLPGTNTQPM
                PETPINKNAT KLPGTNTQPM
                        KLPGTNTQPM
    
```

```

DRTSSETPGA QTESKEAAAEE RSMKHKDKTH GKHKDSNVTE KTKTKQ
DRTSSE  3270-27
DRTSSETPGA 3270-31
DRTSSETPGA QTESKEAAAEE 3270-41
DRTSSETPGA QTESKEAAAEE RSMKHKDKTH 3270-51
          QTESKEAAAEE RSMKHKDKTH GKHKDSNVTE 3270-61
                RSMKHKDKTH GKHKDSNVTE KTKTKQ 3270-71
    
```

Figure 7. 9 Peptides synthesis illustration for PSPTO\_3270

Signal peptide was detected at the beginning of protein, which was exclusive from the synthesized peptides. The Clustal W alignment shows the conservative region among different lines of species. The nested peptides are around 30 amino acids long and they have 20 amino acids overlapped with neighbored peptides. Peptides' names are indicated in boxes, immediately after the sequences. Two active peptides are indicated as red boxes.

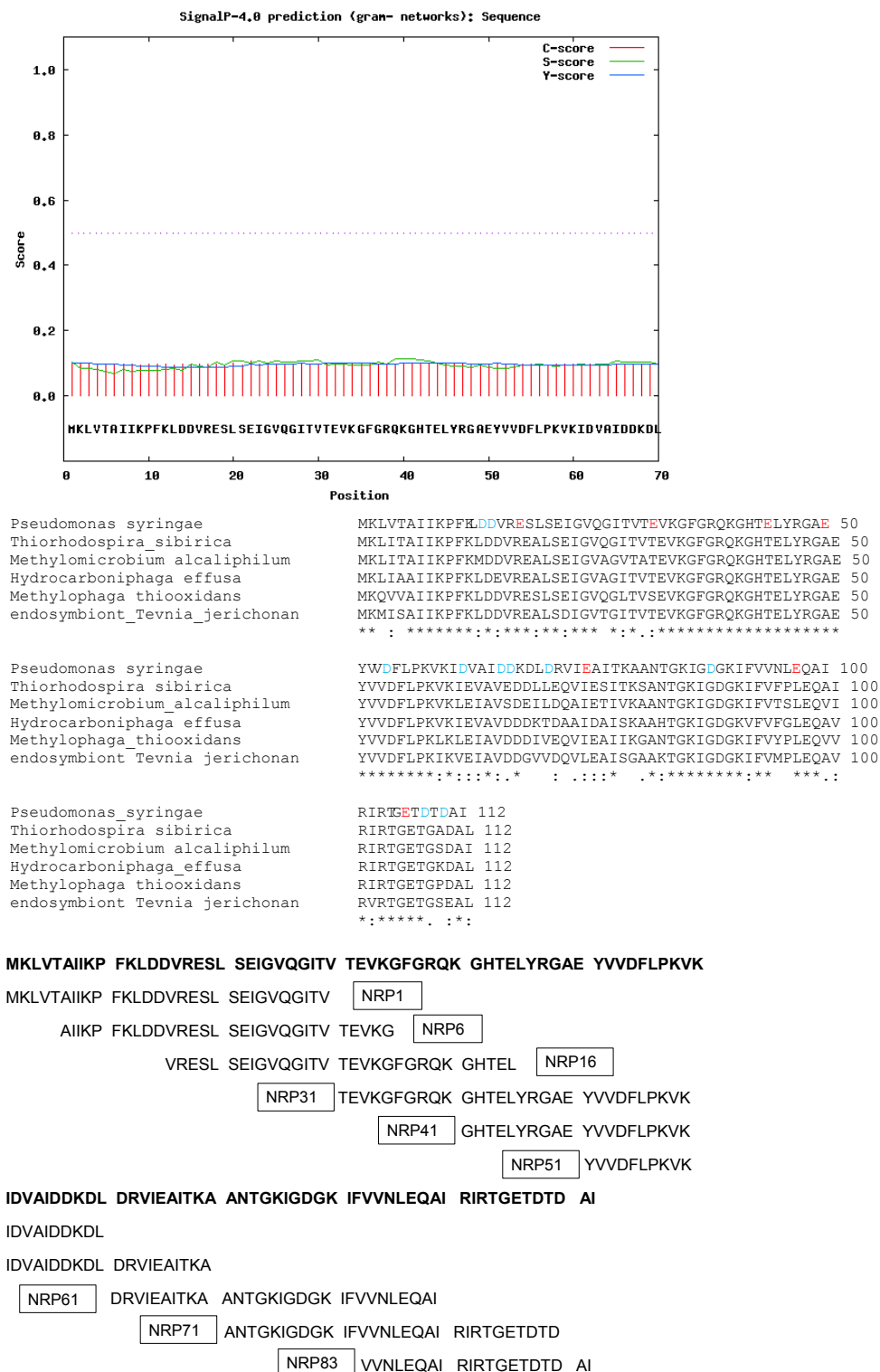


Figure 7. 10 Peptides synthesis illustration for PSPTO\_0217

No signal peptide was detected on this protein. The Clustal W alignment shows the conservative region among different species. The nested peptides are around 30 amino acids long and they have 15-20 amino acids overlapped with neighbored peptides. Peptides' names are indicated in boxes, immediately before or after the sequences.

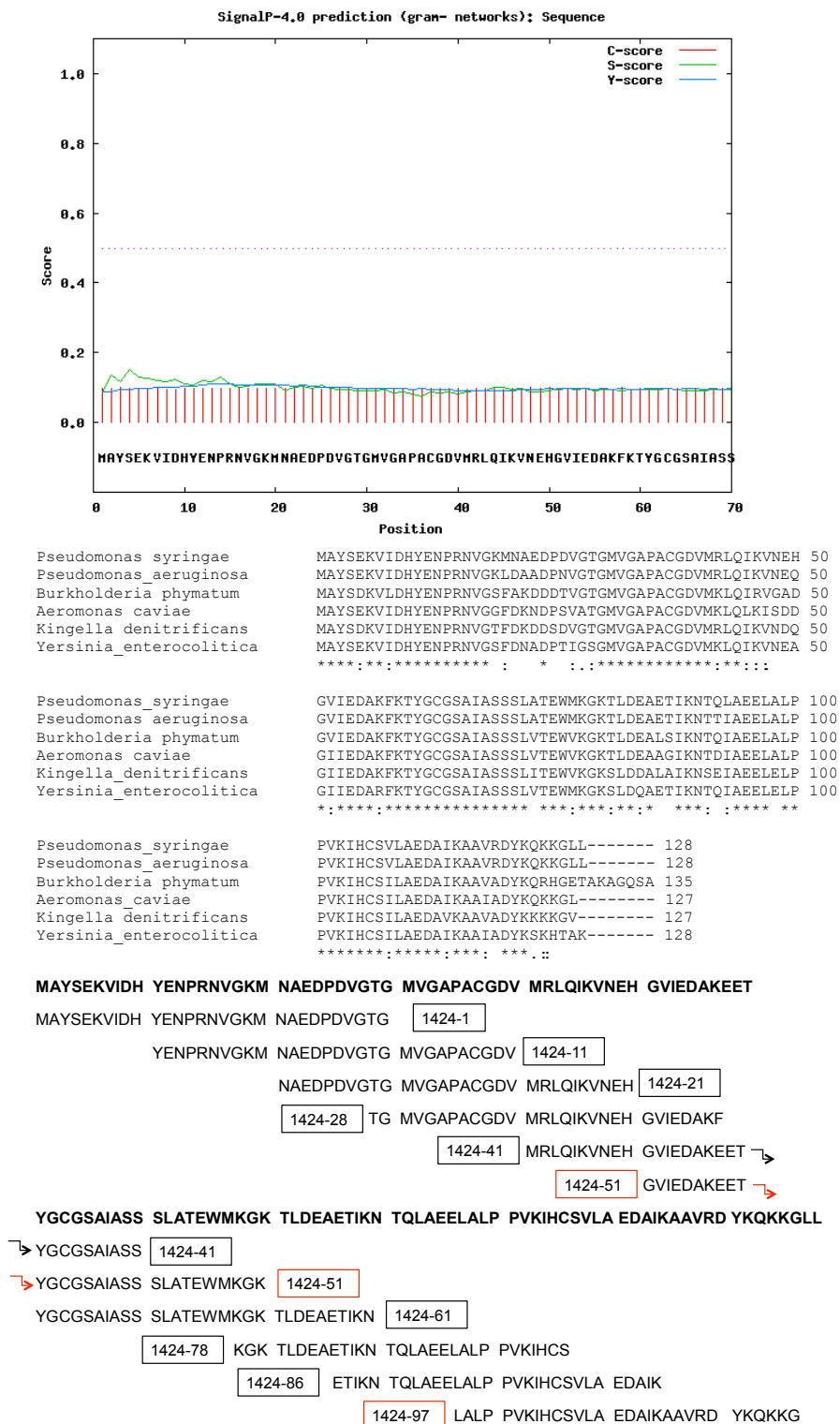


Figure 7. 11 Peptides synthesis illustration for PSPTO\_1424

No signal peptide was detected on this protein. The Clustal W alignment shows the conservative region among different species. The nested peptides are around 30 amino acids long and they have ~20 amino acids overlapped with neighbored peptides. Peptides' names are indicated in box, immediately before or after the sequences. Two active peptides are indicated as red boxes.

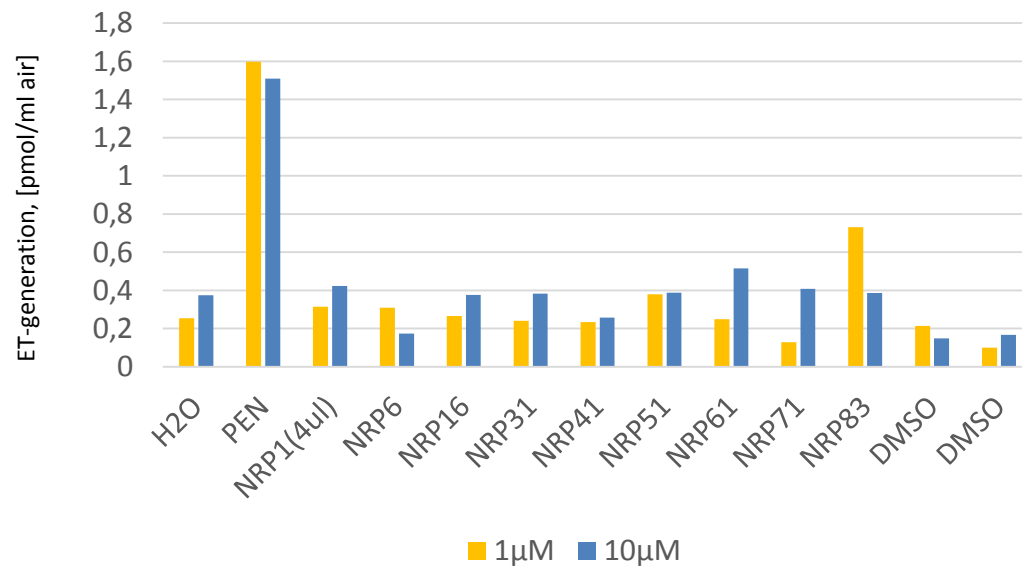


Figure 7. 12 Peptides from PSPTO\_0217 (known as NRPII protein) could not induce ethylene responses in double-mutant plants

Unlike the PSPTO\_3270 and PSPTO\_1424, the peptides synthesized based on the sequence of protein PSPTO\_0217 could not induce ethylene responses in *fls2/efr* double mutant plants with concentration as high as 10µM. The concentration of PEN is 33ng/µl.